

UC San Diego

Scripps Institution of Oceanography Technical Report

Title

Influence of Oceanographic Variability on the Planktonic Prey and Growth of Sardine and Anchovy in the California Current Ecosystem

Permalink

<https://escholarship.org/uc/item/307453xf>

Author

Rykaczewski, Ryan R

Publication Date

2009-05-28

UNIVERSITY OF CALIFORNIA, SAN DIEGO

Influence of Oceanographic Variability on the Planktonic Prey and
Growth of Sardine and Anchovy in the California Current Ecosystem

A dissertation submitted in partial satisfaction of the
requirements for the degree of Doctor of Philosophy

in

Oceanography

by

Ryan Ross Rykaczewski

Committee in charge:

Professor David M. Checkley, Jr., Chair
Professor Richard Carson
Professor Peter J. S. Franks
Professor Michael R. Landry
Professor Daniel L. Rudnick

2009

©

Ryan Ross Rykaczewski, 2009

All rights reserved.

The Dissertation of Ryan Ross Rykaczewski is approved, and it is acceptable in quality and form for publication on microfilm and electronically:

Chair

University of California, San Diego

2009

For my parents,

Bob and Lisa

TABLE OF CONTENTS

Signature Page.....	iii
Dedication.....	iv
Table of Contents.....	v
List of Tables.....	vii
List of Figures.....	viii
Acknowledgements.....	x
Vita.....	xiv
Abstract.....	xv
Chapter 1. Introduction.....	1
1.1. Background.....	1
1.2. Outline of the dissertation.....	6
1.3. References.....	10
Chapter 2. Differences between the branchial sieves of Pacific sardine and northern anchovy of the California Current Ecosystem.....	13
2.1. Abstract.....	13
2.2. Introduction.....	14
2.3. Methods.....	17
2.4. Results.....	18
2.5. Discussion.....	20
2.6. Conclusions.....	24
2.7. References.....	32
Chapter 3. Changes in mesozooplankton size structure along a trophic gradient and implications for small pelagic fish.....	34
3.1. Abstract.....	34
3.2. Introduction.....	35
3.3. Methods.....	39
3.4. Results.....	48
3.5. Discussion.....	54
3.6. Conclusions.....	63
3.7. Acknowledgements.....	65

3.8. References.....	78
Chapter 4. Influence of ocean winds on the pelagic ecosystem in upwelling regions.....	84
4.1. Abstract.....	84
4.2. Introduction.....	85
4.3. Methods.....	89
4.4. Results and discussion.....	96
4.5. Acknowledgements.....	104
4.6. References.....	114
Chapter 5. Conclusions.....	118
5.1. Summary and future directions.....	118
5.2. References.....	124

LIST OF TABLES

Table 2.1. ANCOVA table comparing changes in inter-raker spacing with size between anchovy of the BCE and CCE.....	25
Table 2.2. ANCOVA table comparing changes in inter-raker spacing with size between sardine of the BCE and CCE.....	25
Table 3.1. Taxonomic categories and length to dry-weight conversions applied in Zooscan analysis.....	66
Table 3.2. Linear Pearson correlation coefficients between nutrient concentrations and measurements of the plankton community.....	67
Table 3.3. Median dry weights of individual zooplankters and linear Pearson correlation coefficients between mesozooplankton normalized-biomass spectral slopes and the median weights of major taxonomic groups.....	67
Table 3.4. Taxonomic composition and linear Pearson correlation coefficients between total mesozooplankton biomass and relative contributions of major taxonomic groups.....	68
Table 3.5. Differences in individual copepod sizes during two CalCOFI cruises for which detailed species distributions were published by Fleminger (1964, 1967) and Bowman and Johnson (1973)	68
Table 4.1. Pearson correlation coefficients between upwelling and water-column properties.....	105

LIST OF FIGURES

Figure 1.1. Commercial landings of Pacific sardine and northern anchovy in the state of California, 1929 to 2007.....	9
Figure 2.1. Gill arch of northern anchovy, <i>Engraulis mordax</i>	26
Figure 2.2. Anterolateral view of the branchial sieves of sardine and anchovy of the CCE.....	27
Figure 2.3. Magnified examples of anchovy (A) and sardine (B) gill rakers.....	28
Figure 2.4. Comparison of measures describing the branchial sieves of sardine and anchovy species.....	29
Figure 2.5. Dorsal view of a single gill raker of anchovy and sardine, highlighting the differences in denticle structure.....	30
Figure 2.6. Conceptual diagram displaying the possible configurations of sardine denticles during filtering.....	31
Figure 3.1. Locations of experimental cycles in reference to MODIS chlorophyll <i>a</i> concentrations and estimates of curl-driven upwelling.....	69
Figure 3.2. Physical and chemical conditions observed during sampling of phytoplankton and zooplankton communities.....	70
Figure 3.3. Measures of biomass and size structure of the phytoplankton community.....	71
Figure 3.4. Typical normalized-biomass spectra.....	72
Figure 3.5. Mesozooplankton community biomass and size structure estimated by different methods.....	73
Figure 3.6. Comparison of biomass spectral slopes between phytoplankton and mesozooplankton communities observed together in the CCE.....	74
Figure 3.7. Estimates of normalized-biomass spectral slopes for phytoplankton and mesozooplankton communities observed in the CCE.....	75
Figure 3.8. Median dry weights of individual copepods in relation to the spectral slope of the mesozooplankton community.....	76

Figure 3.9. Egg distributions and potential, specific growth rate of individual sardine and anchovy for the plankton conditions observed during cruises in May 2006 and April 2007 off of Pt. Conception, CA.....	77
Figure 4.1. Conceptual diagram displaying the hypothesized relationship between wind-forced upwelling and the pelagic ecosystem.....	106
Figure 4.2. Domain of the upwelling model, locations of zooplankton collections, and CalCOFI stations.....	107
Figure 4.3. Relationship between zooplankter size and upwelling rate.....	108
Figure 4.4. Mean summertime (May-July) wind stress and upwelling rate from 1984-2004.....	109
Figure 4.5. Upwelling changes in the CCE.....	110
Figure 4.6. Summertime upwelling, σ_θ , nutricline depth, and chlorophyll <i>a</i> concentration.....	111
Figure 4.7. Upwelling and surplus production per unit biomass of Pacific sardine.....	112
Figure 4.8. Observed and modeled surplus production in the Pacific sardine population for two periods (1948-1962 and 1983-2004).....	113

ACKNOWLEDGEMENTS

The list of those who have aided in this endeavor is numerous, and more people deserve thanks than I can express here. My advisor, Dave Checkley, has tried his best to impart me with some of his expert understanding of fisheries oceanography over the passed six years. In the process, Dave has provided me not only with an education in the discipline, but also with an appreciation for seagoing research and “true-blue oceanography.” Dave’s experience at sea and knowledge of biological oceanographic techniques are paralleled by few. His unfaltering patience and encouragement have also served me well: more than once during my studies I have left his office lacking the discouragement and frustration which I carried when I entered. I am fortunate and grateful to have Dave as a friend and mentor.

The members of my committee have each uniquely contributed to this dissertation. Dr. Carson has an interest in the dynamics and management of fisheries that is rarely found outside of the oceanographic community. The advice of both Peter Franks and Dan Rudnick has been indispensable, and I would be a better oceanographer if I retained half of what they have taught me over the years. I admire Peter’s ability to concisely convey his teachings in format that even I could understand. I periodically turned to Dan for advice on techniques of data analysis, and he has always offered sound recommendations in addition to spirited discussion; I wish I had spent more time in his office. Mike Landry has supported my research on several fronts. Mike was the first to introduce me to the endless joys of a repetitive cycle of net tows, zooplankton size fractionation, and microzooplankton incubation experiments when I volunteered to help on a scientific voyage during December and

January of my second year at Scripps, but he has more than repaid this debt by generously sharing his time and guidance in the years since.

Mark Ohman has played a formative role in shaping parts of this dissertation. I am amazed by Mark's daily enthusiasm for research. In addition to granting me free rein to his laboratory resources, Mark leads the CCE Long-Term Ecological Research (LTER) Program. The CCE LTER Program was initiated shortly after I began my studies at Scripps. Coincidentally, my personal research interests are largely encompassed by the goals of the CCE LTER program. This program has not only expanded my research opportunities, but also provided a larger context in which to place my research. The prospect of continued, focused investigation of ecosystem processes (which augment the essential and ongoing hydrographic and biological surveys of the CCE by the California Cooperative Oceanic Fisheries Investigations) is exciting. I look forward to seeing the results of this new program as it develops in the coming decades and thank Mark for carrying the torch high. The students, staff, and volunteers associated with the CCE LTER also deserve recognition, as much of my work has relied on their collaboration, support, and sweat, both at sea and on shore.

My introduction to the community of fisheries oceanographers, and specifically those concerned with small pelagic fish, has shown me that this eclectic group of scientists is welcoming, close knit, and full of interesting characters. Discussions with these oceanographers at conferences around the globe and at the Southwest Fisheries Science Center have influenced my research greatly, and this dissertation would not have been possible without their help and dedication. The little

that I have attempted to contribute to our scientific understanding of fisheries ecology is built on the decades that others have devoted to the study of small pelagic fish.

A number of research groups at Scripps have aided in this research. In particular, the Landry, Ohman, Goericke, and Koslow Labs have contributed time, data, laboratory resources, and thoughts on this project. Art Miller and Masao Kanamitsu have also provided ideas and resources, and Don Olson (at the University of Miami) was certain to do his best to provide me with some quantitative understanding of oceanography.

It has been a pleasure working in the Checkley Lab, and Dave's propensity for international collaboration has brought a number of unique perspectives into the group. I thank Motomitsu Takahashi, Pete Davison, Sarah Glaser, Rebecca Asch, Peter Grønkjær, and Rafa Gonzalez-Quiros for their thoughtful discussion.

I am grateful to the institutions and organizations that provided funding for this project and my studies at Scripps, including the National Science Foundation Graduate Research Fellowship Program, the NASA Earth and Space Science Fellowship Program, the San Diego chapter of the ARCS Foundation, the Ellen Browning Scripps Foundation, and the Michael M. Mullin fellowship.

The encouragement and devotion of my parents, Bob and Lisa, has been unwavering. This dissertation is dedicated to them. I could not ask for better friends than my two brothers, Kyle and Sam. My grandparents Roy and Margarete and cousins Ken and Maylette have supported me with their love and generosity during the passed six years. Perhaps most importantly, the friends I have made at Scripps will undoubtedly be friends for life.

Chapter 4 of this dissertation has been published elsewhere as: Rykaczewski, R.R. and Checkley, D. M., Jr. (2008) Influence of ocean winds on the pelagic ecosystem in upwelling regions. *Proceedings of the National Academies of Sciences U. S. A.* **105**:1965-1970. I was the primary researcher and author of this article.

Chapter 3 is in preparation for publication as: Rykaczewski, R.R. Changes in mesozooplankton size structure along a trophic gradient and implications for small pelagic fish.

VITA

- 2000-2001 Undergraduate research assistant, University of Miami, Molecular and Cellular Pharmacology
- 2001-2002 Undergraduate research assistant, University of Miami, Rosenstiel School of Marine and Atmospheric Science
- 2002 B.S., Biology and Marine Science, Chemistry, University of Miami, School of Arts and Sciences, Coral Gables, FL
- 2002-2003 Northwest Observers, Inc., National Marine Fisheries Service observer, Bering Sea/Gulf of Alaska
- 2003-2009 Graduate student researcher; University of California, San Diego; Scripps Institution of Oceanography
- 2008 Teaching assistant; “Biological Oceanography;” University of California, San Diego
- 2009 Ph.D., Oceanography; University of California, San Diego; Scripps Institution of Oceanography; La Jolla, CA

ABSTRACT OF THE DISSERTATION

Influence of Oceanographic Variability on the Planktonic Prey and Growth of Sardine and Anchovy in the California Current Ecosystem

by

Ryan Ross Rykaczewski

Doctor of Philosophy in Oceanography

University of California, San Diego, 2009

Professor David M. Checkley, Jr., Chair

Populations of Pacific sardine (*Sardinops sagax*) and northern anchovy (*Engraulis mordax*) have responded differently to oceanographic changes in the California Current Ecosystem (CCE) over the past century. Similar multi-decadal scale variability has been observed in sardine and anchovy populations around the world. Although correlations between ocean temperatures and fish biomasses are evident, the underlying processes relating ocean conditions to fish production remain unknown. Here, I examine the ecological differences between sardine and anchovy in

the CCE and consider the oceanographic conditions that affect the planktonic prey utilized by the two species.

Sardine and anchovy are planktivorous fish that consume a wide range of prey items. However, direct comparison of the gill rakers of the two species indicate that sardine are better adapted to retain smaller plankters than anchovy. Oceanographic conditions influence the size spectrum of zooplankton communities in the CCE, with larger individual plankters relatively more abundant in the eutrophic region nearshore. I hypothesize that this relationship results from size-dependent trophic interactions between zooplankton and their phytoplanktonic prey. Model results indicate that changes observed in the biomasses and size structure of zooplankton communities in offshore, oligotrophic waters influence the potential growth rate of sardine, while anchovy growth is uniformly negative in the offshore region. Positive growth by anchovy is possible only in the nearshore, eutrophic zone. Different atmospheric conditions control the nutrient supply to these regions of the CCE. The nearshore area is enriched by rapid upwelling of nutrient-rich waters resulting from coastal upwelling, while slow upwelling resulting from positive wind-stress curl supplies nutrients to the offshore area. Estimates of curl-driven upwelling are associated with pycnocline and nutricline shoaling in the southern CCE over the passed decades, and sardine production is more strongly related to changes in curl-driven upwelling than with coastal upwelling or sea-surface temperature. Upwelling rate is a fundamental determinant of the biological structure and production in coastal pelagic ecosystems, and future changes in the magnitude and spatial gradient of wind stress may have important and differing effects on these ecosystems.

Chapter 1. Introduction

1.1. Background

Fisheries oceanographers have long recognized the importance of ecosystem variability to the productivity of marine fisheries, and the desire to better understand this relationship has been the impetus for a number of focused, oceanographic survey programs over the last century. Decades of research by these programs have led to one unanimous conclusion: the relationships between ocean conditions and the production of marine fisheries are ambiguous and complex. From the inception of fisheries oceanography, researchers have been certain that the environment influences the population variability of fish stocks, but the ecological processes responsible for these relationships were not adequately understood. The first Commissioner of the US Commission of Fish and Fisheries, Spencer Fullerton Baird, actively advocated for a mechanistic understanding of the relationships between oceanographic changes and population variability in the 1870s and 1880s (Kendall and Duker 1998). More than a century later, little progress has been made on this front. Examinations of mechanistic processes are often limited to relatively short investigations with focused effort (*e.g.* Lasker 1975), and consideration of longer-term changes have often been limited to correlation between fisheries production and an easily and regularly measured environmental variable (*e.g.*, sea-surface temperature). Not surprisingly, predictions based on these correlations have usually failed with time (Myers 1998). Such relationships are usually based on the past statistical behavior of a physical parameter without a clear understanding of the processes that are ecologically relevant to fish

growth and survival. This lack of understanding leaves fisheries managers incapable of properly incorporating environmental conditions into management decisions. As a result, management plans are often based on simple stock-recruitment relationships and fail to account for the effects of changing environmental conditions. A mechanistic understanding of the effects of climate variability on fish populations is necessary if we intend to prudently manage resources with an ecosystem approach. The aim of this dissertation is to examine the effects of oceanographic and atmospheric conditions on the prey field and production of sardine and anchovy.

The California Current Ecosystem (CCE) is an ideal environment in which to study fisheries oceanography. An impressive amount of research has been focused on the population dynamics of Pacific sardine (*Sardinops sagax*) and northern anchovy (*Engraulis mordax*) of the CCE, not only because of their ecologic and economic value, but also because of the prominent decadal-scale variability in population biomasses that are shared with similar species around the world. Plentiful catches of one species have often alternated with the other, and these fluctuations have had severe consequences to the fishing, processing, and farming (*e.g.*, poultry, swine, and tuna) industries dependent on the fisheries' landings for income and feed (Schwartzlose *et al.* 1999). Sardine in the CCE supported a prosperous commercial fishery during the 1930s and early 1940s, and the astounding and inexplicable decline in landings of sardine off the west coast of North America in the late 1940s prompted an ecological investigation unparalleled in scale—the California Cooperative Sardine Research Program, now known as the California Cooperative Oceanic Fisheries Investigations (CalCOFI) Program. Landings of anchovy in California increased

during the 1960s and 1970s, and though the catches never reached the earlier magnitude of the sardine landings, anchovy supported a valuable commercial fishery until declining in the late 1970s. The sardine population recovered during the 1980s. In 2007 landings of sardine were the highest recorded since the 1950s (Figure 1.1), and sardine is currently the largest fishery in the state of California (CDFG 2008).

Early hypotheses proposed to account for the apparent replacement of the sardine population by anchovy in the CCE considered three principles of population dynamics: interspecific competition between the two species (Silliman 1969); failed sardine recruitment due to intense overfishing of adults, with successive replacement by anchovy (Iles 1973); and differential response of each species to changing climate factors (Marr 1960). From the establishment of CalCOFI, it was recognized that a combination of factors was likely responsible for growth and decline in each fish population. These hypotheses are not mutually exclusive; sardine and anchovy exist in an environment subject to numerous influences by abiotic and biotic factors, including exploitation by humans.

The negative effects of overfishing and the resulting increase in the susceptibility of fish populations to environmental changes are unmistakable (Hsieh *et al.* 2006). However, paleoceanographic records and comparison among biomass estimates of sardine and anchovy populations from around the world suggest that commercial exploitation and interspecific competition may be less significant than the effect of climate variability on sardine and anchovy populations. Analysis of scale deposition in anaerobic sediments of the Santa Barbara Basin by Soutar and Isaacs (1969) and Baumgartner *et al.* (1992) indicate that the annual biomasses of sardine

and anchovy populations in the CCE varied considerably during the past 2000 years due to natural environmental factors, independent of fishing pressure. The multi-decadal time scale of the variability observed during the recent period of commercial exploitation was also evident in the sediment records. In addition, these reconstructed estimates of biomass suggest sardine and anchovy are not strict competitors; both species may be abundant or absent at a given time period. This evidence supports the hypothesis that climate variability is a major influence on the biomasses of sardine and anchovy in the CCE. Subsequent realization that populations of sardine and anchovy share similar time periods of growth and decline in each of the major upwelling ecosystems around the globe (and in the Kuroshio/Oyashio Reion) further suggests that large-scale climate variability has a differential affect on the growth of the two taxa (Schwartzlose *et al.* 1999).

In light of the increasing evidence that sardine and anchovy are subject to climate variability, countless hypotheses have been proposed to account for different responses of the populations to changing environmental conditions. The environment may affect fish directly by changing abiotic conditions (*e.g.*, advection or physiologic response to temperature) or indirectly through food-web processes (*e.g.*, prey distribution or predation pressure). Among these hypotheses, the relationship between sardine and anchovy abundance with water temperature is most renowned (Chavez *et al.* 2003). Sardine production has been favored during warm periods, most recently from the 1920s to the mid-1940s and from 1977 through the present. A cool period, favorable for anchovy, occurred from the mid-1940s through 1976 (Lluch-Belda *et al.*

1989, Chavez *et al.* 2003). A shift to another cool period may have occurred after the 1997-1998 El Niño (Peterson and Schwing 2003).

The mechanism relating sardine and anchovy growth to warm and cool periods (respectively) remains unknown. However, the relationship between warmer waters and sardine abundance has been considered reliable enough that a three-year running mean of summertime sea-surface temperature at the pier of the Scripps Institution of Oceanography is currently used by the Pacific Fishery Management Council as a factor in determining the harvest guideline for sardine along the west coast of the US (Hill *et al.* 2008). Temperature is an emergent property of the ocean, meaning it is descriptive of conditions, but alone, it is not indicative of oceanographic or biological dynamics. Temperature itself may have a direct and differing effect on the physiology of the sardine and anchovy, but clear evidence for such effect is lacking and ignores other changes in the ecosystem. Temperature variability may be symptomatic of several different physical changes (Chavez *et al.* 2003). For example, a decrease in sea-surface temperature may be indicative of increased upwelling of cold waters from below the thermocline or a decrease in heat flux from the atmosphere. The ecological consequences of these changes would certainly differ, and we would be ill-fated to predict ecosystem state based on temperature alone.

Consideration of the underlying oceanographic processes affecting sardine and anchovy is necessary if we intend to apply a more comprehensive strategy of ecosystem-based management. Knowledge of how these taxa differ in their ecological function is necessary before we understand why their populations respond differently to environmental forcing. The approach taken here focuses on the factors affecting the

prey available to juveniles and adults of the taxa. Variability in the survival and growth of larval fish has long been considered a critical factor in determining growth in fish populations (Hjort 1926), but evidence for a relationship between survival of the larval survival and recruitment is equivocal for these small pelagic fish (Peterman *et al.* 1988). Survival through the larval stage is a prerequisite to recruitment and population growth, but it is clear that factors affecting juvenile and adult stages of the population are also important (Bradford 1992).

1.2. Outline of the dissertation

At first glance, sardine and anchovy of the CCE appear strikingly similar in their morphological and ecological characteristics. Both taxa are small, silvery, pelagic fish that form massive schools and feed upon the abundant zooplankton and phytoplankton present in upwelling ecosystems. Sardine and anchovy are iteroparous, meaning that each adult spawns several times throughout the course of a season, and individual females release tens of thousands of eggs in each batch (Butler *et al.* 1993). Both species are important prey items in the diet of larger, piscivorous predators, and they have been valued commercially as food, as fertilizer, and as feed for livestock and aquaculture industries. However, in considering why sardine and anchovy respond differently to changes in ocean conditions, it is necessary to examine the dissimilarities in their ecology. These fishes tend to occupy distinct habitats within the CCE, with sardine occupying warmer waters more characteristic of the open ocean and anchovy occupying more saline areas closer to the coast that are associated with recently upwelled waters. (Checkley *et al.* 2000). The diets of the two species also

differ. Analysis of stomach contents and stable isotopes indicate that anchovy tend to feed on large phyto- and zooplankters, while smaller zooplankters and an increased amount of phytoplankton comprise the diet of sardine (Miller 2006). What biological differences are responsible for the distinctions in habitat and diet? Comparison of the morphology of the gill rakers used in filter feeding between sardine and anchovy of the Benguela Current Ecosystem suggests that differences in diet are related to the minimum prey sizes efficiently retained during filter feeding (King and MacLeod 1976). In Chapter 2, I compare the inter-raker spacing between *S. sagax* and *E. mordax* collected in the CCE. I consider the implications of these morphological differences given observations of swimming speed during feeding. Based on these results, I conclude that differences in the morphology of gill rakers between the sardine and anchovy of the CCE are similar to those identified for congeneric species in the Benguela Current Ecosystem, and these differences are likely to result in partitioning of prey resources between the sardine and anchovy.

What are the implications of this difference in prey retention for the bioenergetics and potential habitat of each species in the CCE? In Chapter 3, I present data relating changes in zooplankter sizes and abundances to environmental factors and consider the implications of these changes for the nutritional budgets of sardine and northern anchovy in the CCE. Anchovy appear to be more susceptible to changes in the nearshore environment and are unable to meet their daily nutritional requirements in the offshore, oligotrophic region. In contrast, sardine growth is not strongly favored in eutrophic environments, and they are able to meet their daily nutritional requirements under moderately oligotrophic conditions.

In Chapter 4, I consider the large-scale environmental conditions that may influence the small pelagic fish populations in the southern portion of the CCE over interannual and decadal time periods. As noted above, cold periods have been correlated with growth in the anchovy population, while warm periods favor sardine production. Since cold periods are often associated with increased coastal upwelling and nutrient supply along the coast, the growth observed in the anchovy population during these phases is expected. However, the paradoxical growth of a massive sardine population during warm periods with weak coastal upwelling has puzzled fisheries oceanographers for decades (Baumgartner *et al.* 1992, Bakun and Broad 2003). What atmospheric conditions might influence changes in the size structure of the plankton community? I hypothesize that that rapid rate of upwelling resulting from coastal, alongshore wind stress may result in larger plankters, while the relatively slow rate of upwelling related to positive wind-stress curl in offshore regions of the CCE results in the production of small plankters. Although the rate of upwelling driven by wind-stress curl is slow, the areal extent of wind-stress curl indicates that this slow upwelling may be more important (in terms of total magnitude of volume transport) than coastal upwelling in the southern CCE. Summertime estimates of coastal and curl-driven upwelling appear to vary independently during the past 60 years, and the magnitude of curl-driven upwelling over a broad area is positively related with shoaling of the pycnocline and nutricline, increased chlorophyll concentration, and greater productivity in the sardine population. This chapter was published in 2008 in the *Proceedings of the National Academy of Sciences* (Rykaczewski and Checkley 2008). Concluding remarks are presented in Chapter 5.

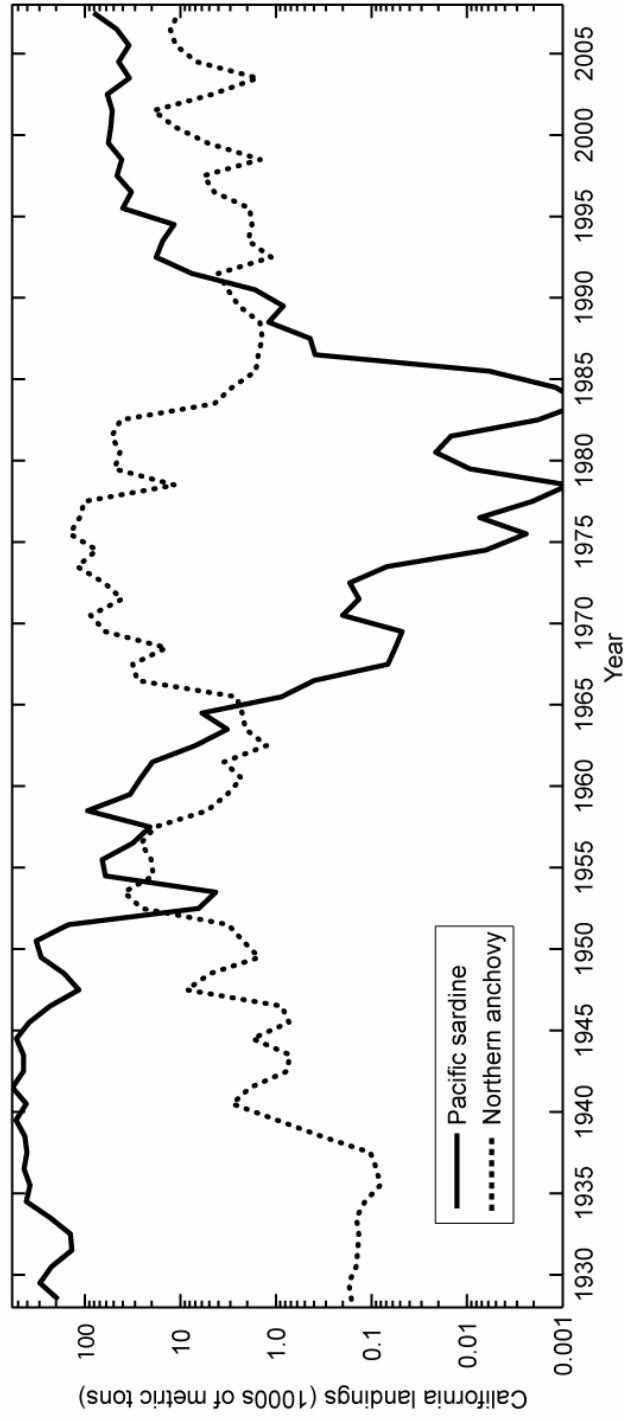


Figure 1.1. Annual commercial landings of Pacific sardine and northern anchovy in the state of California, 1929 to 2007.

1.3. References

- Bakun, A. and Broad, K. (2003) Environmental 'loopholes' and fish population dynamics: comparative pattern recognition with focus on El Niño effects in the Pacific. *Fish. Oceanogr.* **12**:458-473.
- Baumgartner, T.R., Soutar, A. and Ferreirabartolina, V. (1992) Reconstruction of the history of Pacific sardine and northern anchovy populations over the past two millennia from sediments of the Santa-Barbara Basin, California. *CalCOFI Rep.* **33**:24-40.
- Bradford, M.J. (1992) Precision of recruitment predictions from early life stages of marine fishes. *Fish. Bull.* **90**:439-453.
- Butler, J.L., Smith, P. and Lo, N.C.H. (1993) The effect of natural variability of life-history parameters on anchovy and sardine population growth. *CalCOFI Rep.* **34**:104-111.
- CDFG (2008) Review of some California fisheries for 2007: coastal pelagic finfish, market squid, dungeness crab, California spiny lobster, highly migratory species, ocean salmon, groundfish, California halibut, hagfish, Pacific herring, and recreational. *CalCOFI Rep.* **49**:15-38.
- Chavez, F.P., Ryan, J., Lluch-Cota, S.E. and Niquen, M. (2003) From anchovies to sardines and back: multidecadal change in the Pacific Ocean. *Science* **299**:217-221.
- Checkley, D.M., Jr, Dotson, R.C. and Griffith, D.A. (2000) Continuous, underway sampling of eggs of Pacific sardine (*Sardinops sagax*) and northern anchovy (*Engraulis mordax*) in spring 1996 and 1997 off southern and central California. *Can. J. Fish. Aquat. Sci.* **47**:1139-1155.
- Hewitt, R.P. and Methot, R.D., Jr. (1982) Distribution and mortality of northern anchovy larvae in 1978 and 1979. *CalCOFI Rep.* **23**:226-245.
- Hill, K., Dorval, E., Lo, N.C.H., Macewicz, B.J., Show, C. and Felix-Uraga, R. (2008) Assessment of the Pacific sardine resource in 2008 for U.S. management in 2009. *U.S. Dep. Commer., NOAA Tech. Memo. Report No.* **413**, 176 pp.
- Hjort, J. (1926) Fluctuations in year classes of important food fishes. *J. Cons. Perm. Int. Explor. Mer.* **1**:5-38.
- Hsieh, C.H., Reiss, C.S., Hunter, J.R., Beddington, J.R., May, R.M. and Sugihara, G. (2006) Fishing elevates variability in the abundance of exploited species. *Nature* **443**:859-862.

- Iles, T.D. (1973) Interaction of environment and parent stock size in determining recruitment in the Pacific sardine as revealed by analysis of density-dependent 0-group growth. *Rapp. P.-V. Réun. Cons. Int. Explor. Mer.* **164**:228-240.
- Kendall, A.W. and Duker, G.J. (1998) The development of recruitment fisheries oceanography in the United States. *Fish. Oceanogr.* **7**:69-88.
- King, D.P.F. and MacLeod, P.R. (1976) Comparison of the food and the filtering mechanism of pilchard *Sardinops ocellata* and anchovy *Engraulis capensis* off South West Africa, 1971-1972. *Invest. Rep. Sea. Fish. Brch. S. Afr.* **111**:1-29.
- Lasker, R. (1975) Field criteria for survival of anchovy larvae: relation between inshore chlorophyll maximum layers and successful first feeding. *Fish. Bull.* **73**:453-462.
- Lluch-Belda, D., Crawford, R.J.M., Kawasaki, T., MacCall, A.D., Parrish, R.H., Schwartzlose, R.A. and Smith, P.E. (1989) Worldwide fluctuations of sardine and anchovy stocks: the regime problem. *S. Afr. J. Mar. Sci.* **8**:195-205.
- Marr, J.C. (1960) The causes of major variations in the catch of the Pacific sardine, *Sardinops caerulea* (Girard). *Proceedings of the World Scientific Meeting on the biology of sardines and related species, FAO* **3**:677-791.
- Miller, R.W. (2006) Trophic dynamics of marine nekton and zooplankton in the Northern California Current ecosystem. Ph.D. thesis. Oregon State University, Corvallis.
- Myers, R.A. (1998) When do environment-recruitment correlations work? *Rev. Fish Biol. Fish.* **8**:285-305.
- Peterman, R.M., Bradford, M.J., Lo, N.C.H. and Methot, R.D. (1988) Contribution of early life stages to interannual variability in recruitment of northern anchovy (*Engraulis mordax*). *Can. J. Fish. Aquat. Sci.* **45**:8-16.
- Peterson, W.T. and Schwing, F.B. (2003) A new climate regime in Northeast Pacific ecosystems. *Geophys. Res. Lett.* **30**:10.1029/2003GL017528.
- Ryckaczewski, R.R. and Checkley, D.M. (2008) Influence of ocean winds on the pelagic ecosystem in upwelling regions. *Proc. Natl. Acad. Sci. U. S. A.* **105**:1965-1970.
- Schwartzlose, R.A., Alheit, J., Bakun, A., Baumgartner, T.R., Cloete, R., Crawford, R.J.M., Fletcher, W.J., Green-Ruiz, Y., Hagen, E., Kawasaki, T., Lluch-Belda, D., Lluch-Cota, S.E., MacCall, A.D., Matsuura, Y., Nevarez-Martinez, M.O., Parrish, R.H., Roy, C., Serra, R., Shust, K.V., Ward, M.N. and Zuzunaga, J.Z.

(1999) Worldwide large-scale fluctuations of sardine and anchovy populations. *S. Afr. J. Mar. Sci.* **21**:289-347.

Silliman, R.P. (1969) Population models and test populations as research tools. *Bioscience* **19**:524-528.

Soutar, A. and Isaacs, J.D. (1969) History of fish populations inferred from fish scales in anaerobic sediments off California. *CalCOFI Rep.* **13**:63-70.

Chapter 2. Differences between the branchial sieves of Pacific sardine and northern anchovy of the California Current Ecosystem

2.1. Abstract

Resource partitioning has been hypothesized to account for the different responses of sardine and anchovy populations to changing environmental conditions. Previous examinations of these clupeid taxa from the Benguela Current Ecosystem (BCE) have shown that the spacing between the gill rakers of sardine is smaller than that of anchovy. This difference confers a competitive advantage on sardine for the efficient retention of small planktonic prey during filter feeding. Although direct comparison of gill-raker morphology has only been conducted for the sardine and anchovy species of the BCE, the hypothesis of resource partitioning has been applied to sardine and anchovy populations in upwelling ecosystems worldwide. Here, I examine the gill rakers of *Sardinops sagax* and *Engraulis mordax*, the sardine/anchovy pair inhabiting the California Current Ecosystem (CCE). Differences in gill-raker morphology between these species are similar to those between the sardine and anchovy of the BCE; the inter-raker spacing in juvenile anchovy is about 140% that of juvenile sardine, and this difference continues to increase with growth in each species, reaching 200% when the fishes are 150 mm in standard length. These observations support the hypothesis that sardine and anchovy of the CCE are adapted to consume prey in different portions of the plankton size spectrum. Retention of prey items by gill rakers appears to occur at a Reynolds number greater than 1. However, the small denticles which extend from the sides of each gill raker operate at a

Reynolds number less than 1 and may augment capture of larger plankters by the gill rakers through retention of particles smaller than the inter-raker spacing in both sardine and anchovy.

2.2. Introduction

Sardine (*Sardinops* spp. and *Sardina* spp.) and anchovy (*Engraulis* spp.) inhabit major eastern boundary currents of the ocean's subtropical gyres. These species support valuable commercial fisheries and are ecologically important as consumers of biological production and as forage for mammals, birds, and piscivorous fishes. Populations of sardine and anchovy display prominent variability on a multi-decadal scale, with the biomass of one species often alternating with that of the other (Schwartzlose *et al.* 1999). Current hypotheses explaining the differing responses of each taxon to environmental changes are related to the distinct size classes of zooplankters and phytoplankters on which they feed (Alheit and Niquen 2004, Rykaczewski and Checkley 2008, van der Lingen *et al.* in press). Studies of diet and feeding behavior have revealed that anchovy (*Engraulis encrasicolus* and *Engraulis mordax* of the Benguela and California Currents, respectively) selectively feed on the largest plankters available (Koslow 1981, Louw *et al.* 1998). In contrast, Pacific sardine (*Sardinops sagax*) is thought to be a generalist predator, capable of feeding more efficiently on smaller zooplankters and phytoplankters than anchovy. This division of a common resource (*i.e.*, planktonic prey) between co-occurring species is known as resource partitioning (Ross 1986).

The concept of resource partitioning between sardine and anchovy arises from two lines of evidence: 1) morphological differences in the structure of the branchial apparatus, specifically the distances between adjacent gill rakers (referred to as the inter-raker spacing), which determine the minimum prey sizes efficiently retained during filter feeding (King and MacLeod 1976); and 2) differences in feeding behavior and bioenergetics (van der Lingen *et al.* in press). Here, I aim to address this first line of evidence by examining the morphology of the branchial apparatus for the sardine and anchovy species inhabiting the CCE.

The gill rakers of clupeid fishes have evolved to efficiently capture planktonic prey, analogous to the baleen plates of mysticete whales, and are long and numerous in comparison to other fish taxa. Gill rakers extend anteriorly from the upper- and lower-gill arches, opposite the gill filaments used in gas exchange (Figure 2.1). Gill rakers develop early in the life history of sardine and anchovy and become functional after metamorphosis from the larval to the juvenile stage (Schumann 1963, Schmitt 1986). With the opening of the mouth during filter feeding, the gill rakers are extended distally from the gill arches (Figure 2.2) and form a structural barrier which acts as a sieve through which water must pass before exiting the oral cavity. Filtration of plankton by this branchial sieve is considered to be the primary means of prey capture during filter feeding (Lazzaro 1987).

Direct comparison between the gill rakers of sardine and anchovy has been limited to *S. sagax* and *E. encrasicolus* of the BCE. King and MacLeod (1976) estimated inter-raker spacing by dividing the length of the gill arch by the number and mean thickness of individual rakers, concluding that the inter-raker spacing of juvenile

and adult anchovy is greater than that of sardine. The hypothesis that sardine is more efficient in retaining small prey items than anchovy has also been supported by dietary comparisons (King and MacLeod 1976, Louw *et al.* 1998). In addition to noting differences in the inter-raker spacing, King and MacLeod (1976) described species differences in the morphology of denticles (or “branchiospinules”), the small protrusions located along the sides of the gill rakers. The denticles of anchovy are described as simple, spine-like projections located randomly along the gill rakers. Sardine denticles are evenly distributed along the rakers and are more robust and elaborate in structure, possessing a specialized nodule at the tip of each denticle. The function of these specialized tips remains unknown, though they are thought to aid in retention of small particles (Scofield 1934).

Morphology of the branchial sieve is variable among fish species, even among congeners. Gill-raker counts are often used to differentiate between closely related species and subpopulations (McHugh 1951), and the morphological differences between the gill rakers of *E. encrasicolus* and *S. sagax* of the BCE do not necessitate similar differences between *E. mordax* and *S. sagax* of the CCE. James and Chiappa-Carrara (1990) compared the length of the gill arch and the number of gill rakers between *E. mordax* and *E. encrasicolus*. The authors found minor differences in the number of gill rakers present along the first gill arch of these two anchovy species but concluded that these differences in morphology did not influence the ability of each species to capture and retain prey. However, differences in the inter-raker spacing were not measured directly.

Comparison between the branchial sieves of sardine and anchovy of the CCE is prudent before further consideration of resource partitioning between these species. Here, I compare the inter-raker spacing between *S. sagax* and *E. mordax* collected in the CCE. I consider the implications of these morphological differences given observations of swimming speed during feeding.

2.3. Methods

Fish were obtained from the commercial fishery in San Diego, CA and were captured by purse seine near La Jolla Canyon during fall 2006 and 2007. All individuals were frozen and stored at -11°C . Approximately 30 fish from each species were analyzed. The standard lengths of individuals were measured to the nearest millimeter. Sardine ranged in size from 74 to 165 mm in standard length, corresponding to juvenile and 1-year-old fish (Butler *et al.* 1996). Anchovy ranged in size from 73 to 150 mm in standard length, corresponding to juvenile through 3- or 4-year-old fish (Mallicoate and Parrish 1981). An attempt was made to sample fish of various sizes, but the size structure of the population at time of sampling prevented collection of sardine between 120 and 140 mm in standard length.

Fish were thawed at room temperature, and the complete branchial sieve was removed by dissection. The first gill arch was separated from the branchial sieve and examined with light microscopy. The number of gill rakers and length of the gill arches (upper and lower) were measured for each individual to the nearest $15\ \mu\text{m}$ at 60x magnification. Gill rakers were photographed with a digital camera mounted to a light microscope at 250x to 500x magnification, and a computer micrometer was used

to measure the raker widths and inter-raker spacing. At least 30 measurements were taken from upper and lower gill arches to the nearest micrometer. Rakers were oriented perpendicular to the gill arch during measurement, and measurements were taken near the midpoint of each raker. In addition, individual gill rakers were removed from the gill arch, and the anatomy of the denticles located along the dorsal and ventral sides of the gill rakers was examined. The methods applied here only permit discussion of denticle morphology in a qualitative manner.

2.4. Results

There were significant differences between the inter-raker spacing of *S. sagax* and *E. mordax* over the size range of fish examined, and these differences increased with the standard body lengths of the fish. Differences in inter-raker spacing are apparent with gross comparison (Figure 2.2) as well as with microscopic examination (Figure 2.3). The measurements of inter-raker spacing are displayed in Figure 2.4. There was no significant difference between the inter-raker spacing of anchovy species of the CCE (analyzed here) and BCE (as analyzed by King and MacLeod, 1976; Table 2.1). Comparison of the inter-raker spacing of sardine between the two upwelling systems did show a minor, but significant difference; estimates of inter-raker spacing for sardine of the CCE were consistently smaller than those of sardine of the BCE ($p < 0.05$). The trend in inter-raker spacing with fish length was the same between the two regions (Table 2.2). The slight difference in inter-raker spacing of sardine between the two regions is likely due to differences in methodology, as King and MacLeod (1976) did not measure inter-raker spacing directly.

The spacing between the gill rakers of sardine increased from about 190 μm in a fish 80 mm in length to 280 μm in a 160-mm fish. The increase in inter-raker spacing with individual length was greater in anchovy, increasing from 270 μm in an 80-mm fish to 470 μm in a 140-mm fish (Figure 2.4a). As noted by King and MacLeod (1976) for species of the HCE, the increased difference in inter-raker spacing with standard body length is attributed to the length of the gill arch in relation to the number of gill rakers. The length of the gill arch is proportional to fish length in both sardine and anchovy (Figure 2.4b), but the number of rakers along the first gill arch remains relatively constant with length in anchovy (79 rakers, ± 2 s.d.), while sardine continue to add gill rakers to the arch as length of the gill arch increases (increasing from about 74 to 140 rakers as fish length increased from 80 to 165 mm; Fig 4c). The width of each raker increased with increased sardine length, widening from 23 to 38 μm over the size range examined. The gill rakers of anchovy, in contrast, became narrower with increased fish length, decreasing from about 140 to 115 μm for fish ranging in size from 80 to 140 mm (Figure 2.4d).

Observation of the denticles of *E. mordax* and *S. sagax* of the CCE are similar to those described by King and MacLeod (1976) for *E. encrasicolus* and *S. sagax* of the BCE, though some qualitative differences are worth noting. King and MacLeod (1976) described the denticles of *E. encrasicolus* as a random distribution of spines along the sides of each raker. Although the arrangement of denticles in *E. mordax* of the CCE appears random when viewed from the dorsal or ventral perspective (Figure 2.5a), the anterior view shows rows of denticles arranged regularly along each raker (Figure 2.3a). There are multiple rows of denticles along the side of each gill raker,

with the longest denticles aligned closest to the posterior edge of the gill raker and additional rows of smaller denticles located closer to the anterior edge of the raker (Figure 2.5a).

In sardine, a single row of denticles is located along the sides of each gill raker (Figure 2.5b). Sardine denticles are laterally compressed, triangular flaps of tissue attached at their base along the medial axis of each gill raker, and the anterior tip of each denticle is modified into a hexagonally shaped, plate-like nodule. The function of these modified denticles remains unknown. Scofield (1934) was the first to describe the denticles in Pacific sardine of the CCE and suggested that the nodules located at the end of each denticle aid in the retention of small prey items. I further speculate on their function below.

2.5. Discussion

The differences observed between inter-raker spacing of *E. mordax* and *S. sagax* of the CCE are similar to those described for *E. encrasicolus* and *S. sagax* of the HCE. The spacing between the gill rakers is significantly greater in sardine than in anchovy. Before concluding that the finer branchial sieve of sardine might confer an advantage for retention of small plankters, it is informative to briefly consider the Reynolds number (Re , non-dimensional) involved during filter feeding:

$$Re = \frac{ul}{\nu},$$

where u is the velocity of the fluid at the point of filtration, l is the diameter of the filtering fiber (*i.e.* the gill raker or denticle), and ν is the kinematic viscosity. If

viscous forces dominate the filter feeding process ($Re < 1$), the analogy between gill rakers and a mechanical sieve is inappropriate, and alternate methods of prey capture should be considered (Rubenstein and Koehl 1977). A larger Re suggests that simple filtration by gill rakers is a possible mechanism of particle retention.

The gill rakers of sardine have widths ranging from 23 to 38 μm , and van der Lingen (1994) observed a minimum swimming speed of 1.5 body lengths s^{-1} during active filter feeding. It is problematic to estimate the water velocity between the gill rakers as water exits the oral cavity, but we can estimate the minimum Re for a water velocity 60% of the swimming speed (Cheer *et al.* 2001), an approximation of the water velocity observed in the vicinity of the gill rakers during filter feeding for a different fish species. Given a kinematic viscosity of $10^{-6} \text{ m}^2 \text{ s}^{-1}$ and a water velocity of 0.07 m s^{-1} (corresponding to a swimming speed of 113 mm s^{-1}), the minimum Re is estimated at about 2. If the maximum swimming speed (2.5 body lengths s^{-1}) and body length examined here (160 mm) are considered, Re equals 9. A similar calculation can be performed for anchovy. Given raker widths ranging from 130 μm to 110 μm and swimming speeds from 0.07 to 0.2 m s^{-1} , Re ranges from 9 to 25. These Re values are consistent with the perception that gill rakers act as a sieve, and the spacing between adjacent gill rakers may influence the minimum size of prey that can be efficiently retained.

A difference in inter-raker spacing of 100 to 200 μm is minor in comparison to the wide range of plankter sizes; copepods alone range in length from tens of micrometers to more than 6 mm in the CCE (Hopcroft *et al.* 2001). Maximum width is probably the more critical dimension when considering retention by a mesh or sieve.

If we assume a width:length ratio of 0.25 for copepods, then a difference in inter-raker spacing of 100 μm represents less than 7% of the total range of copepod widths.

However, it is important to note that the fractions of plankton biomass in evenly spaced size categories declines logarithmically with linear increases in size (Sheldon *et al.* 1972). A fish species capable of efficiently retaining prey 100 to 200 μm smaller than another species (*e.g.*, sardine and anchovy, respectively) may have a considerable advantage in environments where ingestion of food limits growth and reproduction.

Although the morphology of the denticles was not analyzed quantitatively for individuals of various sizes, the observations made are worthy of discussion. In both sardine and anchovy, the minimum widths of these projections are less than 10 μm , and the associated Re 's are less than 1 at most swimming speeds. This suggests that prey items smaller in diameter than the spacing of the gill rakers may be retained with some efficiency, possibly explaining previous observations of these prey items in the stomachs of both species (Lewis 1929, Loukashkin 1970). Van der Lingen (1994) examined the retention efficiency during filter feeding for sardine about 230 mm in standard length (larger than the individuals examined here). The smallest particles considered (phytoplankter cells of about 14 μm maximal length) were retained with about 8% efficiency, and retention rates increased linearly for larger particles and reached a maximum of 93% for lengths greater than about 400 μm . Were simple sieving the sole method of prey retention, prey items greater than the inter-raker spacing would be retained with near 100% efficiency, and smaller particles would not be retained. The observations of that retention decreases linearly for particles smaller

than the inter-raker spacing opposes the idea that simple sieving the sole method of prey retention and suggests that processes at low Re may be important for the retention of these small particles. For example, the efficiency of retention by direct inception of particles by the denticles is expected to increase linearly with increasing in the particle diameter (Rubenstein and Koehl 1977).

Given the presence of denticles in both taxa, it is valid to question whether these structures obviate the differences between inter-raker spacing in sardine and anchovy. The simple, spine-like denticles of anchovy are flexible at their narrow base (Figure 2.5) and do not form a structure as rigid as gill rakers. The ability of these simple denticles to retain relatively large copepods and other large prey items is therefore questionable and deserves further investigation. The utility of the larger, modified denticles of sardine has not been addressed in the literature, but the qualitative observations of morphology permit speculation about the function of these structures. When viewed under the light microscope in laboratory conditions, these denticles lie nearly flat against the gill rakers (as in Figure 2.5b). However, simple manipulations under the microscope revealed that the denticles are flexible at their broad base where they join the gill raker, and water pressure (as during active filtration) forces the denticles to spread away from the sides of the gill raker and form a plane nearly orthogonal to that of the rakers. The distance between adjacent rakers may be bridged by the flexing of the denticles during filtration, and the denticles along adjacent rakers may either interlock or overlap in the space between the rakers. Interlocking denticles would substantially reduce the effective inter-raker spacing (Figure 2.6a). Overlapping of the plate-like nodules at the tips of the denticles would

prevent the flux of elongated particles through the branchial sieve, retaining plankters based on two morphological dimensions (*i.e.*, length and width) as opposed to one dimension (Figure 2.6b). The simple spine-like denticles of anchovy do not appear to confer the same advantage. Anchovy denticles do spread away from the gill raker under water pressure, but they are thin, cylindrical, and lack the laterally compressed shape necessary to form a plane orthogonal to that of the gill rakers.

2.6. Conclusions

The morphology of the gill rakers in *S. sagax* and *E. mordax* support the hypothesis that resource partitioning may act to distinguish prey fields in the CCE. The inter-raker spacing of anchovy is about 140% that of sardine for juveniles 80 mm in standard length, and the differences in the inter-raker spacing between the two species increases with growth of the fish. For fish of standard lengths of 150 mm, the inter-raker spacing of anchovy is about 200% that of sardine. The gill rakers of anchovy lack the modified denticles found along the gill rakers of sardine. These differences in functional morphology of the branchial sieve may offer sardine a competitive advantage over anchovy for the efficient retention of small plankters. These results support the hypothesis of resource partitioning among the two prominent planktivorous fishes of the CCE.

Table 2.1. ANCOVA table comparing changes in inter-raker spacing with size between anchovy of the BCE and CCE.

Source	d.f.	sum of squares	mean squares	F-value	p-value
location	1	660	660	1.96	0.168
standard length	1	$2.55 \cdot 10^5$	$2.55 \cdot 10^5$	755	0
interaction	1	163	163.268	0.484	0.490
error	52	$1.75 \cdot 10^4$	337.4269		

Table 2.2. ANCOVA table comparing changes in inter-raker spacing with size between sardine of the BCE and CCE.

Source	d.f.	sum of squares	mean squares	F-value	p-value
location	1	$2.41 \cdot 10^4$	$2.41 \cdot 10^4$	26.5	$1 \cdot 10^{-5}$
standard length	1	$3.30 \cdot 10^4$	$3.30 \cdot 10^4$	364	0
interaction	1	14.4	14.4	0.16	0.690
error	36	3270	90.8		

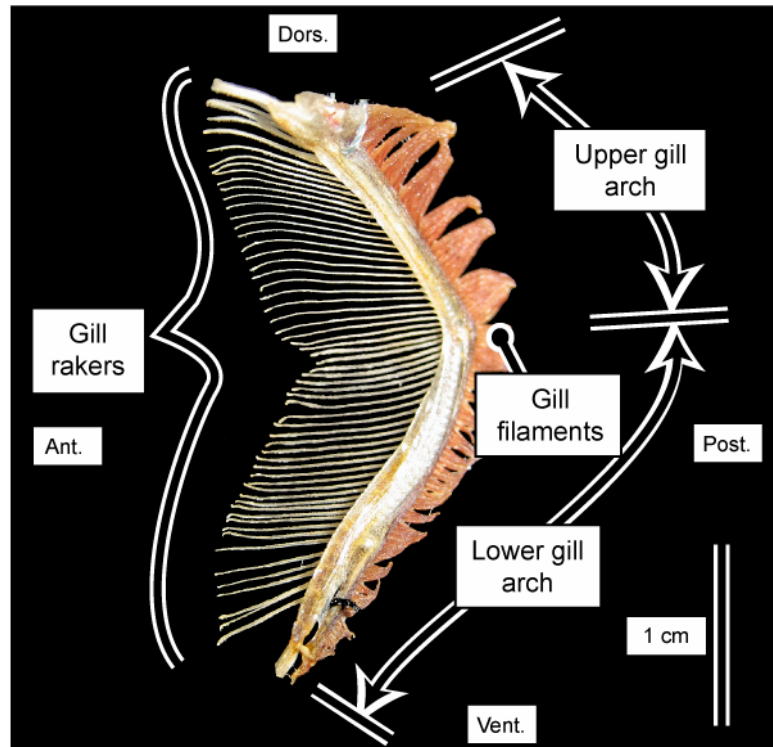


Figure 2.1. Gill arch of northern anchovy, *Engraulis mordax*. The gill rakers are used for retaining plankton that have entered the mouth before exiting the oral cavity. Each arch is composed of an upper and lower section. This particular example is the first gill arch from the right side of an anchovy 124 mm in standard length. Orientation is noted: anterior (ant.), posterior (post.), dorsal (dors.), and ventral (vent.).

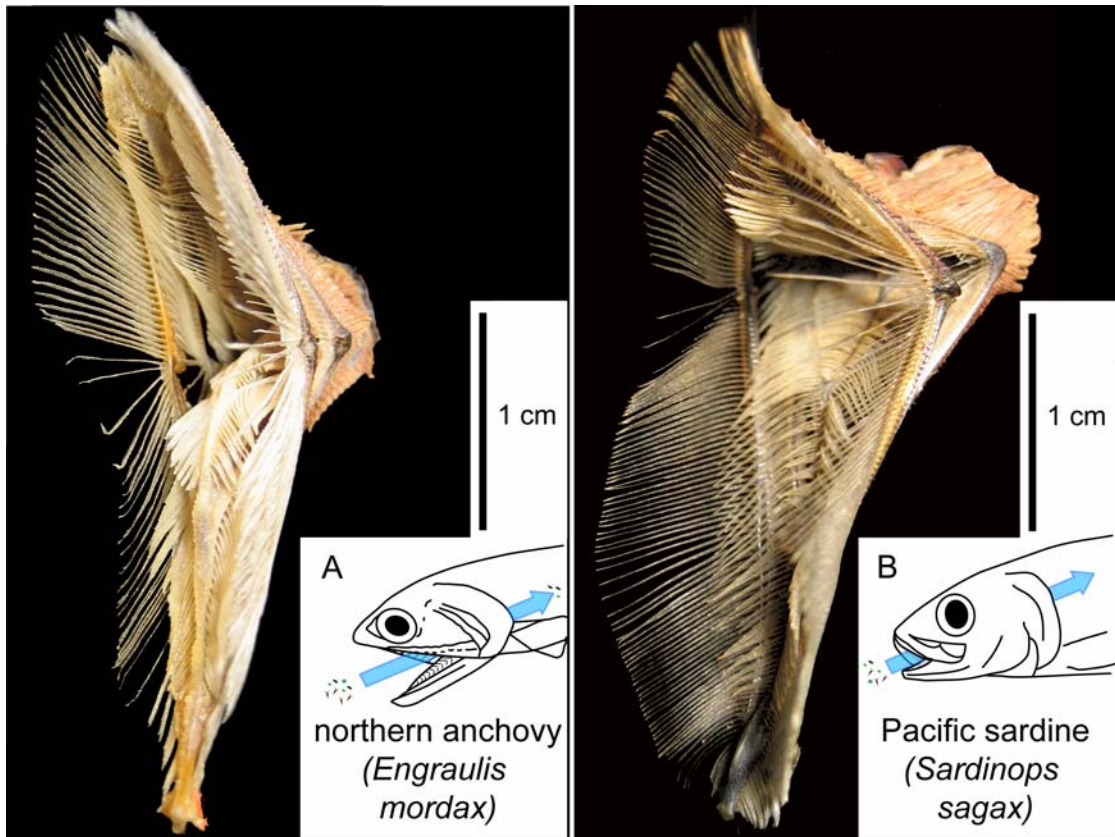


Figure 2.2. Anterolateral view of the branchial sieves of sardine and anchovy of the CCE. The gill filaments have been removed for clarity. The inset is intended to approximate the orientation of each fish, and arrows display the flow of water and plankton through the branchial sieve. In these examples, the standard length of anchovy (A) was 150 mm, and the standard length of sardine was 155 mm (B). A section of the lower gill rakers on the first gill arch are further magnified in Figure 2.3.

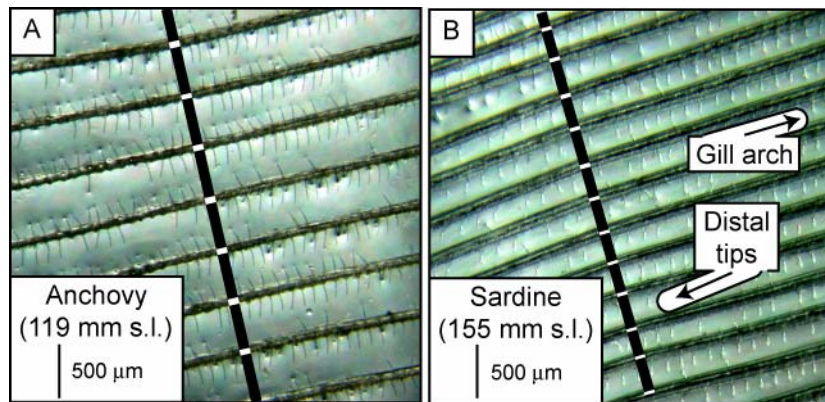


Figure 2.3. Magnified examples of anchovy (A) and sardine (B) gill rakers. Black bars denote inter-raker distances, and white bars indicate raker widths. Denticles are regularly spaced along the gill rakers of both species. Note that the sardine rakers in B lie laterally to show the denticles along one side of the rakers, and this lateral view of the rakers does not correspond to the raker width indicated by the white bars. A magnified portion of a single gill raker from each species is displayed in Figure 2.5.

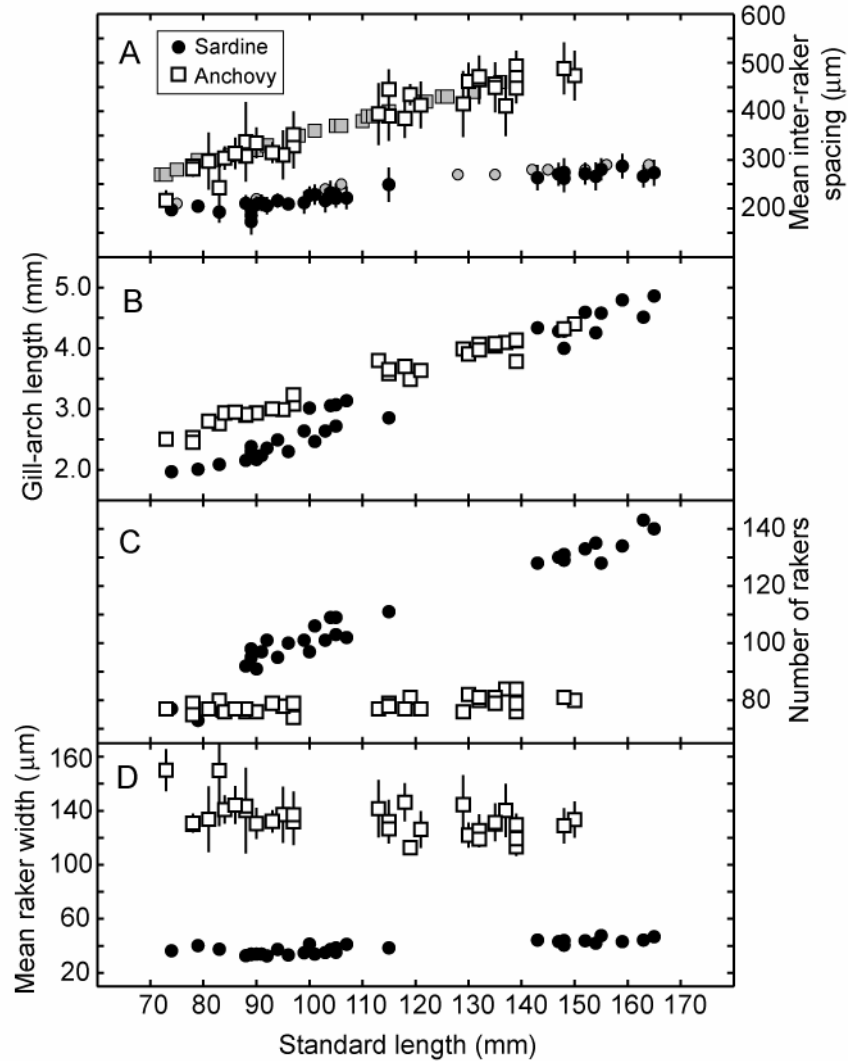


Figure 2.4. Comparison of measures describing the branchial sieves of sardine and anchovy species. A) Black and white symbols represent measurements for species of the CCE, and the solid gray symbols are measurements presented for species of the BCE by King and MacLeod (1976). B) The total length of the first gill arch was taken as the sum of upper- and lower-arch lengths. C) The total number of rakers on the gill arch of sardine continues to increase with fish length over the fish sizes examined, while the number of raker remains fairly constant in anchovy. D) The width of the rakers vary little with fish length. Lines in A and D denote ± 1 standard deviation.

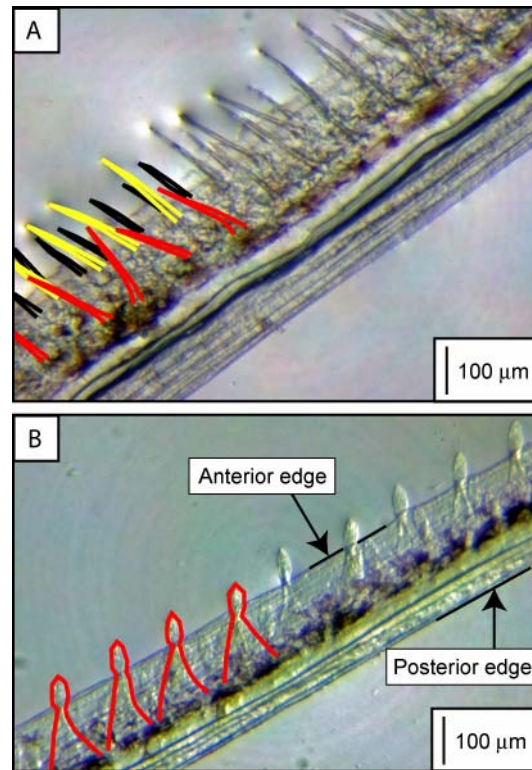


Figure 2.5. Dorsal view of a single gill raker of anchovy and sardine, highlighting the differences in denticle structure. The anterior edge of each raker is presented to the water and plankton exiting the oral cavity through the branchial sieve. This dorsal view shows the denticles along one side of the gill raker. Denticles along the opposite side are similar. For each microscope image, half of the denticles have been outlined in bold. A) The denticles of anchovy are thin, spine-like projections. Denticles in *E. mordax* were evenly spaced and present in three rows, highlighted here in red, yellow, and black. B) The denticles of sardine appear in a single row, are laterally compressed and triangular in shape. A hexagonal, plate-like structure is present at the tip of each denticle.

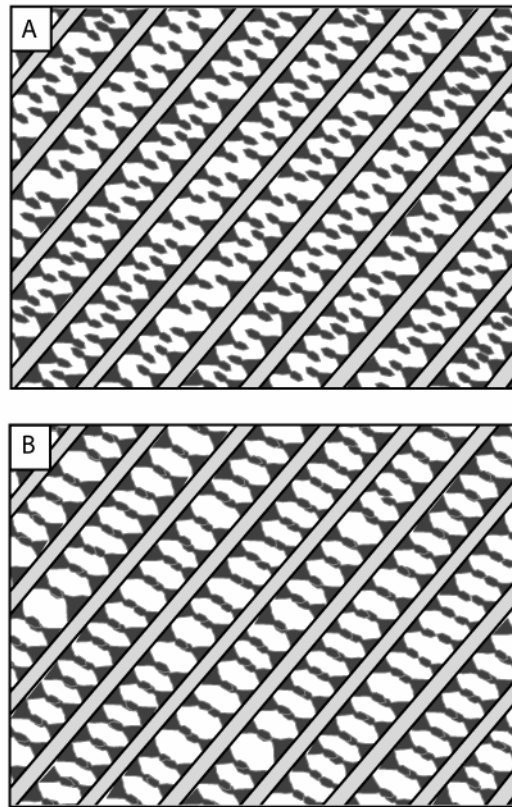


Figure 2.6. Conceptual diagram displaying the possible configurations of sardine denticles during filtering. A) Denticles may either interlock during filtering, reducing the inter-raking spacing, or B) overlap, forming a mesh structure. Here, gill rakers are shown in light gray; denticles are shown in dark gray.

2.7. References

- Alheit, J. and Niquen, M. (2004) Regime shifts in the Humboldt Current Ecosystem. *Prog. Oceanogr.* **60**:201-222.
- Butler, J.L., Granados, M.L., Barnes, J.T., Yaremko, M. and Macewicz, B.J. (1996) Age composition, growth, and maturation of the Pacific sardine (*Sardinops sagax*) during 1994. *CalCOFI Rep.* **37**:152-159.
- Cheer, A.Y., Ogami, Y. and Sanderson, S.L. (2001) Computational fluid dynamics in the oral cavity of ram suspension-feeding fishes. *J. Theor. Biol.* **210**:463-474.
- Hopcroft, R.R., Roff, J.C. and Chavez, F.P. (2001) Size paradigms in copepod communities: a re-examination. *Hydrobiologia* **453**:133-141.
- James, A.G. and Chiappa-Carrara, X. (1990) A comparison of field based studies on the trophic ecology of *Engraulis capensis* and *E. mordax*. In: *Trophic Relationships in the Marine Environment: Proceedings of the 24th European Marine Biology Symposium*. M. Barnes, R.N. Gibson (eds.) Aberdeen: Aberdeen University Press, pp. 208-221.
- King, D.P.F. and MacLeod, P.R. (1976) Comparison of the food and the filtering mechanism of pilchard *Sardinops ocellata* and anchovy *Engraulis capensis* off South West Africa, 1971-1972. *Invest. Rep. Sea. Fish. Brch. S. Afr.* **111**:1-29.
- Koslow, J.A. (1981) Feeding selectivity of schools of northern anchovy, *Engraulis mordax*, in the Southern California Bight. *Fish. Bull.* **79**:131-142.
- Lazzaro, X. (1987) A review of planktivorous fishes - their evolution, feeding behaviors, selectivities, and impacts. *Hydrobiologia* **146**:97-167.
- Lewis, R.C. (1929) The food habits of the California sardine in relation to the seasonal distribution of microplankton. *Bull. Scripps Inst. Oceanogr. Univ. Calif. Tech. Ser.* **2**:155-180.
- Loukashkin, A.S. (1970) On the diet and feeding behavior of the northern anchovy, *Engraulis mordax* (Girard). *Proc. Calif. Acad. Sci.* **37**:419-458.
- Louw, G.G., van der Lingen, C.D. and Gibbons, M.J. (1998) Differential feeding by sardine *Sardinops sagax* and anchovy *Engraulis capensis* recruits in mixed shoals. *S. Afr. J. Mar. Sci.* **19**:227-232.
- Mallicoate, D.L. and Parrish, R.H. (1981) Seasonal growth of California stocks of northern anchovy, *Engraulis mordax*, Pacific mackerel, *Scomber Japonicus*, and jack mackerel, *Trachurus symmetricus*. *CalCOFI Rep.* **22**:69-81.

- McHugh, J.L. (1951) Meristic variations and populations of northern anchovy, *Engraulis mordax mordax*. *Bull. Scripps Inst. Oceanogr.* **6**:123-160.
- Ross, S.T. (1986) Resource partitioning in fish assemblages - a review of field studies. *Copeia* **2**:352-388.
- Rubenstein, D.I. and Koehl, M.A.R. (1977) Mechanisms of filter feeding: some theoretical considerations. *Am. Nat.* **111**:981-994.
- Rykaczewski, R.R. and Checkley, D.M. (2008) Influence of ocean winds on the pelagic ecosystem in upwelling regions. *Proc. Natl. Acad. Sci. U. S. A.* **105**:1965-1970.
- Schmitt, P. (1986) Prey size selectivity and feeding rate of larvae of the northern anchovy, *Engraulis mordax* Girard. *CalCOFI Rep.* **27**:153-161.
- Schumann, G.O. (1963) Some aspects of behavior in clupeid larvae. *CalCOFI Rep.* **10**:71-78.
- Schwartzlose, R.A., Alheit, J., Bakun, A., Baumgartner, T.R., Cloete, R., Crawford, R.J.M., Fletcher, W.J., Green-Ruiz, Y., Hagen, E., Kawasaki, T., Lluch-Belda, D., Lluch-Cota, S.E., MacCall, A.D., Matsuura, Y., Nevarez-Martinez, M.O., Parrish, R.H., Roy, C., Serra, R., Shust, K.V., Ward, M.N. and Zuzunaga, J.Z. (1999) Worldwide large-scale fluctuations of sardine and anchovy populations. *S. Afr. J. Mar. Sci.* **21**:289-347.
- Scofield, E.C. (1934) Early life history of the California sardine (*Sardina caerulea*), with special reference to distribution of eggs and larvae. *Fish Bull. Div. Fish Game Cal. Bureau Commercial Fish.* **41**:1-48.
- Sheldon, R.W., Sutcliff, W. and Prakash, A. (1972) The size distribution of particles in the ocean. *Limnol. Oceanogr.* **17**:327-340.
- van der Lingen, C.D. (1994) Effect of particle size and concentration on the feeding behavior of adult pilchard *Sardinops sagax*. *Mar. Ecol. Prog. Ser.* **109**:1-13.
- van der Lingen, C.D., Bertrand, A., Bode, A., Brodeur, R., Cubillos, L.A., Espinoza, P., Friedland, K., Garrido, S., Irigoien, X., Miller, T., Möllmann, C., Rodriguez-Sanchez, R., Tanaka, H. and Temming, A. (in press) Trophic dynamics. In: *Climate Change and Small Pelagic Fish*. D.M. Checkley, Jr., J. Alheit, Y. Oozeki, C. Roy (eds.) Cambridge: Cambridge University Press.

Chapter 3. Changes in mesozooplankton size structure along a trophic gradient and implications for small pelagic fish

3.1. Abstract

Zooplankton sizes and concentrations are hypothesized to be key determinants of growth and behavior of individual sardine and anchovy, yet the factors affecting size structure in mesozooplankton communities are poorly understood.

Mesozooplankton sizes and concentrations were measured for samples collected across a trophic gradient in the California Current Ecosystem with coincident measures of phytoplankton size structures and ecosystem conditions. There was a clear distinction between mesozooplankton sizes in samples collected from oligotrophic and eutrophic communities, with the relative abundance of large individuals being greater in areas where upwelling conditions enhanced nutrient availability and increased abundance of large phytoplankters. The relative contributions of small zooplankters were greater in oligotrophic waters. These changes in the size structure of the zooplankton community are the result of variability in copepod sizes rather than changes in gross taxonomic composition. In light of the observed variability in the biomasses and size structures of phytoplankton and zooplankton communities, the potential growth rates of sardine and anchovy are estimated using previously established models of ingestion, absorption, excretion, and respiration. These bioenergetic models suggest that the potential for growth of anchovy is dependent on the community structure of nearshore, eutrophic waters where large zooplankters are abundant. Growth of anchovy is unlikely in offshore, oligotrophic waters. In contrast, growth of sardine is

possible under more oligotrophic conditions and influenced by oceanographic conditions in the offshore region of the ecosystem.

3.2. Introduction

Concentration and size structure of the zooplankton community are believed to be the main factors influencing individual growth and feeding behavior of mature sardine and anchovy (van der Lingen *et al.* in press). Juvenile and adults of both species are omnivorous planktivores capable of two modes of prey capture: non-selective filter feeding and particulate feeding (active biting of individual prey items). Leong and O'Connell (1972) and James and Findlay (1989) examined the factors influencing feeding mode and rates of prey ingestion for anchovy from two upwelling systems, finding that northern anchovy (*Engraulis mordax*) from the California Current and cape anchovy (*Engraulis encrasicolus*) of the Benguela Current employ particulate feeding when large zooplankters compose a significant portion of the zooplankton community. Filter feeding is utilized only as the concentration of large prey items declines. Closer investigation of the prey consumption and bioenergetic expenditure of anchovy demonstrated that filter feeding is an inefficient mode of prey capture, and exclusive filtering is unlikely to provide the level of nutrition necessary to meet daily requirements (O'Connell 1972, James *et al.* 1989). Observations of prey consumption in the field substantiate these laboratory findings; Koslow (1981) and Louw *et al.* (1998) observed that anchovy actively select the largest plankters available in the environment.

Examinations of sardine (*Sardinops sagax*) feeding behavior and prey consumption show that individual growth is also subject to limitations related to prey size and concentration. However, the fine-mesh branchial sieve of sardine is capable of capturing much finer planktonic prey than *E. encrasicolus* and *E. mordax* (van der Lingen 1994). In comparison to anchovy, sardine filter feed over a greater portion of the plankton size spectrum and are capable of retaining prey items smaller than 20 μm . Selection of individual prey items by particulate feeding is energetically inefficient in comparison to filter feeding (van der Lingen *et al.* in press). When presented with similar prey communities in the natural environment, items consumed by sardine are distinctly smaller than those consumed by anchovy (Louw *et al.* 1998). An understanding of how the biomass size spectra of phytoplankton and zooplankton communities vary with respect to environmental conditions may elucidate the factors influencing production and growth of sardine and anchovy populations.

The relationship between the size structure of marine phytoplankton communities and resource availability is well documented. The relative contribution of small phytoplankters decreases as total chlorophyll *a* increases. Oligotrophic communities are dominated by small cells, and the proportion of large cells increases with increasing availability of nutrients (Chisholm 1992). Allometric relationships governing rates of nutrient uptake, cell respiration, and the response of zooplankton grazing pressure are often cited as the underlying ecological processes responsible for the relationship between community size spectra and nutrient concentrations. Small cells have a large surface-area-to-volume ratio, conferring a competitive advantage over large cells in regard to nutrient-uptake rate (Morel *et al.* 1991). In eutrophic

environments where nutrient constraints are reduced, populations of large cells flourish while smaller phytoplankters are restricted by size-dependent microzooplankton grazing (Riegman *et al.* 1993). An alternate hypothesis suggests that upward vertical velocity in the water column, independent of nutrient supply, may result in an increased contribution of large cells to the phytoplankton community by decreasing the net sinking rate of large cells from the euphotic zone. The sinking rates of small phytoplankters, which experience relatively low-Reynolds-number environments where viscous forces dominate, are not influenced by differences in vertical motion (Rodriguez *et al.* 2001).

In contrast, factors influencing the size structure of the mesozooplankton prey relevant for sardine and anchovy remain unclear. Many previous investigations of zooplankton size structure in the marine environment have emphasized changes over the complete size spectrum (ranging from bacteria to metazoa) and commonly attribute the shape of the biomass spectrum to allometric scaling of physiological rates, predator-prey interactions, and the efficiency of energy transfers among trophic levels within the ecosystem (Zhou and Huntley 1997). These studies provide insight into the characteristics of the ecosystem as a whole but provide little understanding of the structure and function of the particular biological communities of direct importance to planktivorous fish. Few studies have examined size structure specifically within the mesozooplankton, and these previous investigations have focused on changes over large latitudinal gradients rather than on changes within an ecosystem (Hopcroft *et al.* 2001, San Martin *et al.* 2006).

In addition to controlling the transfer of nutrients and organic matter to higher predators, the size structure of mesozooplankton communities is an important factor influencing carbon export and nutrient regeneration. Vertical particle flux attributed to the fecal pellets of mesozooplankters and macrozooplankters contributes to the export of organic carbon, while the high metabolic rates of small zooplankters promote rapid nutrient regeneration. Understanding of mesozooplankton size structure is important in partitioning production between microbial recycling and export to higher trophic levels (Legendre and Michaud 1998) and is a key component of ecosystem and biogeochemical models (Moloney and Field 1991, Buitenhuis *et al.* 2006).

How might we expect zooplankter sizes to vary across a trophic gradient? There is abundant evidence to suggest that large zooplankters are inefficient at utilizing small phytoplankters as prey, and there is an optimal predator:prey ratio which maximizes the transfer of energy and organic matter from phytoplankton to zooplankton in pelagic ecosystems (Frost 1974, Moloney and Field 1991, Hansen *et al.* 1994). Hence, a decrease in zooplankter sizes with decreases in phytoplankter sizes and nutrient supply is expected. Here, I posed the question: How does the size spectrum of the mesozooplankton vary with changes in the sizes of their phytoplanktonic prey in the marine environment? I address this question by examining biomass spectra of phytoplankton and mesozooplankton communities in relation to the nutrient content and physical conditions for samples collected across a trophic gradient in the California Current Ecosystem (CCE). The implications of

changes in plankton sizes for the nutritional budgets of sardine and northern anchovy are considered in the context of previously established bioenergetic models.

3.3. Methods

3.3.1. Process cruises

Ecosystem structure was investigated in the southern region of the CCE during two research cruises (May 2005 and June 2006) as part of the CCE Long-Term Ecological Research Program. Water masses of differing characteristics were tracked with a subsurface drogue over several days while intensively sampling chemical, physical, and biological properties at a diel frequency. This 4-5 day sampling “cycle” was successfully repeated eight times during the two cruises in regions ranging from the eutrophic coastal zone to the oligotrophic region offshore (Figure 3.1). Cycle locations were selected along a transect line approximately normal to the coast. One of these experimental cycles was conducted in shallow water ranging from 68 to 200 m, and data from this cycle were excluded from further analysis as the methods applied were not uniform with those at other locations.

Zooplankton were collected with a 0.71-m diameter paired BONGO net with 202- μ m Nitex mesh towed obliquely to 210 m between 2100 and 0400 hours (local time). I focused on nighttime samples so that diel changes in zooplankton abundance would not confound possible differences in size structure. The volume of water filtered was estimated using calibrated flowmeters in the mouth of each net. Zooplankton from one of the paired nets were preserved in sodium-borate buffered formaldehyde for microscopic analysis. A portion of the zooplankton from the other

paired net was split into size fractions using nested Nitex filters of decreasing mesh size, and zooplankton concentrations in these five size categories were measured by dry-weight analysis (Rykaczewski and Checkley 2008).

Water column properties were measured using a CTD/rosette cast between 0100 and 0240 each morning. Water samples for macronutrient content were collected from at least eight depths above the thermocline and stored at -20°C , and concentrations of nitrate were determined calorimetrically by an automated analyzer (Marine Science Institute, Santa Barbara, California). The nutricline location was determined by locating the largest gradient in nitrate concentration with depth. Water samples for analysis of phytoplankton size spectra were collected from the mixed layer and filtered onto six filters of differing pore size (256 ml each onto a $0.7\ \mu\text{m}$ glass-fiber filter and nested 1-, 3-, 8-, and $20\text{-}\mu\text{m}$ polycarbonate filters) and repeated in triplicate fashion. Chlorophyll was extracted from the each filter overnight while immersed in 7 ml of 90% acetone at -2°C and analyzed for chlorophyll *a* concentration using a Turner Designs fluorometer (Goericke, pers. comm.).

Wind stress and upwelling rate resulting from wind-stress curl (*i.e.*, Ekman pumping) at each sampling location were calculated using a wind product generated from a blending of wind stress measured by a satellite scatterometer and a mesoscale atmospheric model (Chao *et al.* 2003). Use of the blended model allowed estimation of wind speed and upwelling rate at locations inshore of 50 km where satellite scatterometer measurements are unreliable. Curl-driven upwelling rate was estimated at the base of the mixed layer (Smith 1968) and averaged over seven days prior to

zooplankton sampling. Wind-stress magnitude was similarly averaged over the seven days prior to sampling.

3.3.2. Zooplankton Sample Preparation and Enumeration

A fraction of each zooplankton sample was optically imaged using the Zooscan system (Grosjean *et al.* 2004). Prior to scanning, the preserved samples were split into two coarse size fractions using a 1-mm sieve. Two sets of Zooscan images were created for each zooplankton sample; one set for each of the size fractions. Separating the sample into these coarse fractions was intended to allow identification of relatively scarce, large individuals that would not have been detected had the sample been considered en masse. Between 0.5% and 10% of each sample volume (at least 3000 individual particles) was imaged using Zooscan.

Automated measurements of particle size, shape, and gray-scale density were performed using Zooprocesss analysis software (Benfield *et al.* 2007). Each particle was described by 22 measurements and classified into one of nine broad taxonomic categories (Table 3.1) using the random forest technique (Breiman 2001). Taxonomic categories were chosen to resolve the dominant members of the mesozooplankton as observed during sample collection. The copepod assemblage composed the majority of the biomass in each sample and was further classified into six categories representing distinctive body shapes. A training set of manually identified zooplankters was compiled in collaboration with other researchers investigating mesozooplankton communities in the CCE (namely Ohman and Cawood). Zooplankters were sorted among these taxonomic categories with a success rate

greater than 80%. Items identified as detritus were excluded from further analysis. Here, the term “Zooscan” will be used to refer to the joint method Zooscan scanning and Zooprocess analysis.

Zooscan measurements of zooplankter lengths were converted to manually measured lengths using taxonomically specific, linear relationships developed for a subset of preserved individuals collected in the CCE (Ohman and Cawood, unpubl.). Body lengths were converted to individual dry mass using relationships from the literature (Table 3.1). Estimation of zooplankter sizes using Zooscan offers some advantage over *in situ* measures (*e.g.* optical plankton counters) which have difficulty distinguishing between living zooplankters and detrital aggregates (Gonzalez-Quiros and Checkley 2006, Checkley *et al.* 2008). Use of Zooscan permits a broad level of taxonomic resolution, and aggregates of phytoplankton in the samples may be intentionally excluded from analysis of zooplankton, as was done here. Furthermore, the rapid scanning and machine identification techniques associated with Zooscan processing allows examination of a greater number of individuals than would be permitted by manual microscopic identification.

3.3.3. Estimation of Normalized-Biomass Spectral Slopes

Zooplankters were grouped into logarithmically increasing size categories (equally spaced on a log scale base $2^{0.333}$), and the summed dry weight in each category was divided by the change in weight across the category to create a normalized-biomass spectrum for each sample (Platt and Denman 1978). A linear

least-squares line was fit to the spectrum to describe the change in normalized biomass with individual body weight for each sample:

$$\log\left(\frac{B_w}{\Delta w}\right) = m[\log(w)] + b$$

where B_w is the sample biomass in each dry-weight category w , Δw is the biomass interval for each fraction, and m and b are the slope and y-intercept of the linear, best-fit line. The dry weight (w) of each zooplankton size category was taken as the geometric mean of the weight values bounding the category. Individuals with an estimated dry weight greater than 80 μg (equivalent to a copepod of 2 mm prosome length) were excluded from the calculation of spectra slope. Exclusion of these largest individuals was warranted for three reasons: 1) The grazing efficiencies of both sardine and anchovy are dependent on the variability of prey sizes smaller than 2000 μm (van der Lingen 1994); changes in the size distribution of larger individuals is not thought to influence ingestion rate. 2) Individual abundances of zooplankters decrease with increasing sizes, while net avoidance increases. The calculation of biomass spectral slope is increasingly susceptible to biases as larger, rarely sampled individuals are considered. Although attempts were made to avoid undersampling of large individuals by fractionating the sample prior to Zooscan analysis, artifacts remained obvious after recombination of the small and large size fractions. 3) This division excludes individuals with generation times greater than about 30 days (Gillooly 2000), allowing examination of community structure influenced by the local environment separate from those consisting of individuals with life histories influenced by a variety of conditions over a longer period of time.

Normalized-biomass spectra were also used to describe size structure in phytoplankton communities. Conversion of size-fractionated chlorophyll measurements to phytoplankton dry weight requires use of three ratios, the carbon:chlorophyll *a*, carbon:wet-weight, and volume:wet-weight ratios. Carbon:chlorophyll *a* ratios were measured in the mixed layer during each sampling cycle using epifluorescence microscopy. This ratio ranged from 34 to 151 by weight (Landry and Taylor, unpubl.). Phytoplankton carbon content was assumed equal to 37% of dry weight (Strickland 1960). The equivalent-spherical diameters of the phytoplankton size classes were taken as the geometric mean of the pore sizes of the two filters defining the size categories, and a diameter of 80 μm was taken as the upper boundary of the largest size class. To convert from size categories based on individual diameters to categories based on individual mass, I applied the volume:wet-weight conversion of Mullin *et al.* (1966). A linear least-squares estimate of the normalized-biomass spectrum was calculated for each phytoplankton sample in a manner identical to that applied to the zooplankton.

3.3.4. Bioenergetic modeling of sardine and anchovy growth

Alheit and Niquen (2004), van der Lingen *et al.* (2006), and Rykaczewski and Checkley (2008) hypothesized that the major difference in the response of sardine and anchovy to changing environmental conditions is related to their use of different sizes of prey and the efficiency at which they capture and retain organic matter over different portions of the plankton size spectrum. Laboratory examinations of feeding behavior, respiration, ingestion, and excretion support this hypothesis. To examine the

plausibility of this hypothesis, I used the equations describing the carbon and nitrogen budgets developed by James *et al.* (1989) and van der Lingen (1999) to estimate specific growth rates of sardine and anchovy given the plankter sizes and concentrations sampled across the CCE. These models are convenient because they estimate fish growth rates given plankter sizes and concentrations. However, cursory examination of these previously established bioenergetic models suggest that the estimated growth rates at high concentrations and large sizes of plankters are unrealistic. Gross-growth efficiencies exceed 0.7 for models of the carbon budgets of both species and exceed 0.4 and 0.2 for the nitrogen budget models of anchovy and sardine, respectively. Actual gross-growth efficiencies for fishes rarely exceed 0.2 (Brett and Groves 1979). It is important to stress that the results from these models may approximate the spatial pattern of growth changes, but the absolute values of estimated growth under high abundances and large sizes of zooplankters are expected to overestimate actual growth rates.

The linear approximations of mesozooplankton biomass size spectra were extended to estimate the prey available at individual sizes ranging from 200 to 4000 μm total length. Model inputs of the concentrations and size structure of the phytoplankton communities and were identical to those observed across the CCE; no extrapolation was necessary. Persistent and dense aggregations of plankters likely influence feeding behavior and growth rates of fish. The phytoplankton and zooplankton concentrations used in this exercise represent spatial averages measured by oblique net tows over a towing distance of about 1 km, and the effects of vertical and horizontal variability at scales less than a kilometer were not considered here.

Estimates of mesozooplankton community sizes and biomasses combined with the basic bioenergetic equations derived empirically by James *et al.* (1989) and van der Lingen (1999) allow approximation of the ingestion and growth of individual sardine and anchovy. I applied these equations to estimate mass-standardized specific growth rates based on rates of ingestion, assimilation, excretion, and respiration. In these models, ingestion and respiration rates change with swimming speed and feeding mode (*i.e.*, filter feeding or particulate feeding), and both of these behavioral changes are functions of prey size and concentration. Metabolic rates were scaled to adjust for differences between the mixed-layer temperatures observed in the CCE during zooplankton sampling and laboratory temperatures at which the bioenergetic budgets were developed and literature values of Q_{10} for sardine and anchovy genera (van der Lingen 1995).

The equations provided by James *et al.* (1989) and van der Lingen (1999) are based on single prey sizes, and I modified these equations slightly to account for the variety of prey sizes available. Clearance rate of anchovy, F_A , is related to the concentrations of prey in each of n size classes (modified from James' "Equation 5"):

$$F_A = \sum_n^{i=1} 17.7623 \cdot e^{(-e^{2.1897-1.8868P_{x_i}/1000})} \text{ l fish}^{-1} \text{ min}^{-1}$$

where x_i is the length (in μm) of a prey item in size class i . When particulate feeding, clearance rates for prey sizes below $710 \mu\text{m}$ were set at zero. When filter feeding, clearance rates for particles larger than $710 \mu\text{m}$ were given a value equal to the clearance rate at $710 \mu\text{m}$. James *et al.* (1989) observed that swimming speed in anchovy was observed to be related to prey size—individuals swam faster when

presented with larger prey items, likely a response to the increased escape capabilities of larger individuals. The prey size governing swimming speed in James' "Equation 20" was taken as the prey size equivalent to the 90th biomass percentile. Other equations representing the bioenergetics of anchovy were unmodified.

The fifth-order polynomial describing the clearance rate of sardine (F_S) as presented by van der Lingen (1999) is inappropriate for prey sizes greater than 2.7 mm total length, and I chose to modify van der Lingen's "Equation 5," fitting a more appropriate equation to the same data:

$$F_S = \sum_n^{i=1} 30.81895 \cdot 0.32323 \cdot \frac{e^{0.0084263 \cdot (x_i - 800)}}{30.81895 + 0.32323 \cdot e^{0.0084263 \cdot (x_i - 800)}} + 12.02961 \cdot 0.75040 \cdot \frac{e^{0.019776 \cdot (x_i - 15)}}{12.02961 + 0.75040 \cdot e^{0.0084263 \cdot (x_i - 15)}}$$

in $l \text{ fish}^{-1} \text{ min}^{-1}$. Clearance rates during different feeding modes were adjusted in a manner similar to that for anchovy. When particulate feeding, clearance rates for prey sizes below $1230 \mu\text{m}$ were set at zero. When filter feeding, clearance rates for particles larger than $1230 \mu\text{m}$ were given a value equal to the clearance rate at $1230 \mu\text{m}$.

James *et al.* (1989) and van der Lingen (1999) noted thresholds governing switches in feeding mode based on the length of a limited variety of prey items. Here, I modified this condition so that feeding mode was based on the mean biomass of individual particles in the community. Strict adherence to the mean length of particles proposed by James *et al.* (1989) and van der Lingen (1999) would consistently result in filter feeding by both species, since small phytoplankters and zooplankters are

always numerically dominant. A threshold based on biomass spectra is more appropriate. In the model applied here, fish switched from filter feeding to particulate feeding if more than 50% of the biomass in the zooplankton community was contained in size classes greater than the thresholds identified in the laboratory experiments of James (1989) and van der Lingen (1999).

The single remaining free parameter in the budget equations presented by James (1989) and van der Lingen (1999) is the amount of time spent filter feeding or particulate feeding per day. As the objective of this exercise is to explore the maximum habitat available given the observed prey sizes, I held the feeding time during particulate feeding at 12 hours day⁻¹ and the time spent feeding during filter feeding at 24 hours day⁻¹. Particulate feeding is dependent on visual identification and active selection of prey items. Particulate feeding by anchovy is possible even under low-light conditions (O'Connell 1972) and shows marked periodicity with peaks at dawn and dusk (James 1987). Filter feeding is not light dependent and does not show regular periodicity (Emmett *et al.* 2005, van der Lingen *et al.* in press).

3.4. Results

Curl-driven upwelling and nitrate content of the mixed layer decreased rapidly with distance offshore during both cruises, and these changes were mirrored by the depth of the 25.5 kg m⁻³ σ_θ isopycnal. Winds were predominantly from the northwest (daily mean = 305°, s.d. = 8°), and the peak in wind stress magnitude occurred between 25 and 130 km from shore during sampling for both cruises (Figure 3.2a-c). The influence of coastal upwelling in the nearshore region was not distinguished from

curl-driven upwelling, wind-driven mixing, or mesoscale dynamical processes, as it is difficult to interpret the location from which the sampled waters originated and the physical processes responsible for the flux of nutrients into the euphotic zone. Given the weekly averaged estimates of wind stress for sampling locations nearest to the coast and assuming that upwelling from Ekman transport away from the coast occurs over a Rossby radius of 10 km, coastal upwelling rates during the cruises ranged from 1.4 to 5.7 m day⁻¹, or up to an order of magnitude greater than the largest rates of curl-driven upwelling (Smith 1968). Coastal upwelling, turbulent mixing across the nutricline, and high rates of curl-driven upwelling are probable processes responsible for the increased nutrient content of the nearshore waters. The influence of coastal upwelling decreases with increased distance from the coast as nutrients are utilized by phytoplankton as water masses advect away from the coastal area. In these offshore regions, curl-driven upwelling and turbulent mixing likely contribute a greater portion of nutrient input to the euphotic zone than in regions closer to the coast.

Concentrations of phytoplankton declined with distance offshore (Figure 3.3a). The slopes of the linear fits to each spectrum became more negative as the pycnocline deepened and the nutrient concentration, wind stress, and curl-driven upwelling rate declined with distance offshore, indicating that the relative contribution of small individuals to the phytoplankton community was greater in more oligotrophic environments (Figure 3.3b).

Normalized-biomass spectra of zooplankton typically displayed local minima for the smallest biomass classes (Figure 3.4). These minima are sampling artifacts related to incomplete retention of small organisms. Organisms with body widths 1.33

times the mesh size of the net are captured with about 95% efficiency (Harris *et al.* 2000). If we assume a width:length ratio of 0.25 for copepods, then individuals with total length less than 1075 μm will be captured with less than 95% efficiency by the 200- μm mesh net used here. I excluded all organisms less than 1100 μm total length (corresponding to calanoid copepods less than 8 μg per individual), and this truncation of the biomass spectra avoided biases due to incomplete retention of small zooplankters.

To examine the capability of the Zooscan analysis to approximate zooplankton biomass and spectral slope, these estimates were compared with those measured by sequential mesh fractionation and oven drying (Rykaczewski and Checkley 2008). The latter dataset was converted to account for fractionation based on individual linear dimension rather than on dry weight, as used here. The spectral slopes and biomass estimates calculated by the oven-dried method agree well with Zooscan estimates and show similar declines with distance offshore (Figure 3.5). However the slopes calculated by mesh fractionation and oven drying were consistently biased negative, describing a smaller community structure. The small individuals deliberately excluded from Zooscan analysis could not be removed from the wet-sieved samples, and this bias is apparent in the comparison. Similarly, biomasses estimated by mesh fractionation and oven drying were greater than those estimated by Zooscan analysis for samples collected near the coast where large phytoplankters clogged the mesh sieves and were unintentionally included in estimates of zooplankton biomass. For these reasons, only the biomasses and size spectra estimated by Zooscan will be discussed further.

Mean mesozooplankton biomass ranged from 2 mg m^{-3} offshore to 54 mg m^{-3} at a nearshore location. Spectral slopes ranged from -1.5 to 0.5 with a mean of -1.0. In light of the high degree of covariation between physical and chemical measurements of the ecosystem (Figure 3.2), I chose to represent trophic state by the logarithm of nitrate concentration above the nutricline rather than by each oceanographic data series individually. The relationship between nitrate concentration and the spectral slopes of the phytoplankton and mesozooplankton communities was significant (Table 3.2). The relationship between the spectral slopes of the phytoplankton and zooplankton communities was also positive, though there was considerable variability in estimates of zooplankton spectral slopes within samples collected at the same location. For each experimental cycle location, the mean and standard deviation of the estimates of spectral slope are plotted with the complete data in Figure 3.6. The logarithmic relationship describing the association between nitrate concentration and spectral slopes of the phytoplankton and zooplankton communities is displayed in Figure 3.7. Slopes of community size spectra are most negative at low concentrations of nitrate and increase to an asymptotic maximum as nitrate levels increase. This relationship is more descriptive of changes in the size structures observed at high and low concentrations of nitrate than of changes in size over a small range of nutrient conditions.

To investigate whether the relationship observed within the mesozooplankton community was the result of shifts in taxonomic composition or of changes in the sizes of individual members of dominant taxonomic groups, I examined the correlation between estimated slope and two measures of community change: median

dry weight of individual zooplankters (Table 3.3) and percentage composition of major taxa (Table 3.4). I also examined mean size and taxonomic composition between inshore areas with nitrate concentrations above the nutricline greater than $1.0 \mu\text{M l}^{-1}$ and offshore areas with lower nitrate concentrations. The five most abundant taxa identified were copepods, euphausiids, chaetognaths, ostracods, and appendicularia. More specific changes within the copepod group were not examined. Although all major taxa (except ostracods) displayed larger individual size and variability in the eutrophic region nearshore, an analysis of variance (ANOVA) revealed that only the change in copepod sizes was significant between the two regions. A decrease in the median weight of copepods was strongly associated with a more negative spectral slope of the mesozooplankton community (Figure 3.8). Euphausiid individual weights also showed a positive correlation with spectral slope. Changes in taxonomic composition across the ecosystem were minor. However, decreasing spectral slopes were associated with a shift towards a greater contribution of chaetognaths and a slight decrease in the contribution of copepods (Table 3.4).

What are the implications of the observed relationships between oceanographic conditions and plankton size structure for populations of small pelagic fish? Estimates of specific growth rates in terms of carbon are displayed in Figure 3.9a. Growth rates for anchovy show a distinct maximum in the eutrophic region nearshore, and growth rates decrease as plankton sizes and concentrations are reduced with distance offshore. Growth in the nearshore region is highly variable and strongly dependent on changes in spectral slope; a slight change in the slope results in a considerable increase in the concentration of large zooplankters and has a positive effect on the growth rate of

anchovy. This variability decreases offshore, where zooplankton are at low concentrations, and slight changes in concentration and slope are of little benefit to anchovy growth. Between 100 and 150 km from the coast, estimated growth rates are about 20% of the nearshore maximum, and growth rates are uniformly negative in the oligotrophic region offshore.

Like anchovy, sardine growth rates are also highest inshore of 100 km. However, sardine growth rates are less variable and decline only gradually with distance offshore. Sardine are capable of obtaining their required prey from a wider range of plankter sizes and are less susceptible to changes in the spectral slope of the zooplankton and phytoplankton communities in the nearshore region. At 100 to 150 km offshore, growth rates of sardine are about 50% of the maximum closer to the coast, and sardine are capable of meeting daily nutrition requirements under some of the prey conditions observed offshore of 250 km.

The distribution of sardine and anchovy eggs were sampled by the National Marine Fisheries Service using a Continuous Underway Fish-Egg Counter (Checkley *et al.* 2000) during surveys in spring 2006 and 2007. Data from these cruises are displayed in Figure 3.9b and 3.9c (respectively) for the transect line corresponding to the zooplankton sampling locations offshore of Pt. Conception, CA. In both years, anchovy eggs are present in the nearshore, eutrophic area and absent from the oligotrophic waters offshore. The opposite is true of the distribution of sardine eggs; sardine eggs are only found in offshore waters.

3.5. Discussion

3.5.1. Size structure of zooplankton and phytoplankton communities

The covariability of upwelling rate, density, and nitrate concentration describe a gradient of conditions between two distinct regions: 1) the eutrophic area nearshore where coastal upwelling and high levels of curl-driven upwelling promote shoaling of the nutricline, and 2) a relatively oligotrophic region offshore where winds and curl-driven upwelling are weak or negative and nutrient concentrations are low. These regions were clearly separated in May 2006 when the wind stress maximum and minimum in curl-driven upwelling were located 125 km from shore. A distinct separation was not as clearly resolved in April 2007, but satellite scatterometry and ocean color indicate that the wind stress maximum, positive curl-driven upwelling, and higher levels of chlorophyll *a* extended further offshore in April 2006 than in May 2007. This contrast between nearshore productive waters with more oligotrophic waters offshore is typical of conditions found in eastern-boundary current ecosystems during the upwelling season (Huyer 1983).

A distinct separation between the nearshore and offshore environments was also evident in the biomass spectra of phytoplankton and mesozooplankton communities (Figure 3.5 and Table 3.3). Larger zooplankters were relatively more abundant in eutrophic areas where the spectral slopes of phytoplankton communities were greatest, and the contribution of these large individuals to total biomass decreased as nutrient levels decreased (Figure 3.7). Increases in nutrients had a greater influence on the slope of the biomass spectra when nutrient concentrations

were low. Increases in nutrient concentration had a lesser effect on the spectral slopes of phytoplankton and zooplankton communities in eutrophic areas.

In addition to the difference in the physical conditions and nitrate concentrations that characterize these regions of large and small individual sizes, there is increasing evidence that phytoplankton communities in offshore regions of the CCE are iron-limited (King and Barbeau 2007). The nearshore environments sampled in 2006 and 2007 were not iron limited (King, pers. comm.), likely because these waters were recently in close proximity to the benthic-boundary layer along the continental shelf where trace metals are abundant. Along with differences in physical conditions and nitrate concentrations, differential supply of these trace metals to the nearshore and offshore environments is also a factor which may influence the size structure of plankton communities.

At each cycle location, the variability of the spectral slopes of the zooplankton community was greater than those of the phytoplankton community. A greater variability in the structure of the zooplankton community relative to chlorophyll *a* concentration has been noted in previous studies of the CCE (Star and Mullin 1981). Zooplankters, in comparison to phytoplankters, have greater ability to swim vertically and control their position in the water column. Such behavior, when coupled with the dynamic, advective flow present in upwelling regions, may result in greater aggregation (*i.e.* patchiness) in vertical and horizontal dimensions (Franks 1992) and explain the increased variability in estimates of zooplankton size structure at each location. Variability in the zooplankton biomass and spectral slope was highest in the nearshore environment (Figs. 3 and 5), consistent with previous observations of

increased patchiness in eutrophic regions of the CCE (Venrick 1972, Star and Mullin 1981).

What underlying principles may be responsible for the apparent relationship between the structure of phytoplankton and zooplankton communities? Poulin and Franks (in press) demonstrate that such relationships may emerge for a variety of reasons dependent on the allometric scaling of biological rates and the assumption that the size ratio between phytoplankton prey and zooplankton predators is applicable across the spectrum of size classes. The results of Moloney and Field (1991) and Hansen *et al.* (1994) demonstrate that the predator:prey ratio is remarkably consistent over a wide range of sizes within a certain taxon. However, if large changes in the taxonomic composition of the zooplankton result from changes in phytoplankton concentration or nutrient content, a clear relationship between phytoplankton and zooplankton size structure may be obscured by changes in the size ratio between predators and prey. Major changes in gross taxonomic composition were not observed across the trophic gradient examined here (Table 3.4). Variability in spectral slope was strongly associated with changes in the individual sizes of copepods rather than with changes in the gross taxonomic composition (Table 3.3), and a conceptual model relating phytoplankton and zooplankton size structure through predator-prey interactions appears to be appropriate.

Is it reasonable to attribute changes observed in mesozooplankton size structure to variability in the copepod community? Regular hydrographic sampling and mesozooplankton collection have been conducted in the CCE by the California Cooperative Oceanic Fisheries Investigations (CalCOFI) Program. Although this

program has maintained regular collections of mesozooplankton, relatively few samples have been identified at the resolution necessary to address changes in copepod size in different hydrographic regions. However, Fleminger (1964, 1967) and Bowman and Johnson (1973) characterized the species distributions and abundances of adult calanoid and eucalanoid copepods during cruises in 1949 (55 dominant species quantified) and 1958 (175 dominant species quantified). I compared the calanoid species abundances described during cruises in May 1949 and April 1958. The two regions chosen (station 801 compared with 803 in 1949 and stations 80.55 and 80.60 compared with 80.90 in 1958) for comparison correspond hydrographically and spatially to the eutrophic and relatively oligotrophic areas studied during May 2006 and April 2007. Individual abundances, minimum female length taken from the literature for each species (Razouls *et al.* 2009), and the length:dry-weight conversions given in Table 3.1 were used to estimate median individual dry weight of copepods in the nearshore and offshore regions. The coarser mesh nets used by the CalCOFI program and the exclusive identification of adults by Fleminger (1964, 1967) and Bowman and Johnson (1973) prohibit a direct comparison of sizes between these historical data and estimates of Zooscan size for samples collected in 2006 and 2007, however, the differences in sizes between the nearshore and offshore stations during each of these investigations can be compared (Table 3.5). The smaller weights of individual copepods observed in the offshore, more oligotrophic region during 1949 and 1958 is consistent with the differences in mesozooplankton size structure described above for 2006 and 2007 and illustrates that individual copepod weights may show significant spatial variation. These results are not meant to imply that

changes in copepod sizes from nearshore to offshore are constant over time. On the contrary, copepod communities of the CCE do display taxonomic variability in response to environmental changes (Rebstock 2002), and sizes of adult copepods within a species grow to larger sizes during periods when their prey are more abundant (Frost 1974). This variability in species sizes and species composition may influence the size structure of the mesozooplankton community and regulate the transfer of organic matter and energy to planktivorous fish. It is interesting to note that the decrease in copepod size with distance offshore is much greater in spring of 1958 than in 1949, and it is tempting to relate the smaller sizes in 1958 to the severe El Niño event and the associated increase in oligotrophy (Mullin 1998), but such inference is not possible based on the few data examined.

An important caveat to the conclusions presented above concerns the lack of consideration of zooplankters smaller than 8 μg dry weight. This includes the naupliar and copepodite stages of numerous copepod species present in the CCE. Here, I deliberately focus on the mesozooplankton community. Assessment of the contribution of smaller individuals to the zooplankton assemblage was prevented by their incomplete retention by the plankton net used in this study. Increased contribution of early developmental stages of zooplankton to the eutrophic nearshore community is a valid hypothesis, as egg production is often considered to be food-limited in the marine environment (Checkley 1980, Runge 1985). However, complete populations of small species were certainly disregarded as well. Given the results presented above, it is plausible that the contribution of small species and their developmental stages increases in oligotrophic environments, and the observed

decrease in mesozooplankton spectral slope with decreasing nutrient concentration may be robust despite the fact that smaller individuals were not considered here.

3.5.2. Potential for growth by small pelagic fish

In the CCE, annual estimates of growth in the anchovy population are high and variable in comparison to that of the sardine population (Jacobson *et al.* 2001). Instantaneous surplus production rates for anchovy range from -0.5 to 1.5 with a standard deviation of 0.68. Instantaneous surplus production rates for sardine range from -0.4 to 0.8 with a standard deviation of 0.46 (Jacobson *et al.* 2001). These differences in population growth rates are reflected in the estimates of growth rates by individuals of each species displayed in Figure 3.9a. For the spectrum of plankton communities examined in the CCE, individual growth rate of anchovy ranged from -9 to 75 mg C (dry g fish)⁻¹ day⁻¹ with a standard deviation of 22 mg C (dry g fish)⁻¹ day⁻¹. Sardine growth rates ranged from -3 to 16 mg C (dry g fish)⁻¹ day⁻¹ with a standard deviation of 5 mg C (dry g fish)⁻¹ day⁻¹. Results, in terms of nitrogen budgets, exhibited similar characteristics with distance offshore. These results are supported by observations of distinct habitat areas measured by the distribution of pelagic eggs (Figure 3.9b and 3.9c; Checkley *et al.* 2000) and further substantiate the idea that variability in the biomass of sardine and anchovy populations may be related to the size structure of the zooplankton community (van der Lingen *et al.* in press) and changes in the productivity of eutrophic and oligotrophic environments over time (Rykaczewski and Checkley 2008).

The absence of sardine eggs in the nearshore region where the potential for individual growth is highest is puzzling. However, this exercise considered only one aspect of fish habitat—the availability of prey. The lack of sardine eggs nearshore may indicate of either active avoidance of nearshore regions where predation on eggs may be high and low temperatures may limit growth physiologically or a direct removal of sardine eggs by abundant predators. Predation on sardine eggs by large zooplankters has been hypothesized to explain observations of complimentary distributions of euphausiids and sardine eggs (Checkley *et al.* 2000). Sardine lose little in terms of potential growth by avoiding the eutrophic, nearshore area where zooplankton biomass and predation on eggs and larvae are higher. The situation for anchovy is different; avoidance of the nearshore region would greatly reduce potential growth (Figure 3.9). Observation that sardines of the eastern Pacific are able to prosper during warm, El Niño periods when production by other species declines led Bakun and Broad (2003) to suggest that sardine exploit an “ecological loophole”—under relatively oligotrophic conditions, sardine populations are sustained by their ability to consume small, planktonic prey, while populations of other taxa, including the predators on the eggs and larvae of sardine, decline. The estimates of specific growth rates presented here support the loophole hypothesis and suggest that it is broadly applicable in describing the growth conditions for small pelagic fish across the large ecosystem and not restricted to comparisons of extremes in oceanographic conditions as during El Niño and La Niña periods.

Estimated growth rates presented in Figure 3.9a are useful for comparison of the habitat available for individual growth, but it is important to stress that these

values are *potential* specific growth rates, representing the upper bound to the daily growth (reproductive and somatic) attainable by adult fish during the most productive period of the year. The laboratory examinations of fish feeding on which the bioenergetics models are based were conducted over feeding periods of several (2 to 3) hours, and the nitrogen and carbon budgets derived from these examinations may not be accurately extrapolated to describe growth processes for longer periods of feeding (James *et al.* 1989, van der Lingen 1999). Furthermore, the rates estimated here do not address seasonal variability in plankton communities and inter- and intraspecific competition for resources. For instance, the maximum specific growth rate of anchovy was estimated to be $75 \text{ mg C (dry g fish)}^{-1} \text{ day}^{-1}$, requiring a prey consumption of $107 \text{ mg C (dry g fish)}^{-1} \text{ day}^{-1}$. Consider a population size of $0.5 \cdot 10^6$ tons (less than half the average estimated biomass during the 1970s) ranging over an area of $40 \cdot 10^3 \text{ km}^2$, the approximate area of the Southern California Bight. If we assume a dry-weight:wet-weight ratio of 0.3 (James *et al.* 1989), adult anchovy would consume $0.40 \text{ g C m}^{-2} \text{ day}^{-1}$ of zooplankton. Assuming 1) that anchovy feed at the second trophic level, 2) a generous 20% conversion efficiency from primary to secondary production and 3) an annually averaged net primary production of $1 \text{ g C m}^{-2} \text{ day}^{-1}$ (Mantyla *et al.* 1995), this level of anchovy consumption would be equivalent to 200% of the available secondary production—a level certainly not attainable on a regular basis. Realized growth rates (somatic and reproductive) for adult anchovy are about $6.5 \text{ mg (dry g fish)}^{-1} \text{ day}^{-1}$ (Hunter and Leong 1981). The majority of this growth is devoted to reproduction. Assuming a carbon:dry-weight ratio of 0.44 for fish (Watanabe and Saito 1998), this growth rate is equivalent to 2.9 mg C (dry g

fish)⁻¹ day⁻¹. This realized level of growth requires a consumption 14.0 mg C (dry g fish)⁻¹ day⁻¹. Based on a population size of $0.5 \cdot 10^6$ tons over an area of $40 \cdot 10^3$ km² and the three assumptions noted above, this consumption rate is equivalent to 26% of the secondary production. Even given this lower estimate of anchovy growth rate, the prey fields observed across the CCE suggest this level of growth may be attainable only in eutrophic environments.

Somatic growth in adult sardine continues after maturity and exceeds the rate of reproductive growth until about age five (Hill *et al.* 2008). Lasker (1970) estimated total specific growth rate for adult sardine at 1.5 mg (dry g fish)⁻¹ day⁻¹, equivalent to 0.65 mg C (dry g fish)⁻¹ day⁻¹ and requiring a prey consumption rate of 6.7 mg C (dry g fish)⁻¹ day⁻¹. Given the prey field observed in the CCE, this level of growth is occasionally attainable in oligotrophic, offshore waters as well as in the more productive waters nearshore. In the recent decade, the adult population of sardine reached an estimated biomass of $0.8 \cdot 10^6$ to $1.5 \cdot 10^6$ tons (Hill *et al.* 2008). If we assume, for sake of comparison, that this population ranged over an area equal to $40 \cdot 10^3$ km², the adult sardine population would require between 20 and 37% of the available secondary production.

These estimates of the secondary production required to support fish growth are subject to assumptions concerning levels of primary production, the spatial distribution of each population, and the trophic transfer efficiency between primary and secondary producers. The distributions of both sardine and anchovy expand in distribution to the north and offshore of the Southern California Bight, especially during periods of greatest biomass (MacCall 1990), likely occupying an area greater

than $40 \cdot 10^3 \text{ km}^2$. In addition, sardine (and anchovy, to a lesser degree) are omnivorous, supplementing their diet of zooplankton with phytoplankton (van der Lingen *et al.* in press). It is also important to note that the zooplankters, which serve as the main prey items for both species, are themselves omnivorous. Consideration of a larger spatial distribution and omnivory by fish would act to decrease the portion of secondary production required to support the populations of sardine and anchovy, while decreasing the trophic transfer efficiency from 20% or considering some degree of omnivory by zooplankton would increase the portion of secondary production required. Furthermore, all secondary production is not equally prone to predation by the planktivorous fish; the size-selective predation by anchovy would disproportionately affect larger zooplankters.

3.6. Conclusions

Spectral slopes of zooplankton assemblages decline with distance offshore in concert with phytoplankton sizes, nutrient concentrations, and physical conditions promoting shoaling of the pycnocline. These observations are consistent with the hypothesis that changes in the biomass and size structure of the zooplankton community are related to the availability of phytoplankton resources. Changes in the size spectra of the zooplankton appear to be dominated by variation in the individual biomasses of copepods rather than by changes in the gross taxonomic composition of the zooplankton community.

Plankton concentrations and size structures have important implications for dominant populations of planktivorous fish found in upwelling ecosystems worldwide.

The combinations of zooplankton sizes and concentrations observed in the CCE during spring 2006 and 2007 suggest that adult anchovy may be restricted to the eutrophic habitat in which daily nutritional requirements are met, even during the upwelling season when primary production is highest. Sardine growth is less dependent on the nearshore environment. These results are consistent with previous description of sardine and anchovy ecology which suggest that anchovy is an opportunistic specialist, taking advantage of highly productive conditions when available but being incapable of sustenance during periods of low productivity. The strategy of sardine is that of a generalist, being less able to exploit periods of high productivity, but able to meet daily nutritional requirements under moderately oligotrophic conditions. The hypothesis that emerges is interesting. Variability in the size structure and abundance of zooplankton in the more oligotrophic waters of the CCE has the potential to influence production of sardine; changes in the zooplankton may promote either positive or negative growth. These changes in the oligotrophic area do not influence anchovy, as growth is uniformly negative over the range of zooplankton assemblages observed. However, the situation is nearly reversed in the eutrophic environment. Changes in the nearshore zooplankton assemblage strongly influence the potential for anchovy production, while the potential for sardine growth remains relatively constant. Changes in the offshore wind stress and wind-stress curl may have a substantial impact on the suitable habitat and growth rate of sardine, while coastal, alongshore wind stress and other nearshore processes may have a stronger influence on anchovy populations (Rykaczewski and Checkley 2008).

The results presented here represent the first unambiguous analysis of mesozooplankton size structure across trophic gradients in the marine environment; previous analyses have employed the use of more optical instruments which provide results, although valuable if interpreted carefully, that are ambiguous in their description of the zooplankton assemblage due to poor resolution of gross taxonomy and complications due to the sampling of detrital aggregates. I would encourage continued efforts to examine the size structure of the mesozooplankton community and consideration of the implications for particle export, planktivorous fish, and plankton dynamics.

3.7. Acknowledgements

I am grateful for the generosity of M. Ohman for use of the Zooscan instrument and advice concerning interpretation of the data. I thank R. Goericke for graciously providing the size-fractionated phytoplankton data. The zooplankton analysis presented would have been much more difficult without the help of J. B. Romagnan and A. Townsend. I thank D. Checkley and A. Pasulka for their comments on the manuscript. Cruises in 2006 and 2007 were supported by the CCE Long-Term Ecological Research Program. In addition, this work was supported by the National Science Foundation Graduate Research Fellowship Program, the NASA Earth and Space Science Fellowship Program, and the San Diego chapter of the ARCS Foundation.

Table 3.1. Taxonomic categories and length to dry-weight conversions applied in Zooscan analysis. TL = total length; PL = prosome length; TrL = trunk length; ShL = shell length.

Taxonomic group	Length-to-dry weight conversion	Reference
copepods		
calanoid copepods	$\log_{10} DW = 3.358 \cdot \log_{10} (PL) - 9.159$	Kobari <i>et al.</i> 2004
eucalanid copepods	$\log_{10} DW = 3.091 \cdot \log_{10} (PL/1000) - 0.0026$	Hopcroft <i>et al.</i> 2002
oithona copepods	$\log_{10} DW = 3.16 \cdot \log_{10} (TL) - 8.18$	Hopcroft <i>et al.</i> 1998
poecilostomatoid copepods	$\ln DW = 2.90 \cdot \ln (TL) - 16.82$	Satapoomin 1999
harpacticoid copepods	$\ln DW = 1.59 \cdot \ln (TL) - 10.23$	Satapoomin 1999
euphausiids	$\log_{10} DW = 0.456 + 2.8 \cdot \log_{10} (TL/1000)$	Lindley 1999
chaetognaths	$\log_{10} DW = 3.24 \cdot \log_{10} (TL/1000) - 0.975$	Uye 1982
appendicularians	$DW = (38.8 \cdot (TrL/1000)^{2.574})^{1.12}$	Laveneigos and Ohman 2007
ostracods	$DW = 17.072 \cdot (TL/1000)^{2.545}$	Laveneigos and Ohman 2007
polychaetes	$DW = 40.322 \cdot TL/1000$	Laveneigos and Ohman 2007
pteropods	$DW = 1.615 \cdot e^{-0.088 \cdot ShL/1000}$	Laveneigos and Ohman 2007
siphonophores	$DW = 20.47 \cdot (TL)^{0.834}$	Laveneigos and Ohman 2007
detritus and other minor zooplankton taxa	excluded from analysis	

Table 3.2. Linear Pearson correlation coefficients (r) between nutrient concentrations and measurements of the plankton community. Bold values represent correlations with p values less than 0.01. Italicized values represent p values less than 0.05.

	log nitrate concentration	phytoplankton concentration	phytoplankton spectral slope	mesozooplankton concentration
phytoplankton concentration	0.72			
phytoplankton spectral slope	0.71	0.91		
mesozooplankton concentration	0.79	<i>0.52</i>	<i>0.45</i>	
mesozooplankton spectral slope	0.61	0.74	0.66	<i>0.46</i>

Table 3.3. Median dry weights of individual zooplankters and linear Pearson correlation coefficients (r) between mesozooplankton normalized-biomass spectral slopes and the median weights of major taxonomic groups. The standard deviation observed for each sample is noted in parentheses. Bold values represent correlations with p values less than 0.01. Italicized values represent p values less than 0.05. Inshore and offshore samples were grouped according to nitrate concentration above the nutricline, with the nearshore group composed of samples with nitrate values greater than $1.0 \mu\text{M l}^{-1}$.

Taxonomic group	inshore median weight, μg (s.d.)	offshore median weight, μg (s.d.)	significant difference (ANOVA)	r (median weight with slope)
copepods	18.8 (2.9)	15.9 (2.5)	Yes	0.91
euphausiids	914 (1400)	415 (450)	No	<i>0.37</i>
chaetognaths	117 (150)	40.2 (22)	No	-0.046
appendicularians	18.0 (8.2)	15.2 (6.8)	No	-0.044
ostracods	37.0 (24)	40.9 (30)	No	0.11

Table 3.4. Taxonomic composition and linear Pearson correlation coefficients (r) between total mesozooplankton biomass and relative contributions of major taxonomic groups. The standard deviation observed for the samples is noted in parentheses. Bold values represent correlations with p values less than 0.01. Italicized values represent p values less than 0.05.

Taxonomic group	inshore composition, % (s.d.)	offshore composition, % (s.d.)	significant difference (ANOVA)?	r (composition with slope)
copepods	92.9 (2.9)	89.2 (5.2)	Yes	<i>0.36</i>
euphausiids	5.79 (5.8)	3.65 (3.0)	No	-0.03
chaetognaths	3.04 (2.5)	6.73 (4.8)	Yes	<i>-0.40</i>
appendicularians	0.079 (0.06)	1.61 (3.5)	No	-0.04
ostracods	1.07 (0.51)	1.41 (0.62)	No	-0.30

Table 3.5. Differences in individual copepod sizes during two CalCOFI cruises for which detailed species distributions were published by Fleminger (1964, 1967) and Bowman and Johnson (1973). The numerical abundance of copepod species was taken as the geometric mean of the copepods abundances provided. Locations of “inshore” and “offshore” stations are noted in the text.

CalCOFI cruise	inshore	offshore	significant difference (ANOVA)?	
May 1949	median dry weight (μg)	108	71.3 (3.78 - 71.3)	Yes
	dominant species	<i>Calanus pacificus</i> (85%)	<i>Metridia pacifica</i> (57%)	
April 1958	median dry weight (μg)	108	11.4 (5.80 - 106)	Yes
	dominant species	<i>Calanus pacificus</i> (67%)	<i>Eucalanus bungii californicus</i> (31%)	

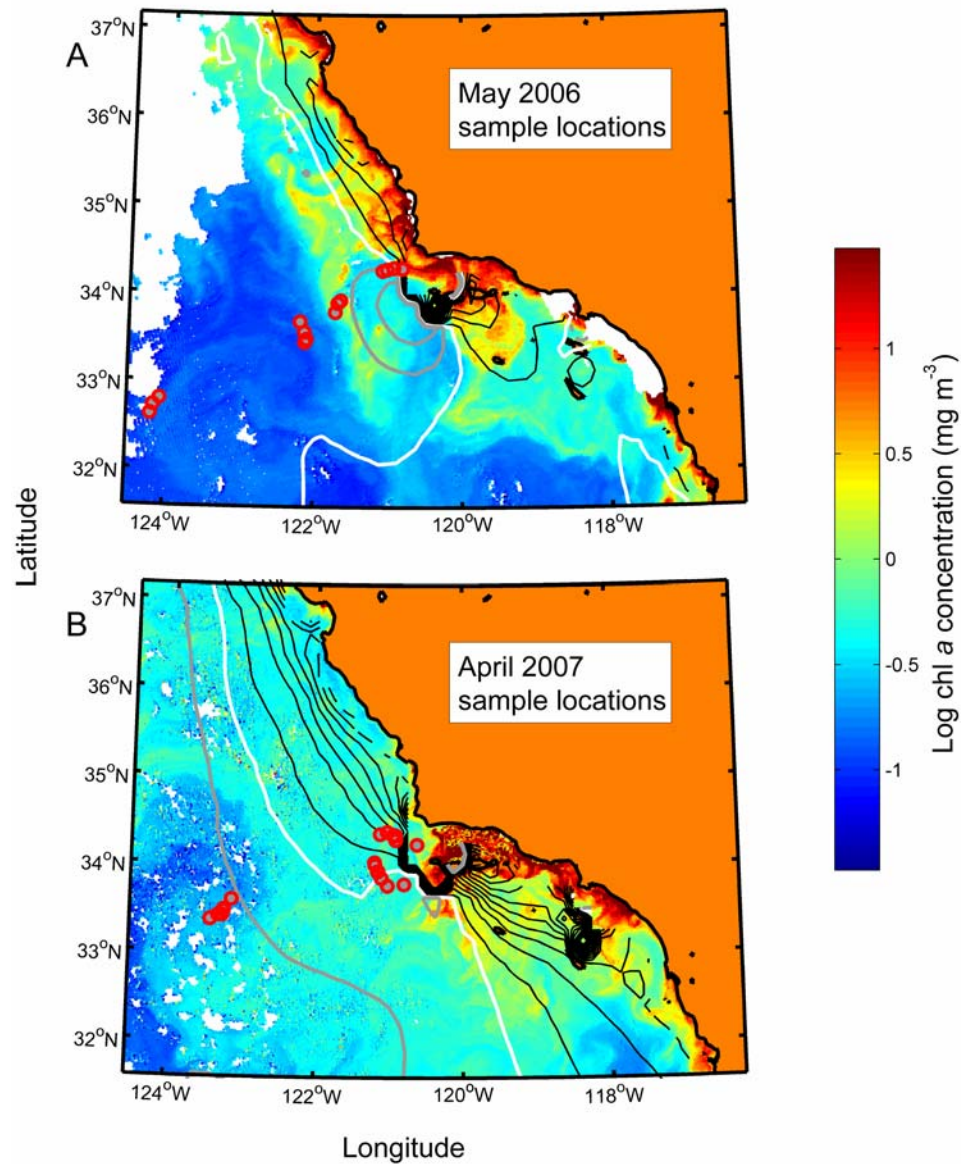


Figure 3.1. Locations of experimental cycles in reference to MODIS chlorophyll *a* concentrations and estimates of curl-driven upwelling. Sampling locations ranged from the eutrophic region nearshore to the oligotrophic region offshore. Contour lines denote curl-driven upwelling rate in 0.1-m-day⁻¹ increments. The zero contour is in white, negative contours are in gray, and positive contours are in black. Each red circle indicates the location of a mesozooplankton sample examined microscopically in the laboratory. These images of conditions on A) May 23, 2006 and B) April 18, 2007 were each one of a few images in which cloud cover did not obscure the study region. Curl-driven upwelling rates are averages over the seven days prior to the dates above.

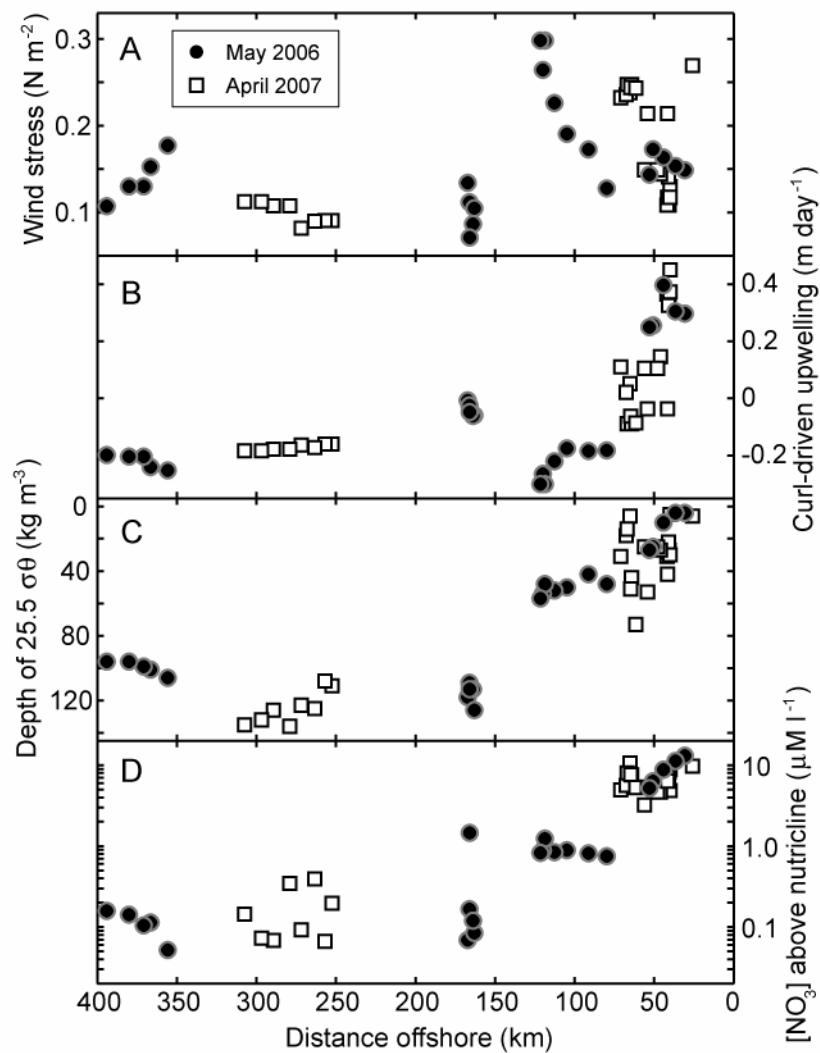


Figure 3.2. Physical and chemical conditions observed during sampling of phytoplankton and zooplankton communities. A) Wind-stress magnitudes, B) curl-driven upwelling rates, C) depths of the $25.5 \sigma_{\theta}$ isopycnal, and D) average nitrate concentrations above the nutricline measured during sampling of phytoplankton community size structure.

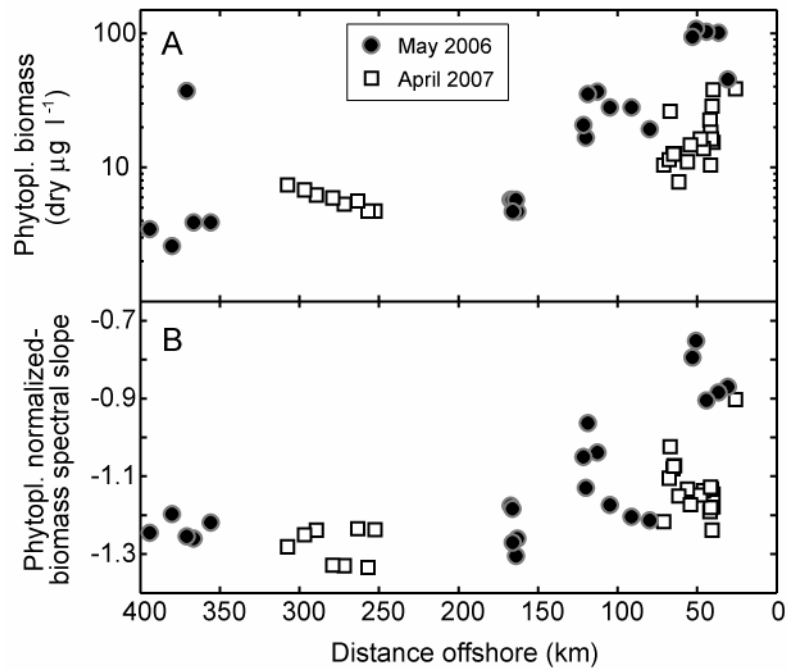


Figure 3.3. Measures of biomass and size structure of the phytoplankton community. A) Phytoplankton concentration was estimated from measures of chlorophyll *a* content and carbon:chlorophyll *a* ratio. B) Slope of the normalized-biomass spectrum for phytoplankton was estimated by chlorophyll *a* fractionation using a series of filters. Phytoplankton size fractionation data are courtesy of R. Goericke.

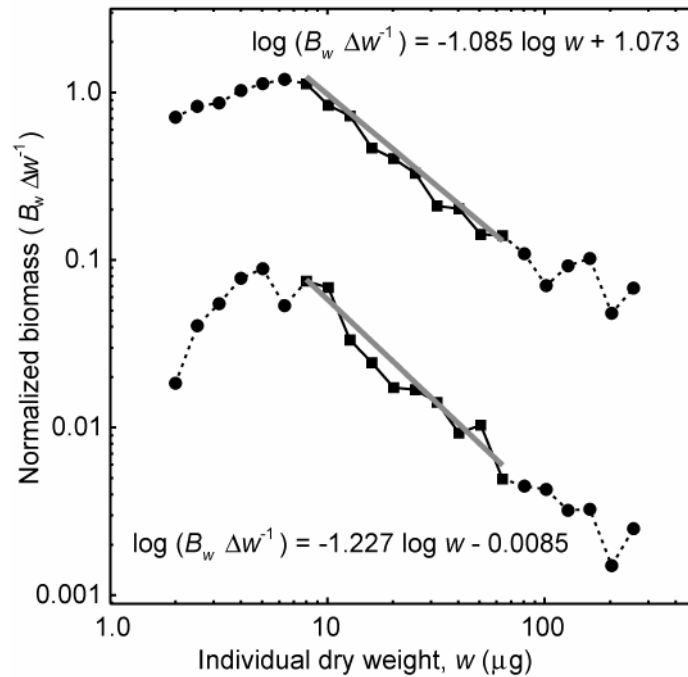


Figure 3.4. Typical normalized-biomass spectra. The upper example is the spectrum from a sample collected in 2007 in the nearshore region (38 km from the coast), and the lower example is from a sample collected in 2006 from the offshore region (385 km from the coast). The straight lines and equations estimate the normalized-biomass spectra over the size ranging from 8 to 80 μg . Dotted lines and circles indicate data excluded from the calculation of biomass spectral slopes. Individuals less than about 8 μg dry weight were incompletely retained by the 202- μm mesh net. Individuals larger than 80 μg dry weight were absent in some samples.

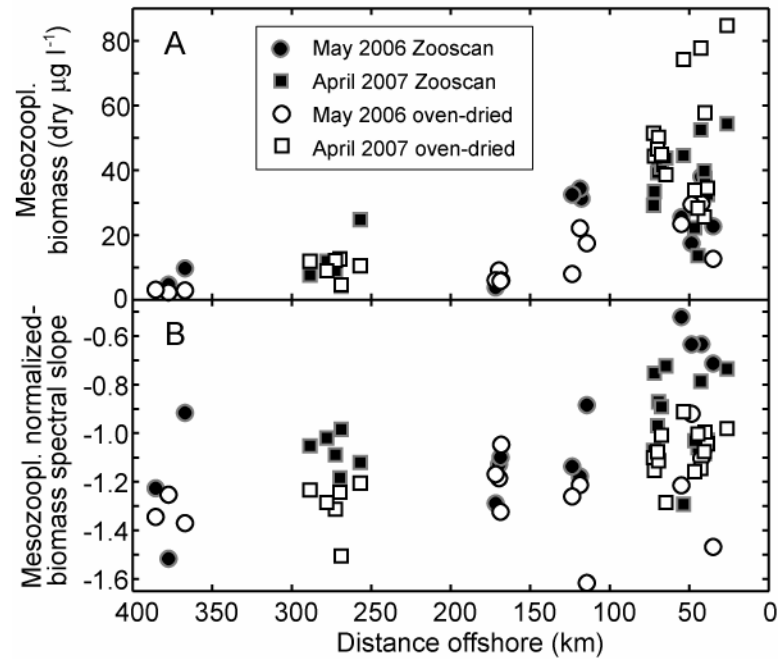


Figure 3.5. Mesozooplankton community biomass and size structure estimated by different methods. Solid symbols indicate estimates of Zooscan analysis, as described in this manuscript. Open symbols indicate estimates by mesh fractionation and oven drying (Rykaczewski and Checkley 2008). A) Estimates of mesozooplankton biomass and B) normalized-biomass spectral slope show similar trends with distance offshore.

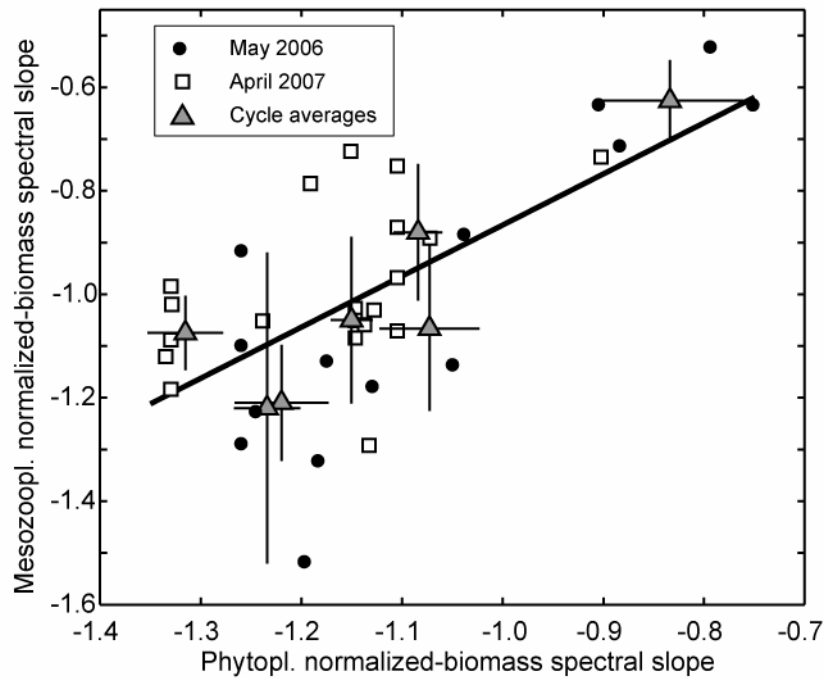


Figure 3.6. Comparison of biomass spectral slopes between phytoplankton and mesozooplankton communities observed together in the CCE. The slopes of the mesozooplankton spectra increase with increases in the phytoplankton spectral slope. The line indicates the linear best fit (mesozoopl. slope = $0.99 \cdot$ phytopl. slope + 0.12, $r = 0.66$, $p < 0.05$). Triangles indicate averages for the seven experimental cycles with an indication of standard deviation among samples at each location.

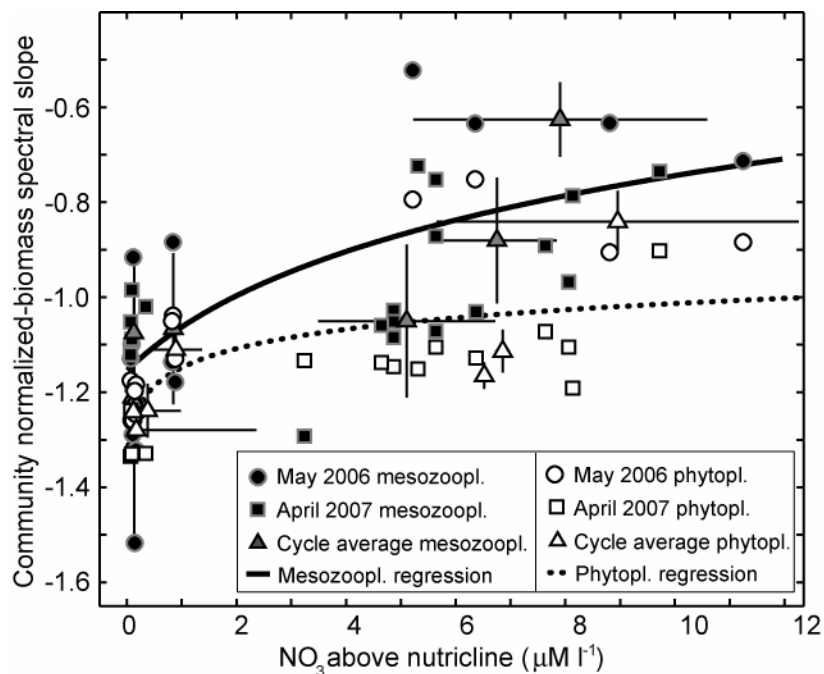


Figure 3.7. Estimates of normalized-biomass spectral slopes for phytoplankton and mesozooplankton communities observed in the CCE. The dotted line indicates the logarithmic best-fit line for the relationship between nitrate concentration and phytoplankton spectral slope (slope = $0.06 \ln([\text{NO}_3] + 0.05) - 1.15$; $r = 0.71$, $p < 0.05$).

The solid line is the logarithmic best fit between nitrate concentration and mesozooplankton spectral slope (slope = $0.23 \cdot \ln([\text{NO}_3] + 2.05) - 1.32$; $r = 0.66$, $p < 0.05$). Triangles indicate averages at experimental cycle locations with an indication of standard deviation among samples at each location.

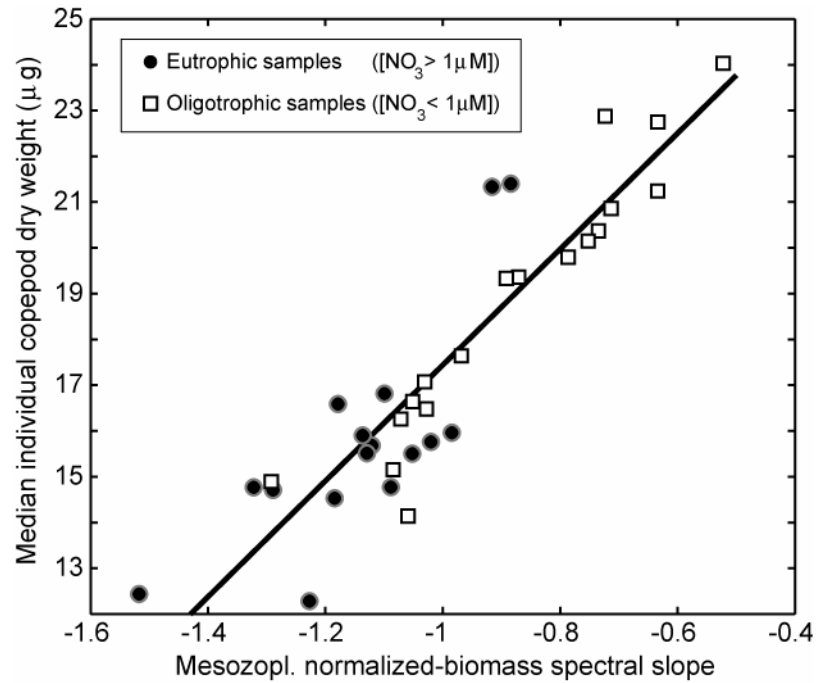


Figure 3.8. Median dry weights of individual copepods in relation to the spectral slope of the mesozooplankton community. Copepods were the most dominant taxa present in both oligotrophic and eutrophic samples, and changes in the sizes of individual copepods were largely responsible for the changes observed in spectral slope. The dark line is the linear best fit (individual weight = $12.7 \cdot \text{slope} + 30.1$; $r = 0.91$, $p < 0.05$).

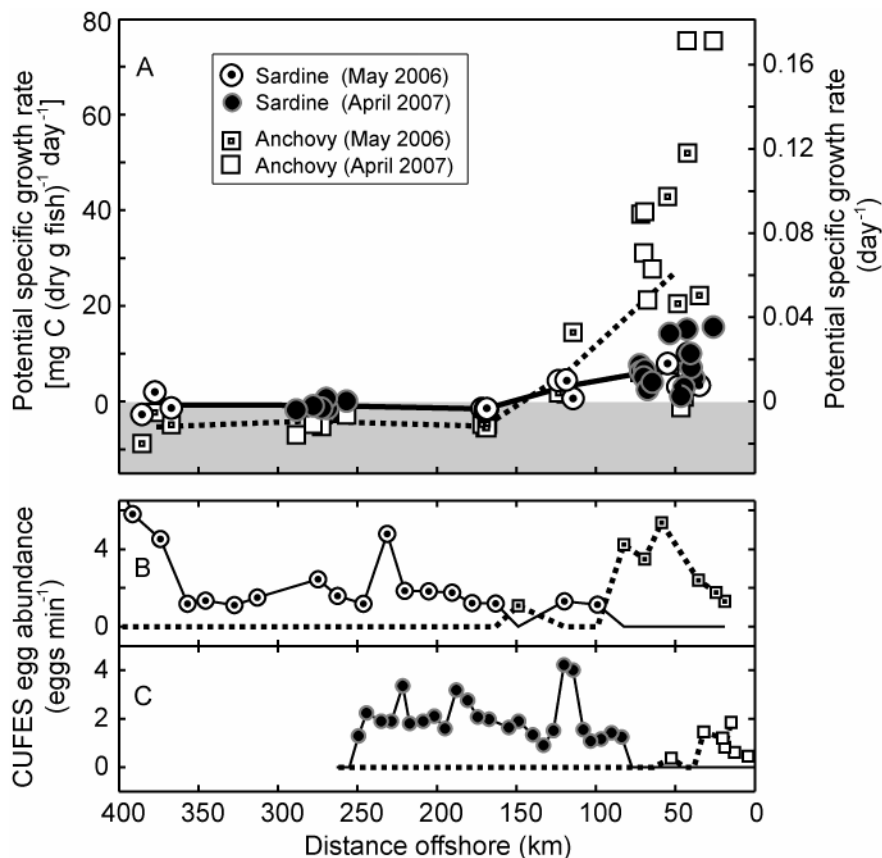


Figure 3.9. Egg distributions and potential, specific growth rate of individual sardine and anchovy for the plankton conditions observed during cruises in May 2006 and April 2007 off of Pt. Conception, CA. A) Specific growth rate is expressed both in units of $\text{mg C (dry g fish)}^{-1} \text{ day}^{-1}$ (left axis) and as day^{-1} (right axis), assuming $0.44 \text{ g C (dry g fish)}^{-1}$. The solid (representing sardine) and dotted (anchovy) black lines connect averages at 50-km intervals using data from both years. The shaded region indicates the region of negative growth. Distributions of sardine and anchovy eggs off of Pt. Conception are shown for CalCOFI cruises in spring 2006 (B) and 2007 (C) as sampled by the Continuous Underway Fish Egg Counter (CUFES). Note the absence of anchovy eggs is approximately coincident with the location of negative growth rate for anchovy. Sardine eggs are distributed widely in the offshore region where there is some potential for positive growth. Eggs were not sampled offshore of 250 km in spring 2007.

3.8. References

- Alheit, J. and Niquen, M. (2004) Regime shifts in the Humboldt Current Ecosystem. *Prog. Oceanogr.* **60**:201-222.
- Bakun, A. and Broad, K. (2003) Environmental 'loopholes' and fish population dynamics: comparative pattern recognition with focus on El Niño effects in the Pacific. *Fish. Oceanogr.* **12**:458-473.
- Benfield, M.C., Grosjean, P., Culverhouse, P.F., Irigoien, X., Sieracki, M.E., Lopez-Urrutia, A., Dam, H.G., Hu, Q., Davis, C.S., Hansen, A., Pilskaln, C.H., Riseman, E.M., Schultz, H., Utgoff, P.E. and Gorsky, G. (2007) RAPID research on automated plankton identification. *Oceanogr.* **20**:172-187.
- Breiman, L. (2001) Random forests. *Mach. Learn.* **45**:5-32.
- Brett, J.R. and Groves, T.D.D. (1979) Physiological energetics. In: *Fish Physiology: Bioenergetics and Growth*. W.S. Hoar, D.J. Randall, J.R. Brett (eds.) New York: Academic Press, pp. 279–344.
- Buitenhuis, E., Le Quere, C., Aumont, O., Beaugrand, G., Bunker, A., Hirst, A., Ikeda, T., O'Brien, T., Piontkovski, S. and Straile, D. (2006) Biogeochemical fluxes through mesozooplankton. *Glob. Biogeochem. Cycles* **20**:doi:10.1029/2005GB002511.
- Chao, Y., Li, Z.J., Kindle, J.C., Paduan, J.D. and Chavez, F.P. (2003) A high-resolution surface vector wind product for coastal oceans: Blending satellite scatterometer measurements with regional mesoscale atmospheric model simulations. *Geophys. Res. Lett.* **30**:10.1029/2002GL015729.
- Checkley, D.M., Jr (1980) Food limitation of egg production by a marine, planktonic copepod in the sea off southern California. *Limnol. Oceanogr.* **25**:991-998.
- Checkley, D.M., Jr, Davis, R.E., Herman, A.W., Jackson, G.A., Beanlands, B. and Regier, L.A. (2008) Assessing plankton and other particles in situ with the SOLOPC. *Limnol. Oceanogr.* **53**:2123-2136.
- Checkley, D.M., Jr, Dotson, R.C. and Griffith, D.A. (2000) Continuous, underway sampling of eggs of Pacific sardine (*Sardinops sagax*) and northern anchovy (*Engraulis mordax*) in spring 1996 and 1997 off southern and central California. *Can. J. Fish. Aquat. Sci.* **47**:1139-1155.
- Chisholm, S.W. (1992) Phytoplankton size. In: *Primary Productivity and Biogeochemical Cycles in the Sea*. P.G. Falkowski, A.D. Woodhead (eds.) New York: Plenum, pp. 213–237.

- Emmett, R.L., Brodeur, R.D., Miller, T.W., Pool, S.S., Krutzikowsky, G.K., Bentley, P.J. and McCrae, J. (2005) Pacific sardine (*Sardinops sagax*) abundance, distribution, and ecological relationships in the Pacific Northwest. *CalCOFI Rep.* **46**:122-143.
- Franks, P.J.S. (1992) Sink or swim: accumulation of biomass at fronts. *Mar. Ecol. Prog. Ser.* **82**:1-12.
- Frost, B.W. (1974) Feeding processes at lower trophic levels in pelagic communities. In: *The Biology of the Oceanic Pacific*. C.B. Miller (ed.) Corvallis: Oregon State University Press, pp. 59-77.
- Gillooly, J.F. (2000) Effect of body size and temperature on generation time in zooplankton. *J. Plankton Res.* **22**:241-251.
- Gonzalez-Quiros, R. and Checkley, D.M. (2006) Occurrence of fragile particles inferred from optical plankton counters used in situ and to analyze net samples collected simultaneously. *J. Geophys. Res.* **111**:10.1029/2005JC003084.
- Grosjean, P., Picheral, M., Warembourg, C. and Gorsky, G. (2004) Enumeration, measurement, and identification of net zooplankton samples using the ZOOSCAN digital imaging system. *ICES J. Mar. Sci.* **61**:518-525.
- Hansen, B., Bjornsen, P.K. and Hansen, P.J. (1994) The size ratio between planktonic predators and their prey. *Limnol. Oceanogr.* **39**:395-403.
- Harris, R., Wiebe, P., Lenz, J., Skjoldal, H.R. and Huntley, M. (2000) *ICES Zooplankton Methodology Manual*. San Diego: Academic Press. pp. 90-94.
- Hill, K., Dorval, E., Lo, N.C.H., Macewicz, B.J., Show, C. and Felix-Uraga, R. (2008) Assessment of the Pacific sardine resource in 2008 for U.S. management in 2009. *U.S. Dep. Commer., NOAA Tech. Memo. Report No.* **413**, 176 pp.
- Hopcroft, R.R., Clarke, C. and Chavez, F.P. (2002) Copepod communities in Monterey Bay during the 1997-1999 El Niño and La Niña. *Prog. Oceanogr.* **54**:251-264.
- Hopcroft, R.R., Roff, J.C. and Chavez, F.P. (2001) Size paradigms in copepod communities: a re-examination. *Hydrobiologia* **453**:133-141.
- Hopcroft, R.R., Roff, J.C., Webber, M.K. and Witt, J.D.S. (1998) Zooplankton growth rates: the influence of size and resources in tropical marine copepodites. *Mar. Biol.* **132**:67-77.

- Hunter, J.R. and Leong, R. (1981) The spawning energetics of female northern anchovy, *Engraulis mordax*. *Fish. Bull.* **79**:215-230.
- Huyer, A. (1983) Coastal upwelling in the California Current System. *Prog. Oceanogr.* **12**:259-284.
- Jacobson, L.D., De Oliveira, J.A.A., Barange, M., Cisneros-Mata, M.A., Felix-Uraga, R., Hunter, J.R., Kim, J.Y., Matsuura, Y., Niquen, M., Porteiro, C., Rothschild, B., Sanchez, R.P., Serra, R., Uriarte, A. and Wada, T. (2001) Surplus production, variability, and climate change in the great sardine and anchovy fisheries. *Can. J. Fish. Aquat. Sci.* **58**:1891-1903.
- James, A.G. (1987) Feeding ecology, diet and field-based studies on feeding selectivity of the cape anchovy *Engraulis capensis* Gilchrist. *S. Afr. J. Mar. Sci.* **5**:673-692.
- James, A.G. and Findlay, K.P. (1989) Effect of particle-size and concentration on feeding behavior, selectivity and rates of food ingestion by the cape anchovy *Engraulis capensis*. *Mar. Ecol. Prog. Ser.* **50**:275-294.
- James, A.G., Probyn, T. and Hutchings, L. (1989) Laboratory-derived carbon and Nitrogen budgets for the omnivorous planktivore *Engraulis capensis* Gilchrist. *J. Exp. Mar. Biol. Ecol.* **131**:125-145.
- King, A.L. and Barbeau, K. (2007) Evidence for phytoplankton iron limitation in the southern California Current System. *Mar. Ecol. Prog. Ser.* **342**:91-103.
- Koslow, J.A. (1981) Feeding selectivity of schools of northern anchovy, *Engraulis mordax*, in the Southern California Bight. *Fish. Bull.* **79**:131-142.
- Lasker, R. (1970) Utilization of zooplankton energy by a Pacific sardine population in the California Current. In: *Marine Food Chains*. J.H. Steele (ed.) Los Angeles, CA: University of California Press, pp. 265-284.
- Lavaniegos, B.E. and Ohman, M.D. (2007) Coherence of long-term variations of zooplankton in two sectors of the California Current System. *Prog. Oceanogr.* **75**:42-69.
- Legendre, L. and Michaud, J. (1998) Flux of biogenic carbon in oceans: size-dependent regulation by pelagic food webs. *Mar. Ecol. Prog. Ser.* **164**:1-11.
- Leong, R.J.H. and O'Connell, C.P. (1969) A laboratory study of particulate and filter feeding of northern anchovy (*Engraulis mordax*). *J. Fish. Res. Board Can.* **26**:557-582.

- Lindley, J.A., Robins, D.B. and Williams, R. (1999) Dry-weight carbon and nitrogen content of some euphausiids from the north Atlantic Ocean and the Celtic Sea. *J. Plankton Res.* **21**:2053-2066.
- Louw, G.G., van der Lingen, C.D. and Gibbons, M.J. (1998) Differential feeding by sardine *Sardinops sagax* and anchovy *Engraulis capensis* recruits in mixed shoals. *S. Afr. J. Mar. Sci.* **19**:227-232.
- MacCall, A.D. (1990) *Dynamic Geography of Marine Fish Populations*. Seattle: Washington Sea Grant, Washington University Press, Inc., pp. 153.
- Mantyla, A.W., Venrick, E.L. and Hayward, T.L. (1995) Primary production and chlorophyll relationships, derived from ten years of CalCOFI measurements. *CalCOFI Rep.* **36**:159-166.
- Moloney, C.L. and Field, J.G. (1991) The size-based dynamics of plankton food webs: 1 - A simulation-model of carbon and nitrogen flows. *J. Plankton Res.* **13**:1003-1038.
- Morel, F.M.M., Hudson, R.J.M. and Price, N.M. (1991) Limitation of productivity by trace-metals in the sea. *Limnol. Oceanogr.* **36**:1742-1755.
- Mullin, M.M. (1998) Interannual and interdecadal variation in California Current zooplankton: *Calanus* in the late 1950s and early 1990s. *Global Change Biology* **4**:115-119.
- Mullin, M.M., Sloan, P.R. and Eppley, R.W. (1966) Relationship between carbon content, cell volume, and area in phytoplankton. *Limnol. Oceanogr.* **11**:307-311.
- O'Connell, C.P. (1972) The interrelation of biting and filtering in the feeding activity of the northern anchovy (*Engraulis mordax*). *J. Fish. Res. Board Can.* **29**:285-293.
- Platt, T. and Denman, K. (1978) The structure of pelagic marine ecosystems. *Rapp. P.-V. Réun. Cons. Int. Explor. Mer.* **173**:60-65.
- Poulin, F.J. and Franks, P.J.S. (in press) Size-structured planktonic ecosystems: constraints, controls, and assembly instructions. *J. Plankton Res.*
- Razouls, C., de Bovée, F., Kouwenberg, J. and Desreumaux, N. (2009) Diversity and geographic distribution of marine planktonic copepods. <http://copepodes.obs-banyuls.fr/en>.

- Rebstock, G.A. (2002) Climatic regime shifts and decadal-scale variability in calanoid copepod populations off southern California. *Global Change Biology* **8**:71-89.
- Riegman, R., Kuipers, B.R., Noordeloos, A.A.M. and Witte, H.J. (1993) Size-differential control of phytoplankton and the structure of plankton communities. *Neth. J. Sea Res.* **31**:255-265.
- Rodriguez, J., Tintore, J., Allen, J.T., Blanco, J.M., Gomis, D., Reul, A., Ruiz, J., Rodriguez, V., Echevarria, F. and Jimenez-Gomez, F. (2001) Mesoscale vertical motion and the size structure of phytoplankton in the ocean. *Nature* **410**:360-363.
- Runge, J.A. (1985) Relationship of egg production of *Calanus pacificus* to seasonal changes in phytoplankton availability in Puget Sound, Washington. *Limnol. Oceanogr.* **30**:382-396.
- Ryaczewski, R.R. and Checkley, D.M. (2008) Influence of ocean winds on the pelagic ecosystem in upwelling regions. *Proc. Natl. Acad. Sci. U. S. A.* **105**:1965-1970.
- San Martin, E., Harris, R.P. and Irigoien, X. (2006) Latitudinal variation in plankton size spectra in the Atlantic Ocean. *Deep-Sea Res. Part II Top. Stud. Oceanogr.* **53**:1560-1572.
- Satapoomin, S. (1999) Carbon content of some common tropical Andaman Sea copepods. *J. Plankton Res.* **21**:2117-2123.
- Smith, R.L. (1968) Upwelling. *Oceanogr. Mar. Biol. Ann. Rev.* **6**:11-46.
- Star, J.L. and Mullin, M.M. (1981) Zooplanktonic assemblages in three areas of the North Pacific as revealed by continuous horizontal transects. *Deep-Sea Res. Part I Top. Stud. Oceanogr.* **28**:1303-1322.
- Strickland, J.D.H. (1960) Measuring the production of marine phytoplankton. *Bull. Fish. Res. Board Can.* **122**:1-172.
- Uye, S. (1982) Length–weight relationships of important zooplankton from the Inland Sea of Japan. *J. Oceanogr. Soc. Japan* **38**:149–158.
- van der Lingen, C.D. (1994) Effect of particle size and concentration on the feeding behavior of adult pilchard *Sardinops sagax*. *Mar. Ecol. Prog. Ser.* **109**:1-13.
- van der Lingen, C.D. (1995) Respiration rate of adult pilchard *Sardinops sagax* in relation to temperature, voluntary swimming speed and feeding behaviour. *Mar. Ecol. Prog. Ser.* **129**:41-54.

- van der Lingen, C.D. (1999) The feeding ecology of, and carbon and nitrogen budgets for, sardine *Sardinops sagax* in the southern Benguela upwelling system. Ph.D. thesis. University of Cape Town, Cape Town.
- van der Lingen, C.D., Bertrand, A., Bode, A., Brodeur, R., Cubillos, L.A., Espinoza, P., Friedland, K., Garrido, S., Irigoien, X., Miller, T., Möllmann, C., Rodriguez-Sanchez, R., Tanaka, H. and Temming, A. (in press) Trophic dynamics. In: *Climate Change and Small Pelagic Fish*. D.M. Checkley, Jr., J. Alheit, Y. Oozeki, C. Roy (eds.) Cambridge: Cambridge University Press.
- van der Lingen, C.D., Hutchings, L. and Field, J.G. (2006) Comparative trophodynamics of anchovy *Engraulis encrasicolus* and sardine *Sardinops sagax* in the southern Benguela: are species alternations between small pelagic fish trophodynamically mediated? *Afr. J. Mar. Sci.* **28**:465-477.
- Venrick, E.L. (1972) Small-scale distributions of oceanic diatoms. *Fish. Bull.* **70**:363-372.
- Watanabe, Y. and Saito, H. (1998) Feeding and growth of early juvenile Japanese sardines in the Pacific waters off central Japan. *J. Fish Biol.* **52**:519-533.
- Zhou, M. and Huntley, M.E. (1997) Population dynamics theory of plankton based on biomass spectra. *Mar. Ecol. Prog. Ser.* **159**:61-73.

Chapter 4. Influence of ocean winds on the pelagic ecosystem in upwelling regions

4.1. Abstract

Upwelling of nutrient-rich, subsurface water sustains high productivity in the ocean's eastern boundary currents. These ecosystems support a rate of fish harvest nearly 100 times the global mean and account for more than 20% of the world's marine fish catch. Environmental variability is thought to be the major cause of the decadal-scale biomass fluctuations characteristic of fish populations in these regions, but the mechanisms relating atmospheric physics to fish production remain unexplained. Two atmospheric conditions induce different types of upwelling in these ecosystems: coastal, alongshore wind stress, resulting in rapid upwelling (with high vertical velocity, w); and wind-stress curl, resulting in slower upwelling (low w). We show that the level of wind-stress curl has increased and that production of Pacific sardine (*Sardinops sagax*) varies with wind-stress curl over the past six decades. The extent of isopycnal shoaling, nutricline depth, and chlorophyll concentration in the upper ocean also correlate positively with wind-stress curl. The size structure of plankton assemblages is related to the rate of wind-forced upwelling, and sardine feed efficiently on small plankters generated by slow upwelling. Upwelling rate is a fundamental determinant of the biological structure and production in coastal pelagic ecosystems, and future changes in the magnitude and spatial gradient of wind stress may have important and differing effects on these ecosystems. Understanding of the

biological mechanisms relating fisheries production to environmental variability is essential for wise management of marine resources under a changing climate.

4.2. Introduction

Worldwide, populations of sardine (*Sardinops* spp. and *Sardina* spp.) and anchovy (*Engraulis* spp.) have varied greatly over time, with plentiful catches of one often alternating with the other on the scale of decades (Lluch-Belda *et al.* 1989). These fluctuations have severe consequences to the fishing, processing, and farming (*e.g.*, poultry, swine, and tuna) industries dependent on the fisheries' landings for income and feed. Since these small pelagic fish often dominate the intermediate trophic level in upwelling ecosystems, their populations are crucial to the transfer of energy and biomass from lower to higher trophic levels (Cury *et al.*). Despite more than 50 years of effort and focused oceanographic research, a mechanistic explanation for the large variability in Pacific sardine and northern anchovy populations in the California Current Ecosystem (CCE) remains obscure. Sediment records suggest that similar fluctuations occurred over the two millennia prior to the development of commercial fisheries (Baumgartner *et al.* 1992). The changes in sardine and anchovy abundance during the past century are therefore thought to reflect natural environmental variability, exacerbated by fishing pressure (Hsieh *et al.* 2006).

Understanding of the mechanisms relating these population fluctuations to environmental variability has not progressed past empirical observations associating sardine and anchovy biomass with temperature (Lluch-Belda *et al.* 1989, Chavez *et al.* 2003). Warm periods, favorable for sardine production, occurred most recently from

the 1920s to the mid-1940s and from 1977 through the present. A cool period, favorable for anchovy, occurred from the mid-1940s through 1976 (Lluch-Belda *et al.* 1989, Chavez *et al.* 2003). A shift to another cool period may have occurred after the 1997-1998 El Niño (Peterson and Schwing 2003). Identification of warm and cold periods favorable for sardine and anchovy production has been important in describing multidecadal changes in pelagic fisheries, but this description does not provide the understanding necessary to predict how populations will vary under future conditions. Since cold periods are often associated with increased coastal upwelling and nutrient supply along the coast, the growth observed in the anchovy population during these phases is expected. However, the paradoxical growth of a massive sardine population (up to four times larger than the maximal anchovy population) during warm periods with weak coastal upwelling has puzzled fisheries oceanographers for decades (Baumgartner *et al.* 1992, Bakun and Broad 2003).

To investigate the relationship between climate and sardine growth in the CCE, we considered the two mechanisms by which winds supply surface waters with the nutrients required for biological production: “coastal upwelling” due to alongshore wind stress and “curl-driven upwelling” due to wind-stress curl. The importance of coastal upwelling to major fisheries production has long been recognized (Ryther 1969). In the traditional view of coastal upwelling ecosystems, biological productivity at all levels of the food web is attributed to persistent, alongshore, and equatorward wind stress in spring and summer. These winds force water away from the coastal boundary, a process known as Ekman transport. Nutrient-rich waters are drawn up into the euphotic zone to replace the surface waters that are forced offshore.

Curl-driven upwelling may also act as a significant source of nutrients in coastal pelagic ecosystems (Yoshida and Mao 1957, Chelton 1982, Pickett and Paduan 2003, Chelton *et al.* 2004, Pickett and Schwing 2006) and is responsible for the shoaling of isopycnals in the southern CCE during summer (Di Lorenzo 2003). Horizontal shear in the wind stress (wind-stress curl) over the open ocean results in a divergence of Ekman transport that is balanced by vertical transport. While most areas of the subtropical ocean gyres are regions of anti-cyclonic wind-stress curl (downwelling), the eastern edge of the gyres (*i.e.*, inshore of the wind-stress maximum) are zones of cyclonic wind-stress curl and upwelling (Chelton 1982, Chelton *et al.* 2004). Small areas of intense, positive wind-stress curl occur in the lee of major headlands leading to curl-driven upwelling with vertical velocity (w) comparable to the high w associated with coastal upwelling (Pickett and Schwing 2006). However, the average w associated with curl-driven upwelling is slow, typically several times smaller than w associated with coastal upwelling in the CCE (Dever *et al.* 2006). The expansive regions of positive curl over the open ocean are the result of two characteristics of the eastern North Pacific: 1) the large-scale change in the orientation of the west coast of North America, from a coastline trending north to south poleward of 40° N latitude to a coastline oriented northwest to southeast in southern California; and 2) the location of the maximal gradient between the pressure systems over the North Pacific and southwest United States (Bakun and Nelson 1991, Edwards *et al.* 2001). Because these areas of positive curl are large compared to the coastal boundary region, the volume of water upwelled by slow, curl-driven upwelling is greater than that upwelled by coastal upwelling or by fast, curl-driven upwelling

near the coast (Dever *et al.* 2006). The intensity of offshore, curl-driven upwelling is hypothesized to be related to the location of the large-scale pressure systems with respect to the coastline of California (Edwards *et al.* 2001).

We expect the type of biological production resulting from coastal and curl-driven upwelling to differ, with high w resulting in larger phytoplankters and low w favoring smaller phytoplankters. The demand for nutrients by a phytoplankton cell is typically a function of cell volume, while the maximal uptake rate is a function of the cell's surface area. For this reason, smaller cells, with higher surface-area:volume ratios, have a competitive advantage in nutrient-limited environments (Margalef 1978, Falkowski and Oliver 2007). The increased nutrient concentrations in vigorously upwelling waters (high w) reduces nutrient limitation and the competitive advantage of small cells, allowing populations of large cells with lower surface-area:volume ratios to develop. Given that prey size correlates positively with predator size (Moloney and Field 1991), larger zooplankters are favored in areas with larger phytoplankters and higher w (Fig.1).

Temporal variability in coastal and curl-driven upwelling may affect populations of planktivorous predators by influencing production of small and large plankters. Pacific sardine spawn in offshore waters, away from areas of coastal upwelling (Checkley *et al.* 2000), and adult and juvenile sardine have a fine mesh of gill rakers with specialized denticles to retain planktonic prey as small as 10 μm in diameter (van der Lingen *et al.*). Even as larvae, sardine appear to specialize on small plankters and are prevented from capturing larger prey by a small mouth-gape diameter (Arthur 1976, van der Lingen *et al.*). In comparison, anchovy spawn near the

coast (Checkley *et al.* 2000) and use coarse gill rakers to capture larger prey (van der Lingen *et al.* 2006). We hypothesize that changes in sardine population growth are related to the production of small plankters and the magnitude of curl-driven upwelling in the CCE. To test this hypothesis, we posed the following questions: Is zooplankter size related to upwelling rate? Have winds favoring curl-driven and coastal upwelling changed over decades and, if so, have these changes influenced hydrography, nutrient supply, and biological production? We examined zooplankter sizes across a gradient of upwelling rates and compared estimates of historical upwelling with concurrent measurements of water-column density, nutricline depth, chlorophyll concentration, and sardine production.

4.3. Methods

4.3.1. May 2006 and April 2007 cruise data

Zooplankton samples were collected during research cruises in May 2006 and June 2007 as part of the CCE Long-Term Ecological Research program. Cruises were structured to sample across the CCE, ranging from areas of coastal upwelling to offshore, oligotrophic areas. Zooplankton were sampled using a BONGO net of 202- μ m-Nitex mesh, towed obliquely to 210 m (depth permitting) between 2100-0400 hours following the strict protocol of the CalCOFI program (Ohman and Smith 1995). Three-eighths of the sample from one BONGO codend was wet sieved through nested screens of 5000, 2000, 1000, 505, and 202 μ m, and dry masses in each size class were determined (Harris *et al.* 2000). A linear least-squares line was fit to approximate the biomass-size spectrum for each sample according to the following formula:

$$\log \frac{B_x}{\Delta x} = m[\log(x)] + b,$$

where B_x is the sample biomass retained on a filter of mesh size x , Δx is the size interval for each fraction (taken here as 5000, 3000, 1000, 495, and 303 μm), and m and b are the slope and y-intercept of the linear, best-fit line.

Wind-stress data collected by the SeaWinds Scatterometer were used to estimate w . For two sampling stations near the coast where scatterometer data are invalid, wind stresses were estimated using data from the shipboard anemometer and moored buoys operated by the National Data Buoy Center. A standard algorithm was used to convert wind speed to wind stress (Yelland *et al.* 1998). Coastal and curl-driven upwelling rates were calculated as described below and averaged over five days prior to zooplankton collection.

4.3.2. Historic upwelling estimates

We used output from a dynamically downscaled model of historic winds (1948-2005) from the National Centers for Environmental Prediction and National Center for Atmospheric Research (NCEP/NCAR) Reanalysis. This model, known as CaRD10 (California Reanalysis Downscaling at 10 km) produces fine-scale, thermodynamically consistent atmospheric variables without deviation from the original NCEP/NCAR reanalysis data (Kanamitsu and Kanamaru 2007). CaRD10 was chosen for use in this analysis because it is the only atmospheric model offering the ability to examine mesoscale variability in curl-driven upwelling at multidecadal scales. The CaRD10 model covers a large spatial area and offers a historical

perspective unparalleled by models of similar resolution. In comparison to observed wind speed, the CaRD10 model shows significant improvement over other models which offer a historical perspective at lower resolution. This improvement is especially evident in the coastal ocean (Kanamitsu and Kanamaru 2007). We recognize that wind stress at the coast is difficult to model, even with grids of higher resolution. However, we feel that the CaRD10 model provides the best available data on the spatial and temporal scales relevant to the sardine habitat in the southern CCE.

Upwelling transport is defined as the upward movement of a volume of water per unit time and results from two different processes: curl-driven upwelling or coastal upwelling. We used monthly averages of surface wind stress (N m^{-2}) produced by the CaRD10 model to calculate the vertical velocity, w_{curl} (m s^{-1} positive upward), of curl-driven upwelling at the base of the mixed layer (Smith 1968):

$$w_{\text{curl}} = \frac{I}{\rho_w f} \nabla \times \tau ,$$

where $\nabla \times \tau$ is the curl of the wind-stress field, ρ_w is seawater density (taken as 1024 kg m^{-3}), and f is the Coriolis parameter. Wind-stress derivatives used in the calculation of curl at a given grid point were taken as the difference between wind stresses at adjacent grid points.

Coastal upwelling due to seaward Ekman transport was also calculated using output from the CaRD10 model. T , the volume of Ekman transport per meter of coastline ($\text{m}^3 \text{ s}^{-1}$ per meter of coast), was estimated (Smith 1968):

$$T = \frac{\tau_a}{\rho_w f} ,$$

where τ_a is alongshore wind stress within 10 km of the coastline. Conservation of mass requires that volume transport by coastal upwelling be equivalent to T . This volume transport was divided by the local Rossby radius of deformation, R_d , to yield a mean vertical velocity of coastal upwelling, w_{coast} (m s^{-1}):

$$w_{coast} = \frac{T}{R_d}.$$

Based on earlier studies in the region, a Rossby radius of 10 km was used in the calculation (Pickett and Paduan 2003, Pickett and Schwing). Upwelling by each mechanism was integrated over the spatial domain to generate indices of upwelling transport by coastal and curl-driven upwelling. The relative magnitudes of coastal and curl-driven upwelling are subject to the R_d used as the location of the boundary between coastal and curl-driven upwelling processes. However, variation in the two time series is not influenced by changes in the boundary location.

4.3.3. Historic hydrographic, chemical, and biological measurements

Temperature, salinity, and concentrations of nitrate and chl a have been regularly measured by the CalCOFI program since 1984 (Hayward 2000). We defined the nutricline depth as the first depth at which nitrate concentration exceeded $1.0 \mu\text{mol l}^{-1}$. Chl a concentration was that measured at 10 m. CalCOFI measurements of temperature, salinity, and pressure at 50 m were used to estimate σ_θ (Gill 1982). These measures of nutricline depth, chl a , and σ_θ were averaged over the standard CalCOFI sampling grid (*i.e.*, lines 76.7 to 93.3 and from station 90.0 to the coast) to yield a mean value for each cruise. Historic upwelling transport was averaged from

June-August for comparison with density, nutricline depth, and chl *a* concentration. This period encompasses the range of summertime CalCOFI sampling (except for 1985 and 1986, when CalCOFI cruises occurred in September). Temperature and salinity at 50 m were sampled by the CalCOFI surveys prior to 1983.

4.3.4. Historic SST

The SST data were from the Comprehensive Oceanographic–Atmospheric Data Set (Woodruff *et al.* 1987) and covered the spatial domain used in the upwelling estimation. Resolution of the data was $1^\circ \times 1^\circ$ from 1960-present and $2^\circ \times 2^\circ$ from 1948-1959.

4.3.5. Pacific sardine production

Stock assessments have been performed for sardine since 1982 using an age-structured population model incorporating both fishery-dependent and fishery-independent data (US Department Commerce, Technical Memorandum NOAA-TM-NMFS-SWFSC-396). Using these data, annual surplus production (ASP) was calculated for the sardine stock from 1983-2004. ASP is as a measure of annual growth in the total biomass of the stock and is largely a function of the recruitment of young fish. ASP in year t is approximated as

$$ASP_t = (b_{0,t} + \delta C_{0,t}) + (b_{1+,t} - b_{1+,t-1} + \delta C_{1+,t}),$$

where $b_{a,t}$ and $C_{a,t}$ are the biomass and catch of age a fish at time t (age 0 fish are those between 0 and 1 year old; age 1+ fish are those older than 1 year), and δ is a catch adjustment factor (0.83) as estimated empirically for the California stock of Pacific

sardine (Jacobson *et al.* 2005). The catch adjustment factor converts the catch during the preceding fishing season to its biomass estimated at the end of the fishing season had the fish remained in the population. This accounts for the portion (δ) of captured fish that would have survived to the end of the fishing season had they not been harvested. Surplus production per unit biomass was calculated by dividing ASP by the biomass of sardine at ages 1+. The time series of surplus production per unit biomass showed a declining trend as the sardine biomass expanded in the 1980s and 1990s. This trend is likely a result of the decrease in recruitment per spawner that is characteristic of an increasing fish population (density-dependent recruitment) and is independent of environmental variability (Beverton and Holt). This linear trend in the time series was removed before comparison with upwelling estimates to prevent correlation based solely on the long-term trend resulting from density-dependent changes in recruitment.

We limited our calculation of surplus production per unit biomass to the period since 1983 when the stock assessment methods have been consistent and incorporated both fishery-independent and fishery-dependent data. No stock assessment for sardine was conducted from 1963-1981. The stock assessments performed prior to 1963 were based on fishery-dependent data (MacCall 1979). We used previously calculated estimates of ASP for the sardine stock from 1948-1962 (Jacobson *et al.* 2005).

4.3.6. Population modeling

We modified the Fox surplus production model so that the carrying capacity of the population varies annually as a function of environmental conditions (Fox 1970).

The conventional Fox model estimates ASP in year t as follows:

$$ASP_t = rB_t \left(1 - \frac{\ln[B_t]}{\ln[K]} \right),$$

where r is the intrinsic rate of increase, B_t is the stock biomass (ages 1+), and K is a constant equal to B_{max} , the population carrying capacity. To construct an EDSP model, an environmentally dependent variable (related to upwelling or SST) was included in the equation such that the carrying capacity K was a function of the environmental condition in year t as well as the population carrying capacity, B_{max} :

$$K = B_{max} (E_t + \alpha),$$

where E_t is an index of environmental condition and α is a constant scaling parameter. Parameters r , B_{max} , and α (each greater than zero) are estimated during the model fitting procedure. This model structure assumes that the environmental variables are positively related to ASP in the sardine population.

Since survival through larval and early juvenile life stages is thought to be a major determinant of stock recruitment (Jennings *et al.* 2001), sardine production is likely affected more by environmental conditions in the first months after the hatching of larvae than by conditions throughout the entire year. Instead of comparing annual fish production with upwelling estimates averaged over a 12-month period, estimates from each period of three consecutive months were averaged to generate annual time series of conditions specific to each three-month period. Each time series was

standardized by subtracting the minimum value and dividing by the standard deviation. The resulting standardized time series was included in the EDSP model as E_t . Model parameters and performance were determined by minimizing the sum of squared deviations between the modeled and observed ASP.

In the stepwise regression procedure, the environmental time series explaining most of the variability in surplus production per unit biomass was included in as the first explanatory time series in the model. Additional environmental time series were included only if inclusion significantly improved model fit ($p < 0.05$).

4.4. Results and discussion

4.4.1. Plankter sizes and upwelling

A combination of data from the SeaWinds Scatterometer and shipboard and moored anemometers were used to compare w resulting from upwelling with the size of zooplankters. Zooplankton were collected during two cruises in May 2006 and April 2007 at locations spanning the CCE west of Pt. Conception, California (Figure 4.2). A normalized biomass spectrum was estimated for the zooplankton collected at each station (Platt and Denman 1978). The slope of the spectrum increased as w increased (Figure 4.3), indicating that zooplankters are relatively larger in areas of coastal upwelling (high w) and smaller in areas of curl-driven upwelling (low w). A similar result has been found for phytoplankton in the CCE; larger phytoplankters are found nearshore where the nutricline is shallow, and smaller phytoplankters are dominant where the nutricline is deep (Mullin 1998).

4.4.2. Historic upwelling rates

To examine the temporal variability in coastal and curl-driven upwelling rates over the past 60 years, we used monthly averages of historic winds to calculate w of curl-driven and coastal upwelling. The geographic range of the analysis was limited to the waters off the southern and central California coasts (from Ensenada, Baja California to Santa Cruz, California), extending approximately 300 km offshore and encompassing the area of sardine spawning off of California (Figure 4.2). We found that regions of intense cyclonic curl are common during summer in the lee of prominent headlands and result in small areas of high w (3 to 7 m day⁻¹). High rates of coastal upwelling were also present at these headlands (w of 7 to 12 m day⁻¹). Further offshore, large regions of positive wind-stress curl and low w (0 to 1 m day⁻¹) were typical (Figure 4.4). These results are consistent with previous studies which have examined coastal and curl-driven upwelling over smaller temporal and spatial scales (Pickett and Paduan 2003, Koracin *et al.* 2004).

Although average w resulting from coastal upwelling is about an order of magnitude larger than w resulting from open-ocean, curl-driven upwelling, curl is more important to total upwelling transport because it covers a spatial area 18 to 22 times larger than the area of coastal upwelling. In our analysis, we found that wind-stress curl has been responsible for at least 60% (and up to 80%) of the annual, wind-forced upwelling transport in the southern CCE. Monthly time series of the two upwelling processes are significantly correlated ($p < 0.001$) and indicate that both coastal and curl-driven upwelling have increased since 1948. However, there are important distinctions between the two records. Vertical transport by curl-driven

upwelling abruptly increased during the winters of 1975 and 1976, and the level of curl-driven upwelling remained elevated through 2004. In contrast, the coastal upwelling record shows a smaller range of variation and no abrupt changes. Coastal upwelling declined after peaking in the early 1980s. Figure 4.5 compares w during two decades, 1950-1959 and 1990-1999.

4.4.3. Effects on water-column properties

The California Cooperative Oceanic Fisheries Investigations (CalCOFI) program has conducted quarterly surveys of temperature, salinity, chlorophyll *a* (chl *a*), and nutrients in the CCE since 1984. We compared the variability of these water-column properties to changes in upwelling during summertime cruises. We chose to focus on summer because this season corresponds to the late-larval and juvenile periods for spring-spawning sardine, and survival through these life stages is thought to be a major determinant of stock recruitment (Jennings *et al.* 2001). Also, by focusing on summer, we avoided the issue of inconsistent timing of the spring transition with respect to the springtime CalCOFI survey.

Nutricline depth and chl *a* concentration at 10 m showed significant correlation with curl-driven upwelling from 1984-2004 (Figure 4.6). The nutricline depth shoaled and the chl *a* concentration increased with increases in curl-driven upwelling. The correlations between these water-column properties and coastal upwelling became significant only when the linear trend was removed from each time series (Table 1). We emphasize that the trend should be considered since decadal-scale variability is known to be important. The change in correlation after removing

the trend indicates that consideration of decadal-scale changes in the CCE is essential to distinguish the effects of coastal and curl-driven upwelling.

We estimated potential density (σ_θ) of the upper water column using CalCOFI measurements of temperature and salinity from 1949 to the present. Surveys with reduced spatial or depth coverage ($< 70\%$ of the currently sampled area) were excluded from our analysis. There were two periods of sufficient sampling: 1950-1969 (16 summers) and 1978-2004 (22 summers). Our analysis indicates that the CCE has changed over the past six decades from a system where coastal upwelling is a major factor influencing σ_θ to a system where curl-driven upwelling controls σ_θ variability (Figure 4.6). Curl-driven upwelling is only correlated with σ_θ during the recent time period. In contrast, coastal upwelling is significantly correlated with σ_θ during the 1950s and 1960s (Table 1). These results are consistent with the observed increase in the contribution of wind-stress curl to the total amount of wind-forced upwelling since the 1950s.

A long-term decrease in density of the upper layers of the CCE is evident despite the increase in the total amount of wind-driven upwelling (Figure 4.6). This result is in conflict with our hypothesis relating increasing wind-driven upwelling with increasing density. Our analysis of historic winds cannot account for the decrease in density between the 1960s and 1980s, suggesting that other factors, in addition to winds, have influenced σ_θ over multidecadal time periods. Vertical heat flux into the surface layers of the CCE and lateral advection of warmer waters from the south increased sharply in the mid 1970s and may be responsible for the observed decline in

σ_0 (Miller *et al.* 1994, Di Lorenzo *et al.* 2005). Poleward transport in the CCE is related to positive wind-stress curl by Sverdrup balance (Munk 1950, Chelton 1982). Increasing levels of wind-stress curl may be associated with the poleward flux of warm waters and partially explain the differences in the relationship between σ_0 and upwelling at interannual and multidecadal scales.

4.4.4. Effects on sardine production

We compared coastal and curl-driven upwelling with surplus production per unit biomass in the sardine population over the past 22 years during which consistent stock-assessment methods have been in use. Curl-driven upwelling during late spring and summer (May-July) was positively correlated with surplus production per unit biomass. Sardine production and coastal upwelling were not correlated during these months (Figure 4.7). In addition, we examined the influence of coastal and curl-driven upwelling on surplus production per unit biomass by using a stepwise regression model. The model which included curl-driven upwelling during May-July explained a significant portion of the variance in production. Addition of coastal upwelling did not significantly improve model fit ($p > 0.05$). Curl-driven and coastal upwelling records were not correlated over this time period (Figure 4.7).

In addition, we compared the influence of coastal upwelling, curl-driven upwelling, and SST on sardine production using environmentally dependent surplus production (EDSP) models during two periods for which environmental and fisheries data are available: 1948-1962 and 1983-2004. Sea-surface temperature (SST) has been shown to be reasonably effective in explaining the dynamics of sardine biomass

in EDSP models (Jacobson *et al.* 2005), and we were interested in testing whether SST or a measure of upwelling produced the best estimate of sardine production. We found that use of curl-driven upwelling in the model produced the best fit to observed production during both periods (Figure 4.8). The model using SST as the environmental variable was more successful than that using coastal upwelling, and all three environmental variables performed better than the null model (which did not include environmental variability). The sum of squared deviations for the model using curl-driven upwelling was 0.30 MT^2 . Values for the models using SST and coastal upwelling were 0.44 MT^2 and 0.47 MT^2 , respectively. The null model resulted in a sum of squared deviations equal to 0.51 MT^2 .

While use of curl-driven upwelling in the EDSP models produced the best estimates of sardine production during both time periods, the months during which curl produced the best estimate shifted between 1948-1962 and 1983-2004. In the more recent period, use of curl-driven upwelling during May-July was optimal for estimating production and suggests that conditions during these months were most influential in determining sardine production. Since 1983, extensive spawning has occurred off of central and southern California in April (Smith 2005). May-July corresponds to the early life-history stages during which the environment has the strongest influence on survival (Jennings *et al.* 2001). Use of curl-driven upwelling during October, November, and December produced the best model performance during the 1948-1962 period. This result is consistent with the observation that spawning in autumn offshore of Baja California is more important to sardine production during periods of low population size (Smith 2005). The months of SST

and coastal upwelling that produced the best estimates of production also shifted from late summer and autumn during the 1958-1962 period to spring and early summer during the 1983-2004 period.

4.4.5. Consideration of other upwelling systems

The CCE is the only upwelling system with the environmental time series required to investigate wind-forced upwelling and the response of water-column properties and fisheries production at decadal and multidecadal scales. Observations of historic, oceanic winds depend on ship traffic, and the number of observations in the CCE is high compared to other eastern boundary currents (Bakun and Nelson 1991). Atmospheric models offering high-resolution estimates of wind stress over the past 60 years have not yet been developed in other regions of the globe. In addition, the long-term hydrographic datasets provided by the CalCOFI program are unique.

Wind-forced upwelling results in high primary and fisheries production in eastern boundary currents around the world (Ryther 1969), and the concepts presented here are applicable to each of these regions. However, the effects of coastal and curl-driven upwelling may vary with conditions specific to each area. For instance, latitudinal differences may have a significant influence on w and production of plankton and fish. The rate of curl-driven upwelling in the Humboldt Current Ecosystem (HCE) off the coast of Peru will be more than three times that in the CCE for a given wind-stress curl due to the difference in the Coriolis parameter with latitude. A wind-stress curl of $0.5 \cdot 10^{-6} \text{ N m}^{-3}$ at 35° N latitude in the CCE will result in w of 0.5 m day^{-1} . The same level of cyclonic wind-stress curl at 10° S latitude in the

HCE will create w of 1.7 m day^{-1} . Much larger plankter sizes may result from curl-driven upwelling in the HCE. Anchovy feed most effectively on large plankters (van der Lingen *et al.* 2006), and we would expect the HCE to be dominated by anchovy and support a larger anchovy population than the CCE under similar curl conditions. Consistent with this hypothesis, anchovy is the dominant fish species in Peru, while sardine is dominant in the CCE. Annual anchovy landings in Peru peaked at more than 13 MT in the mid 1970s, while maximal landings in California peaked at about 0.4 MT in the early 1980s (Lluch-Belda *et al.* 1989).

Our results demonstrate a mechanism, from physics to fish, relating variability in production of Pacific sardine to environmental changes over interannual and decadal scales. We show that the level of production in a large, marine ecosystem depends on wind-stress curl. Coupling predictions of atmospheric winds with a simple hydrographic model will allow forecasting of sardine production in the CCE. Such forecasts have increasing ecological and economic value as globalization of commerce and industrialization of fisheries continues in response to growing demand and utilization of marine resources (Pauly *et al.* 2005). Simultaneously, predictions of future climate conditions are becoming more precise (Barnston *et al.*) and offer an opportunity to more effectively manage fisheries if the biological responses to physical variability are understood. Credible mechanistic hypotheses relating atmospheric physics to variability in the ocean's biota are essential to prudently manage marine resources under a changing climate.

4.5. Acknowledgements

We are grateful to M. Kanamitsu for development of the atmospheric model and thank P. Franks, M. Landry, D. Rudnick, M. Ohman, three anonymous reviewers, and R. Davis, the communicating member, for their comments. The 2006 and 2007 cruises were supported by the CCE Long-Term Ecological Research Program, and the CalCOFI program provided historical data. This work was supported by the National Science Foundation Graduate Research Fellowship Program, the Michael M. Mullin Fund, and the Maxwell-Fenmore Fellowship.

Chapter 4, in full, is a reprint of the material as it appears in Rykaczewski, R.R. and Checkley, D.M., Jr. (2008) Influence of ocean winds on the pelagic ecosystem in upwelling regions. *Proceedings of the National Academies of Sciences U. S. A.* **105**:1965-1970. The dissertation author was the primary investigator and author of this manuscript.

Table 4.1. Pearson correlation coefficients (r) between upwelling and water-column properties. Shown are correlation coefficients (r values) between time series before and after removal of the linear trend from each time series (first and second value in each column, respectively). Bold values are significant at the 95% level.

	period of comparison (number of surveys)	coastal upwelling	curl-driven upwelling
density (σ_θ)	1950 – 1969 (n = 16)	0.62, 0.67	-0.030, 0.034
	1978 – 2004 (n = 22)	0.34, 0.51	0.71, 0.69
nutricline depth	1978 – 2004 (n=22)	-0.37, -0.60	-0.67, -0.62
log chl a	1978 – 2004 (n=22)	0.23, 0.57	0.67, 0.59

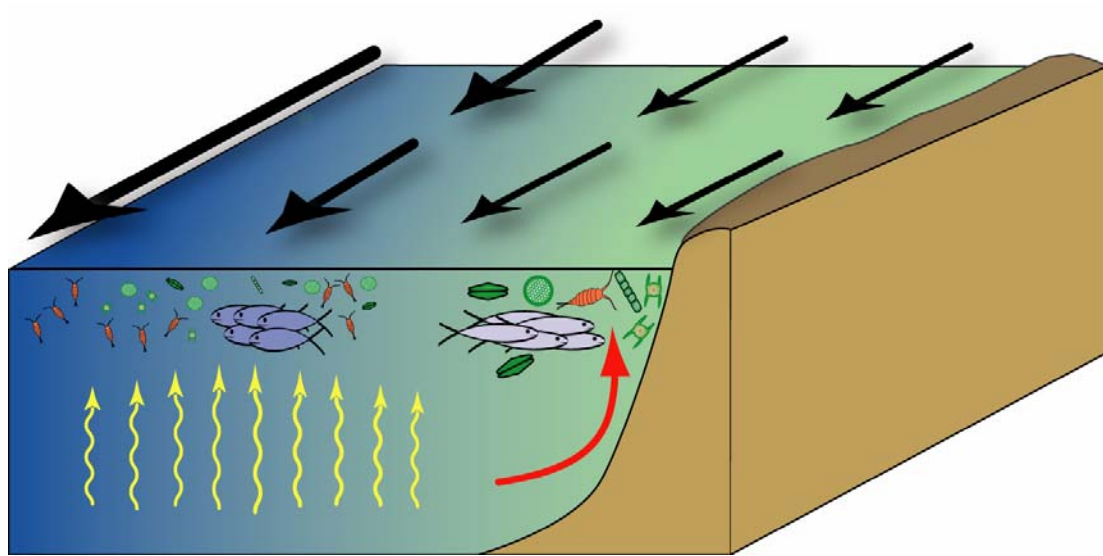


Figure 4.1. Conceptual diagram displaying the hypothesized relationship between wind-forced upwelling and the pelagic ecosystem. Alongshore, equatorward wind stress results in coastal upwelling (red arrow), supporting production of large phytoplankton and zooplankton. Between the coast and the wind-stress maximum, cyclonic wind-stress curl results in curl-driven upwelling (yellow arrows) and production of smaller plankton. Anchovy (gray fish symbols) prey upon large plankton, while sardine (blue fish symbols) specialize on small plankton. Black arrows represent winds at the ocean surface, and their widths are representative of wind magnitude.

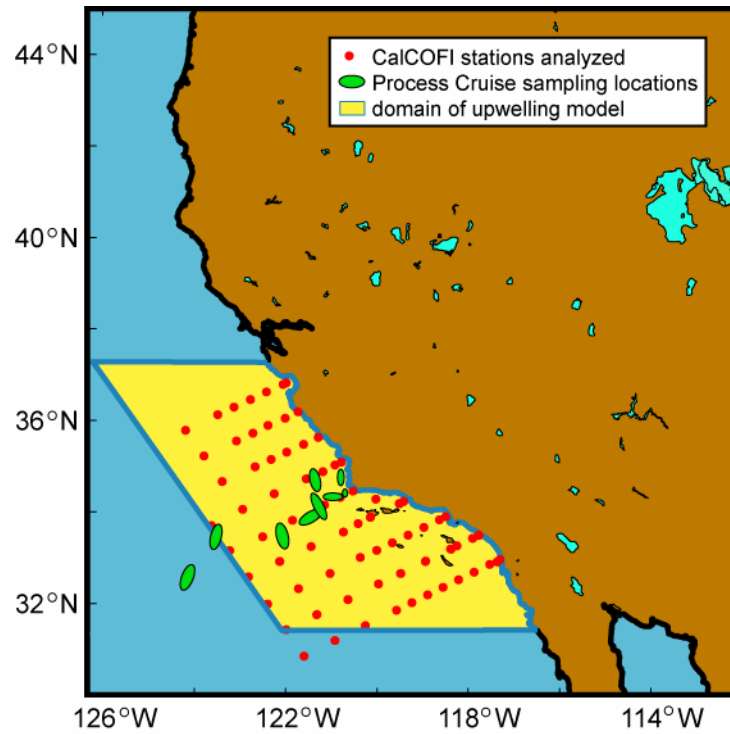


Figure 4.2. Domain of the upwelling model, locations of zooplankton collections, and CalCOFI stations. The domain of the upwelling model is from Ensenada, Baja California to Santa Cruz, California and extends approximately 300 km offshore. Each process cruise station was occupied for three to five days, and zooplankton was collected between dusk and dawn.

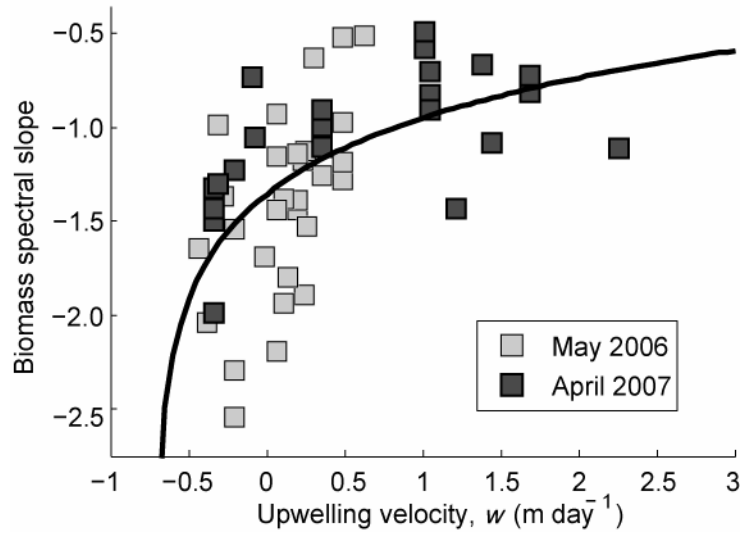


Figure 4.3. Relationship between zooplankton size and upwelling rate. This relationship is modeled using a logarithmic function ($r^2 = 0.32$, $p < 0.001$, $n = 51$, $y = 0.46 \cdot \ln(x + 0.71) - 1.20$). The mean 90% confidence interval around the slopes of the linear least-squares fits to the biomass spectra is $\pm 0.71 \text{ g mm}^{-2}$.

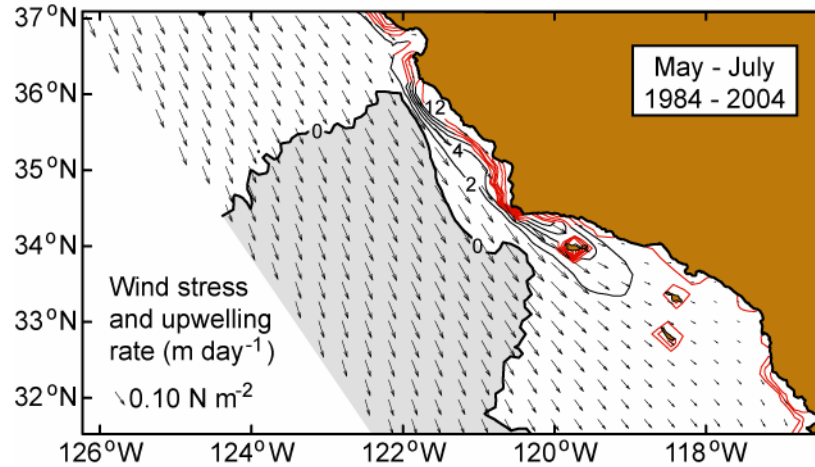


Figure 4.4. Mean summertime (May-July) wind stress and upwelling rate from 1984-2004. Arrows indicate wind stress. Upwelling rates are denoted by contours at an interval of 2 m day^{-1} . Black contours indicate the region of curl-driven upwelling. Red contours denote coastal upwelling. Areas of anti-cyclonic curl (downwelling) are shaded. The years 1984-2004 correspond to the period during which nutrient, chlorophyll, and sardine production data were regularly collected.

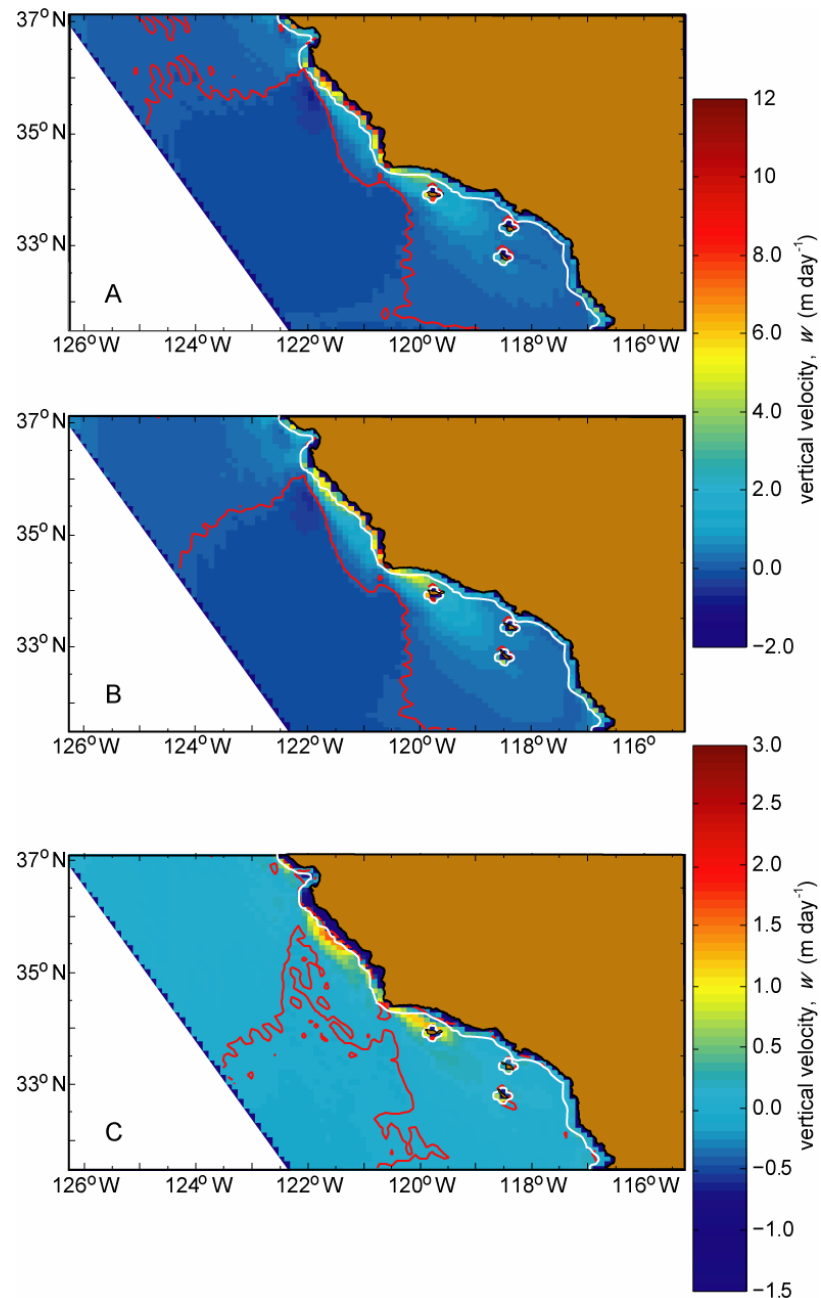


Figure 4.5. Upwelling changes in the CCE. Wind-stress curl and coastal, alongshore winds were used to estimate mean w resulting from coastal upwelling and curl-driven upwelling in May, June, and July during 1950-1959 (A), 1990-1999 (B), and the difference in upwelling between the two periods (1990-1999 minus 1950-1959, C). The zero contour is noted in red. The white line along the coast separates the domains of coastal upwelling and curl-driven upwelling. Note the increase in curl-driven upwelling and the decrease in coastal upwelling in the 1990s relative to the 1950s.

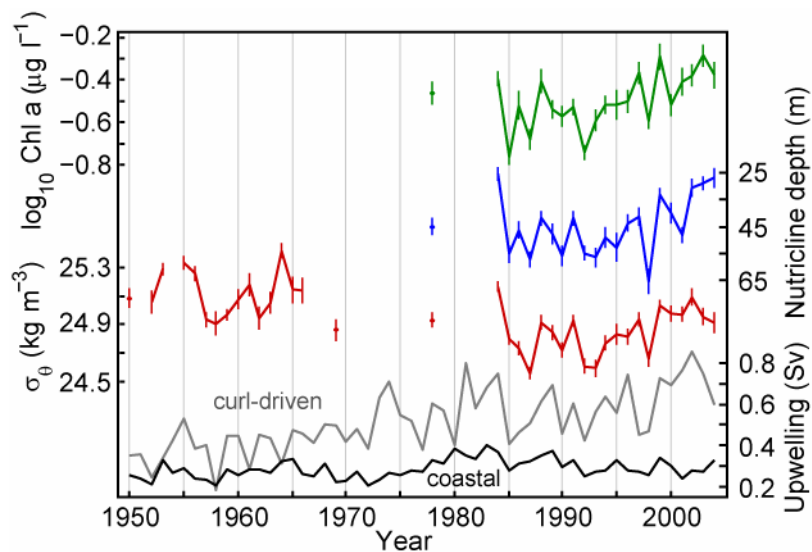


Figure 4.6. Summertime upwelling, σ_θ (red line), nutricline depth (blue line), and chl a concentration (green line). These properties of the water column are more highly correlated with curl-driven upwelling (gray line) than with coastal upwelling (black line) after 1970. Prior to 1970, σ_θ is correlated with coastal upwelling and not curl-driven upwelling. (1 Sverdrup = $1 \times 10^6 \text{ m}^3 \text{ s}^{-1}$)

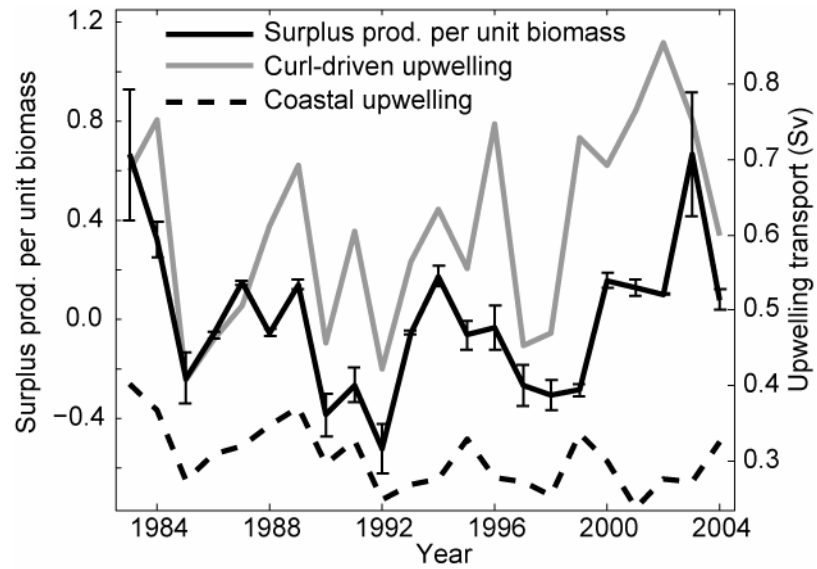


Figure 4.7. Upwelling and surplus production per unit biomass of Pacific sardine. Curl-driven upwelling from May-July showed the highest correlation with surplus production per unit biomass ($r = 0.62$, $p < 0.005$, $n = 22$). Coastal upwelling during the same period was not significantly correlated with production ($r = 0.40$, $p = 0.067$, $n = 22$). Error bars are \pm one standard deviation of the sardine production estimates.

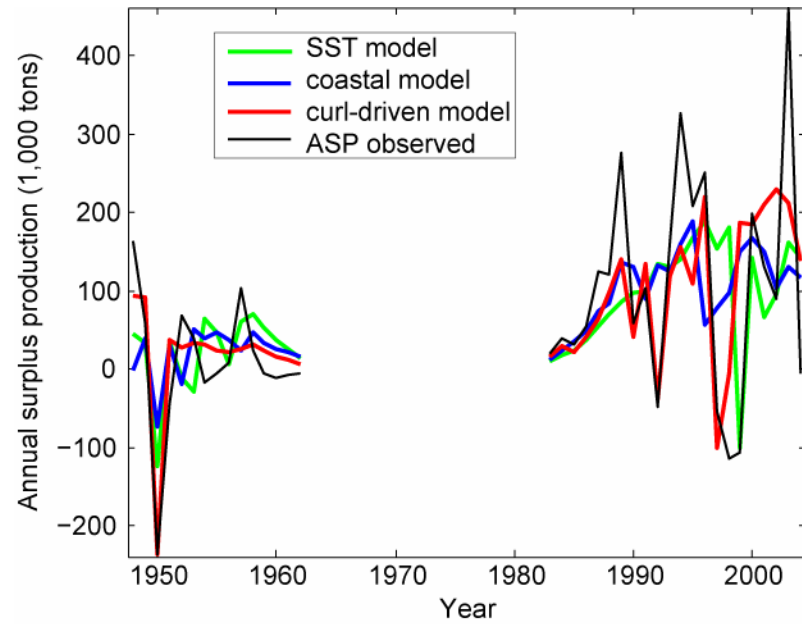


Figure 4.8. Observed and modeled surplus production in the Pacific sardine population for two periods (1948-1962 and 1983-2004). The surplus production model incorporating curl-driven upwelling produced the best fit to observed production during both periods of stock assessment. Coastal upwelling and mean SST were less successful at estimating surplus production.

4.6. References

- Arthur, D.K. (1976) Food and feeding of larvae of three fishes occurring in the California Current, *Sardinops sagax*, *Engraulis mordax*, and *Trachurus symmetricus*. *Fish. Bull.* **74**:517–530.
- Bakun, A. and Broad, K. (2003) Environmental 'loopholes' and fish population dynamics: comparative pattern recognition with focus on El Niño effects in the Pacific. *Fish. Oceanogr.* **12**:458-473.
- Bakun, A. and Nelson, C.S. (1991) The seasonal cycle of wind-stress curl in subtropical eastern boundary current regions. *J. Phys. Oceanogr.* **21**:1815-1834.
- Barnston, A.G., Kumar, A., Goddard, L. and Hoerling, M.P. (2005) Improving seasonal prediction practices through attribution of climate variability. *Bull. Amer. Met. Soc.* **86**:59-72.
- Baumgartner, T.R., Soutar, A. and Ferreirabartrina, V. (1992) Reconstruction of the history of Pacific sardine and northern anchovy populations over the past two millennia from sediments of the Santa-Barbara Basin, California. *CalCOFI Rep.* **33**:24-40.
- Beverton, R.J.H. and Holt, S.J. (1957) *On the Dynamics of Exploited Fish Populations*. London: Chapman and Hall. pp. 44-65.
- Chavez, F.P., Ryan, J., Lluch-Cota, S.E. and Niquen, M. (2003) From anchovies to sardines and back: multidecadal change in the Pacific Ocean. *Science* **299**:217-221.
- Checkley, D.M., Jr, Dotson, R.C. and Griffith, D.A. (2000) Continuous, underway sampling of eggs of Pacific sardine (*Sardinops sagax*) and northern anchovy (*Engraulis mordax*) in spring 1996 and 1997 off southern and central California. *Can. J. Fish. Aquat. Sci.* **47**:1139-1155.
- Chelton, D.B. (1982) Large-scale response of the California Current to forcing by the wind-stress curl. *CalCOFI Rep.* **23**:30–148.
- Chelton, D.B., Schlax, M.G., Freilich, M.H. and Milliff, R.F. (2004) Satellite measurements reveal persistent small-scale features in ocean winds. *Science* **303**:978-983.
- Cury, P., Bakun, A., Crawford, R.J.M., Jarre, A., Quinones, R.A., Shannon, L.J. and Verheye, H.M. (2000) Small pelagics in upwelling systems: Patterns of

- interaction and structural changes in "wasp-waist" ecosystems. *ICES J. Mar. Sci.* **57**:603-618.
- Dever, E.P., Dorman, C.E. and Largier, J.L. (2006) Surface boundary-layer variability off Northern California, USA, during upwelling. *Deep-Sea Res. Part II Top. Stud. Oceanogr.* **53**:2887-2905.
- Di Lorenzo, E. (2003) Seasonal dynamics of the surface circulation in the Southern California Current System. *Deep-Sea Res. Part II Top. Stud. Oceanogr.* **50**:2371-2388.
- Di Lorenzo, E., Miller, A.J., Schneider, N. and McWilliams, J.C. (2005) The warming of the California Current System: Dynamics and ecosystem implications. *J. Phys. Oceanogr.* **35**:336-362.
- Edwards, K.A., Rogerson, A.M., Winant, C.D. and Rogers, D.P. (2001) Adjustment of the marine atmospheric boundary layer to a coastal cape. *J. Atmos. Sci.* **58**:1511-1528.
- Falkowski, P.G. and Oliver, M.J. (2007) Mix and match: How climate selects phytoplankton. *Nat. Rev. Microbiol.* **5**:813-819.
- Fox, W.W. (1970) An exponential surplus-yield model for optimizing exploited fish populations. *Trans. Am. Fish. Soc.* **99**:80-88.
- Gill, A.E. (1982) *Atmosphere-Ocean Dynamics*. New York: Academic Press. pp. 326-408.
- Harris, R., Wiebe, P., Lenz, J., Skjoldal, H.R. and Huntley, M. (2000) *ICES Zooplankton Methodology Manual*. San Diego: Academic Press. pp. 90-94.
- Hayward, T.L. (2000) El Niño 1997-98 in the coastal waters of Southern California: A timeline of events. *CalCOFI Rep.* **41**:98-116.
- Hsieh, C.H., Reiss, C.S., Hunter, J.R., Beddington, J.R., May, R.M. and Sugihara, G. (2006) Fishing elevates variability in the abundance of exploited species. *Nature* **443**:859-862.
- Jacobson, L.D., Bograd, S.J., Parrish, R.H., Mendelsohn, R. and Schwing, F.B. (2005) An ecosystem-based hypothesis for climatic effects on surplus production in California sardine (*Sardinops sagax*) and environmentally dependent surplus production models. *Can. J. Fish. Aquat. Sci.* **62**:1782-1796.
- Jennings, S., Kaiser, M.J. and Reynolds, J.D. (2001) *Marine Fisheries Ecology*. Oxford: Blackwell Science. pp. 78-83.

- Kanamitsu, M. and Kanamaru, H. (2007) Fifty-seven-year California Reanalysis Downscaling at 10 km (CaRD10). Part I: System detail and validation with observations. *J. Clim.* **20**:5553-5571.
- Koracin, D., Dorman, C.E. and Dever, E.P. (2004) Coastal perturbations of marine-layer winds, wind stress, and wind-stress curl along California and Baja California in June 1999. *J. Phys. Oceanogr.* **34**:1152-1173.
- Lluch-Belda, D., Crawford, R.J.M., Kawasaki, T., MacCall, A.D., Parrish, R.H., Schwartzlose, R.A. and Smith, P.E. (1989) Worldwide fluctuations of sardine and anchovy stocks: the regime problem. *S. Afr. J. Mar. Sci.* **8**:195-205.
- MacCall, A.D. (1979) Population estimates for the waning years of the Pacific sardine fishery. *CalCOFI Rep.* **20**:79-82.
- Margalef, R. (1978) Life-forms of phytoplankton as survival alternatives in an unstable environment. *Oceanol. Acta* **1**:493-509.
- Miller, A.J., Cayan, D.R., Barnett, T.P., Graham, N.E. and Oberhuber, J.M. (1994) Interdecadal variability of the Pacific Ocean - model response to observed heat flux and wind stress anomalies. *Clim. Dyn.* **9**:287-302.
- Moloney, C.L. and Field, J.G. (1991) The size-based dynamics of plankton food webs: 1 - A simulation-model of carbon and nitrogen flows. *J. Plankton Res.* **13**:1003-1038.
- Mullin, M.M. (1998) Biomasses of large-celled phytoplankton and their relation to the nitricline and grazing in the California Current System off Southern California, 1994-1996. *CalCOFI Rep.* **39**:117-123.
- Munk, W.H. (1950) On the wind-driven ocean circulation. *J. Met.* **7**:79-93.
- Ohman, M.D. and Smith, P.E. (1995) A comparison of zooplankton sampling methods in the CalCOFI time series. *CalCOFI Rep.* **36**:153-158.
- Pauly, D., Watson, R. and Alder, J. (2005) Global trends in world fisheries: Impacts on marine ecosystems and food security. *Phil. Trans. R. Soc. Lond., Ser. B* **360**:5-12.
- Peterson, W.T. and Schwing, F.B. (2003) A new climate regime in Northeast Pacific ecosystems. *Geophys. Res. Lett.* **30**:10.1029/2003GL017528.

- Pickett, M.H. and Paduan, J.D. (2003) Ekman transport and pumping in the California Current based on the U.S. Navy's high-resolution atmospheric model (COAMPS). *J. Geophys. Res.* **108**:doi:10.1029/2003JC001902.
- Pickett, M.H. and Schwing, F.B. (2006) Evaluating upwelling estimates off the west coasts of North and South America. *Fish. Oceanogr.* **15**:256-269.
- Platt, T. and Denman, K. (1978) The structure of pelagic marine ecosystems. *Rapp. P.-V. Réun. Cons. Int. Explor. Mer.* **173**:60-65.
- Ryther, J.H. (1969) Photosynthesis and fish production in sea. *Science* **166**:72-76.
- Smith, P.E. (2005) A history of proposals for subpopulation structure in the Pacific sardine (*Sardinops sagax*) population off western North America. *CalCOFI Rep.* **46**:75-82.
- Smith, R.L. (1968) Upwelling. *Oceanogr. Mar. Biol. Ann. Rev.* **6**:11-46.
- van der Lingen, C.D., Hutchings, L. and Field, J.G. (2006) Comparative trophodynamics of anchovy *Engraulis encrasicolus* and sardine *Sardinops sagax* in the southern Benguela: are species alternations between small pelagic fish trophodynamically mediated? *Afr. J. Mar. Sci.* **28**:465-477.
- Woodruff, S.D., Slutz, R.J., Jenne, R.L. and Steurer, P.M. (1987) A comprehensive ocean-atmosphere data set. *Bull. Amer. Met. Soc.* **68**:1239-1250.
- Yelland, M.J., Moat, B.I., Taylor, P.K., Pascal, R.W., Hutchings, J. and Cornell, V.C. (1998) Wind stress measurements from the open ocean corrected for airflow distortion by the ship. *J. Phys. Oceanogr.* **28**:1511-1526.
- Yoshida, K. and Mao, H.L. (1957) A theory of upwelling of large horizontal extent. *J. Mar. Res.* **16**:40-54.

Chapter 5. Conclusions

5.1. Summary and future directions

Consideration of the mechanisms relating climate variability to growth of Pacific sardine and northern anchovy is necessary to enhance understanding of the consequences of continued climate change on the California Current Ecosystem (CCE). The research composing this dissertation has helped elucidate the oceanographic conditions and ecological processes underlying the differences in habitat and production of these fishes. The results presented in Chapter 2 support the hypothesis that morphological differences in the branchial sieve of sardine and anchovy are related to resource partitioning of planktonic prey. The inter-raker spacing of anchovy is significantly greater than that of sardine, and the gill rakers of sardine are equipped with specialized denticles that further facilitate retention of small plankters. These differences in functional morphology of the branchial sieve may offer sardine a competitive advantage in relatively oligotrophic environments where the concentration and size structure of plankton are reduced and are consistent with the hypothesis of resource partitioning among the two prominent planktivorous fishes of the CCE.

In Chapter 3, I presented data relating the abundances and size structures of the zooplankton community to changes in oceanographic conditions and considered the implications of these changes for growth in sardine and anchovy. I hypothesize that this relationship results from size-dependent trophic interactions. Zooplankton sizes decline with distance offshore in concert with phytoplankton sizes, nutrient

concentrations, and physical conditions promoting shoaling of the nutricline. The biomasses of individual copepods, rather than changes in gross taxonomic composition of the community, appear to control changes in the spectral slope of the zooplankton community. The potential for growth in the anchovy population is strongly favored by the large plankter sizes and high levels of abundance found in eutrophic areas, and this potential for growth is greatly diminished under oligotrophic conditions. Sardine growth is less variable across the CCE, and the potential for growth exists even under moderately oligotrophic conditions. Changes in the biomass and size structure of zooplankton communities in offshore waters influence the potential growth rate of sardine, but anchovy growth is uniformly negative in the offshore region.

Although the relationship between growth rate and plankton assemblages described in Chapter 3 may be valid, the absolute values of the estimates of growth rate are subject to the bioenergetics models applied. The models of James (1989) and van der Lingen (1999) estimate unrealistically high gross-growth efficiencies for large and abundant plankters, especially in the budgets for carbon analyzed in Chapter 3. It is challenging to examine fish respiration, excretion, and absorption for planktivorous fishes which may feed continuously throughout the day. The laboratory examinations of fish feeding were conducted over feeding periods of several (2 to 3) hours, and the nitrogen and carbon budgets derived from these examinations may not be accurately extrapolated to describe growth processes for longer periods of feeding. If we intend to examine changes in fisheries ecology with a mechanistic approach, it is essential that we have a better understanding of the bioenergetic response of these fishes to

changes in their prey field and readdress model caveats when the models produce unrealistic results.

The distinct spatial areas and oceanographic environments which appear to influence the growth and distribution of sardine and anchovy led me to consider the atmospheric conditions which might affect these distinct regions of the ecosystem, and a hypothesis relating sardine production to wind-stress curl is presented in Chapter 4. Unlike coastal upwelling, the upwelling resulting from wind-stress curl influences both the nearshore and offshore regions of the southern CCE, and estimates of the volume transport resulting from curl-driven upwelling indicate that it is an important mechanism of nutrient supply to the ecosystem. Estimates of curl-driven upwelling are associated with records of pycnocline and nutricline shoaling in the southern CCE since the 1970s, and sardine production is more strongly related to changes in curl-driven upwelling than with estimates of coastal upwelling or measures of sea-surface temperature.

Studies of upwelling ecosystems in the past have largely focused on coastal alongshore wind stress and the resulting upwelling, as this is the most conspicuous upwelling signal at a local scale near the coast. However, the weak upwelling driven by positive wind-stress curl also deserves attention as a factor influencing production away from the coastal boundary. It would be valuable to specifically examine the atmospheric forcing responsible for changes in nutrient supply in different regions of an upwelling ecosystem. What influence does variability in coastal upwelling have, if any, on biological communities 200 or 400 km from the coast? The coupling of atmospheric and hydrographic models with geochemical tracers of shelf interactions

(manganese or radium) may help distinguish between nutrient supply due to local vertical flux and offshore advection of eutrophic waters from the coastal boundary. What is the role of micronutrients (*e.g.* dissolved iron) availability in determining the size structure of phytoplankton and zooplankton communities in different regions of the ecosystem? Are offshore wind stress and wind-stress curl responsible for the interannual and multi-decadal changes in offshore ecosystems, as suggested in Chapter 4, or are the effects of mesoscale circulation features important to consider as well? How do global-scale changes in ocean conditions, such as warming of the surface mixed layer, differentially affect coastal and curl-driven upwelling dynamics? The questions are endless. Such questions addressing the underlying physical and chemical processes that relate atmospheric and biological changes may be pertinent as biological oceanographers consider large-scale spatial and temporal variability in the CCE.

One issue worthy of mention is the sensitivity of the final conclusions in Chapter 4 to caveats in stock assessment methods. Estimating the biomass of sardine is difficult and dependent upon the population model used and several assumptions concerning the distribution of the stock, selectivity of commercial fisheries, and the reliability of data. In 2007, the National Marine Fisheries Service opted to apply a new population model to estimate the population of California sardine, switching from the Age-structured Assessment Program (ASAP) used in earlier years to the Stock Synthesis 2 (SS2) model platform. The SS2 model is more flexible and overcomes several difficulties contained within the ASAP model structure (Hill *et al.* 2008). The range of adult biomass estimates for sardine are similar between the two model

structures. However, biomass changes estimated by the two models do not agree and are uncorrelated over time. This is particularly evident in the second half of the 1990s when the estimates of biomass differ by more than 1 million metric tons, a value equal to about one-half of the biomass maximum over the last five decades. Although it is discouraging to observe such exceptional sensitivity of biomass estimates to the method of estimation, it has increased my recognition of the uncertainties in population assessment. These issues are common to all assessments of marine fish stocks but are especially challenging for the widely ranging and highly variable population of Pacific sardine, which may be distributed from Baja California to the Gulf of Alaska and from the coast to several hundreds of kilometers offshore.

Together, the different elements of this dissertation propose a mechanism accounting for the different responses of sardine and anchovy to environmental changes that is based on the distinct oceanographic conditions which promote growth of each species by changing the abundance and size distribution of their planktonic prey. Recently, other mechanistic hypotheses have been presented to explain variability in sardine and/or anchovy populations (*e.g.*, Logerwell and Smith 2001, van der Lingen 2006, MacCall in press), and countless more have yet to be proposed. Given the new and innovative oceanographic sampling methods (Dickey *et al.* 2008) and atmospheric modeling capabilities (Barnston *et al.* 2005), the time is ripe to examine these hypotheses and readdress basic questions of fisheries oceanography (though funding for process studies from ships continues to be an essential, if costly, component of this research). In the coming decades, fisheries oceanographers will no longer need to ponder over correlations between pier temperatures and fish landings

only to leave true, mechanistic understanding up for speculation. However, even with the recent improvements in the capability to sample the oceanographic environment, the long-term variability characteristic of sardine and anchovy populations may delay answers to this classic fisheries puzzle. In the meantime, I look forward to the continued debate and thoughtful contemplation concerning the responses of small pelagic fish to climate change.

5.2. References

- Barnston, A.G., Kumar, A., Goddard, L. and Hoerling, M.P. (2005) Improving seasonal prediction practices through attribution of climate variability. *Bull. Amer. Met. Soc.* **86**:59-72.
- Dickey, T.D., Itsweire, E.C., Moline, M.A. and Perry, M.J. (2008) Introduction to the Limnology and Oceanography special Issue on autonomous and lagrangian platforms and sensors (ALPS). *Limnol. Oceanogr.* **53**:2057-2061.
- Hill, K., Dorval, E., Lo, N.C.H., Macewicz, B.J., Show, C. and Felix-Uraga, R. (2008) Assessment of the Pacific sardine resource in 2008 for U.S. management in 2009. *U.S. Dep. Commer., NOAA Tech. Memo. Report No.* **413**, 176 pp.
- James, A.G., Probyn, T. and Hutchings, L. (1989) Laboratory-derived carbon and Nitrogen budgets for the omnivorous planktivore *Engraulis capensis* Gilchrist. *J. Exp. Mar. Biol. Ecol.* **131**:125-145.
- Logerwell, E.A. and Smith, P.E. (2001) Mesoscale eddies and survival of late stage Pacific sardine (*Sardinops sagax*) larvae. *Fish. Oceanogr.* **10**:13-25.
- MacCall, A.D. (in press) Mechanisms of low frequency fluctuations in sardine and anchovy populations. In: *Climate Change and Small Pelagic Fish*. D.M. Checkley, Jr., J. Alheit, Y. Oozeki, C. Roy (eds.) Cambridge: Cambridge University Press.
- van der Lingen, C.D. (1999) The feeding ecology of, and carbon and nitrogen budgets for, sardine *Sardinops sagax* in the southern Benguela upwelling system. Ph.D. thesis. University of Cape Town, Cape Town.
- van der Lingen, C.D., Hutchings, L. and Field, J.G. (2006) Comparative trophodynamics of anchovy *Engraulis encrasicolus* and sardine *Sardinops sagax* in the southern Benguela: are species alternations between small pelagic fish trophodynamically mediated? *Afr. J. Mar. Sci.* **28**:465-477.